A Comparison of GIS Approaches to Slope Instability Zonation in the Central Blue Ridge Mountains of Virginia

Jeffrey Sterling Galang

THESIS submitted to the Faculty of

Virginia Polytechnic Institute and State University

in partial fulfillment of the requirements for the degree of

MASTER OF SCIENCE

in

Forestry

Stephen P. Prisley, Chair
A.L. (Tom) Hammett
J.M. (Rien) Visser

October 22, 2004
Blacksburg, Virginia

Keywords: GIS, slope instability, terrain analysis, debris flows

A Comparison of GIS Approaches to Slope Instability Zonation in the Central Blue Ridge Mountains of Virginia

Jeffrey S. Galang

ABSTRACT

To aid in forest management, various approaches using Geographic Information Systems (GIS) have been used to identify the spatial distributions of relative slope instability. This study presents a systematic evaluation of three common slope instability modeling approaches applied in the Blue Ridge Mountains of Virginia. The modeling approaches include the Qualitative Map Combination, Bivariate Statistical Analysis, and the Shallow Landsliding Stability (SHALSTAB) model. Historically, the qualitative nature of the first model has led to the use of more quantitative statistical models and more deterministic physically-based models such as SHALSTAB. Although numerous studies have been performed utilizing each approach in various regions of the world, only a few comparisons of these approaches have been done in order to assess whether the quantitative and deterministic models result in better identification of instability.

The goal of this study is to provide an assessment of relative model behavior and error potential in order to ascertain which model may be the most effective at identifying slope instability in a forest management context. The models are developed using both 10-meter and 30-meter elevation data and outputs are standardized and classified into instability classes (e.g. low instability $\rightarrow$ high instability). The outputs are compared with cross-tabulation tables based on the area (m^2) assigned to each instability class and validated using known locations of debris flows. In addition, an assessment of the effects of varying source data (i.e. 10-meter vs. 30-meter) is performed. Among all models and using either resolution data, the Qualitative Map Combination correctly identifies the most debris flows. In addition, the Qualitative Map Combination is the best model in terms of correctly identifying debris flows while minimizing the classification of high instability in areas not affected by debris flows. The statistical model only performs well when using 10-meter data while SHALSTAB only performs well using 30-meter data. Overall, 30-meter elevation data predicts the location of debris flows better than 10-meter data due to the inclusion of more area into higher instability classes. Of the models, the statistical approach is the least sensitive to variations in source elevation data.

ACKNOWLEDGEMENTS

I would especially like to thank Dr. Stephen Prisley for serving as my committee chair and for all of his valuable advice. Steve has always had an open mind when discussing this project and has always been supportive of my ideas and efforts. Also, Drs. Hammett and Visser have been extremely important in providing advice and direction regarding the output of my work. They both have kept my focus on the applicability of my work which I feel is extremely important. Without the help of these individuals this project may have never ended. I would also like to thank Dr. Gerry Wieczorek of the U.S. Geological Survey for his commentary on my work as well as providing me with the debris flow data and other data necessary to finish this study.

Many thanks again to Dr. Prisley and to Dr. Jeff Kirwan for providing me the funding opportunities to explore my individual research goals. It has been a challenge to work on a research project in which there was no direct funding and these individuals have afforded me the opportunity to pursue my own interests. Without their help this project would not have existed.

I would also like to thank my family and my girlfriend for supporting me throughout this whole endeavor. I don't think anyone thought they would see me go this far and without their support and encouragement it would not have been possible. To all my friends who put up with my two-year hibernation, thank you. And finally, who can forget Mason and Zobo, the best dogs ever!

DEDICATION

For my grandmother.

TABLE OF CONTENTS

LIST OF TABLES

LIST OF FIGURES

CHAPTER 1. INTRODUCTION

Geographical Information Systems (GIS), defined as a "set of tools for collecting, storing, retrieving at will, transforming, and displaying spatial data", have become a valuable tool for planners across a wide array of disciplines (Burrough, 1986). GIS applications in forestry were some of the first and have since become an integral part of many forestry operations. Because everything on the surface of the earth has a spatial position, the ability of GIS to perform spatial analyses has great applications in other fields such as hydrology and community planning. Over the past few decades, the field of natural hazards has found particular use of GIS in its analyses of where hazards might occur. This multidisciplinary approach highlights the power of GIS as a tool that complements other disciplines such as landslide hazard zonation. Landslide hazard zonation refers to the "division of the land surface into areas and the ranking of these areas according to degrees of actual or potential hazard from landslides or other mass movements on slopes" (Varnes, 1984).

Landslides are natural landscape-shaping phenomena, occurring particularly in mountain environments. However, human activities such as timber harvesting and road-building can increase the likelihood of landslides. Nonetheless, forest management continues in many mountain regions throughout the world. Today, active forest management in mountainous terrain is often constrained by the possibility of landslides. Therefore, attempts to define zones of landslide susceptibility (i.e. landslide hazard zonation) have been made throughout the world. Landslide hazard zonation has become a subject of much international interest as evidenced by the large amount of comprehensive work done recently (Brunsden and Prior, 1984; Carrara and Guzzetti, 1995; Crozier, 1986; Schuster and Krizek, 1978; Turner and Schuster, 1996; Varnes, 1984; Zaruba and Mencl, 1982). Moreover, the global interest in this subject is highlighted in the dedication of the 1990's as the International Decade for Natural Disaster Reduction (IDNDR, 1987).

Landslides in mountainous terrain only become problems when social or cultural components (e.g. people, property and livelihoods) are threatened (Crozier, 1986). Unfortunately, as both the world population and the need for natural resources continue to grow, people are forced to live in and/or utilize the marginal environments where landslides commonly occur. Moreover, advances in technical capability that allow humans to modify the natural environment will likely lead to an increased frequency of landslides and the associated damages (Crozier, 1986).

Damage from individual landslides is typically not as catastrophic as earthquakes, floods or hurricanes yet they are more widespread, often reoccur and may cause more cumulative long-term damage than other disasters (Hansen, 1984; Varnes, 1984). The resulting damages from slope movements are classed as either personal, economic and/or environmental and are seen in both developed and developing nations (Crozier, 1986). The most obvious of personal damage of any natural disaster is the loss of life. Since the late 1960's there have been an average 1,650 fatalities from landslides and almost 140,000 people affected by landslides per year (IFRCRCS, 1993; 1994). Most of these occur in developing countries due to a lack of investment in preventative measures such as proper road construction, poor land management strategies, higher population growth

rates and increased marginalization[1] (Alexander, 1995; Guzzetti *et al.*, 1999; Harrison and Pearce, 2000). In addition, many of the fatalities associated with other hazards such as earthquakes and hurricanes are actually due to subsequent landsliding. Other personal damage may include psychological distress due to displacement and the loss of loved ones.

Direct and indirect economic costs include the loss of property, buildings, disruption of transportation routes and the associated costs of recovery and injury. It is estimated that the United States has annual direct and indirect costs associated with landslides in the range of $1.6 – $3.2 billion (Schuster, 1996; Schuster and Highland, 2001; Smith, 1991). In the Blue Ridge of Virginia, two separate storm events caused a total of over $216 million (Gao, 1992; Wieczorek *et al.*, 2004). While the majority of fatalities occur in developing countries, the majority of financial losses occur in the developed countries. Hansen (1984) estimates that of all disaster-related fatalities, 95% occur in developing countries while 75% of financial losses occur in industrialized nations. However, while the largest financial losses occur in wealthy countries, developing countries may have greater losses as a percent of their GNP, up to 20 times greater (Alexander, 1995). Hence, there is incentive to predict and thereby prevent landslides.

The environmental costs associated with landslides include the loss of soil and vegetation, changes in stream morphometry and sedimentation. Landslides, which obviously displace rock, soil and vegetation, further disrupt the pedogenesis of soils and damage the habitats of both belowground and aboveground inhabitants. However, the erosive nature of a landslide has comparable benefits as well. For example, in Nepal landslide deposits are often considered beneficial in the development of agricultural terraces because the loose soil is easier to manage and can provide increased soil fertility (Ives and Messerli, 1989) while in Chile the native *Nothofagus* genus requires disturbed sites for reproduction and landslides are often the necessary disturbance (Veblen, 1982). Stream morphometry changes naturally over time, yet when large deposits dam channels, a subsequent breach of the dam can lead to flash flooding, such as has happened several times in south-central Chile (Davis and Karzulovic, 1963; Veblen, 1982). The increased sedimentation of streams from human activities is another concern that researchers across a wide array of disciplines have extensively studied. Land managers in many countries are regulated in their activities because of the known impacts of sedimentation such as damaged aquatic habitat and reduced water quality.

The related costs of landslides, whether personal, economic or environmental, are substantial and affect many communities throughout the world. Landslides are complex phenomena and are caused by a large and diverse set of factors. However, because landslides affect discrete units of land, an areal zonation of landslide susceptibility is made more feasible than certain other natural hazards such as hurricanes, tsunamis or drought (Hansen, 1984; Varnes, 1984). Moreover, with improved technologies such as desktop PC's, GIS, satellite imagery and Global Positioning Systems (GPS), the handling and processing of data are made much more efficient. In developed countries where financial investments and engineering skills needed to control erosion are abundant, emphasis is on installation of safety controls to prevent landslides from causing damage

[1] When vulnerability to hazards is disproportionate within a country due to military or economic repression, political and social polarization, and/or ethnic or religious dominance, people are forced onto marginal lands where hazards normally occur

whereas developing countries lack the money to implement these controls and must therefore rely on proper planning.

Because areas of potential landsliding can be delineated, forest planners can effectively match management activities with the abilities of the land to support such activities. This is the general purpose behind landslide hazard zonation today and, although it is recognized that the prediction of landslides is an inexact science and only the first step in preventative planning (Varnes, 1984), much progress is being made. Currently, various approaches using Geographic Information Systems (GIS) have been used to identify spatial distributions of relative landslide susceptibility and then classify areas into instability classes (e.g. low → high). However, the decision as to which approach is most appropriate for a site remains somewhat arbitrary. Regardless of the approach, forest managers can use these GIS models to aid in planning activities from timber harvesting to road-building.

Although the use of GIS technology in landslide hazard zonation is more widespread than ever, there are some concerns about the limitations of using GIS (Carrara *et al.*, 1995a). In the transformation from 4-dimensional reality into a 1-dimensional computer file, errors and uncertainties such as generalization and simplification are introduced into the hazard model. In addition, various model approaches produce different outputs resulting in uncertainty among the models. The concepts of error and uncertainty in GIS have been studied extensively by GIS professionals (Bolstad and Smith, 1992); however, in the field of natural hazards, that concept is rarely considered.

Although many models are tested for accuracy against locations known to have been subject to landsliding, error and uncertainty still receive only minor attention. As a result, what may look like reliable output may actually be of little use in forest management. Moreover, most hazard model outputs are considered independently of other model outputs. For example, statistical and deterministic modeling approaches have been developed that are more quantitative and physically-based, respectively, than the earlier qualitative models. Often, these quantitative/deterministic models are assumed to provide better results than qualitative models. The major goal of this study is to provide an assessment of relative model behavior and error potential in a forest management context to determine whether certain modeling approaches are actually better than others at predicting instability. To achieve this goal, the following objectives have been defined:

1) Develop and evaluate the model classifications of three of the most common medium-scale GIS methods for modeling landslide susceptibility;
2) Validate each output with existing landslide inventories in the Blue Ridge, and;
3) Assess the relative sensitivity of each method to variations in source data.

The methodology used will be designed to provide a standardized technique for model comparisons and to provide maximum benefit to individuals from different regions by using the most transportable methods and data requirements. The outputs of this research will be the determination of the most suitable modeling approach for predicting hazard in the Blue Ridge, production of hazard maps for the Blue Ridge and automation of the various models.

CHAPTER 2. LITERATURE REVIEW

Fundamental to the determination of landslide susceptibility is the clarification of definitions and terminologies. Although the zonation of landslide susceptibility has been attempted in numerous countries including China (Dai and Lee, 2002a; 2002b; Wu *et al.*, 2001), Taiwan (Lin and Tung, 2003; Lin *et al.*, 2002), Italy (Carrara *et al.*, 1991; Carrara *et al.*, 1995a; Carro *et al.*, 2003; Clerici *et al.*, 2002; Guzzetti *et al.*, 1999; Turrini and Visintainer, 1998), Colombia (Chung *et al.*, 1995; Leroi *et al.*, 1992; van Westen, 1994; van Westen *et al.*, 1997), the United States (Chen, 1990; Dietrich *et al.*, 2001; Gritzner *et al.*, 2001; Ohlmacher and Davis, 2003) and several countries in the Himalayas (Anbalagan, 1992; Anbalagan and Singh, 1996; Saha *et al.*, 2002), there still remains some disagreement concerning terminology. Moreover, terms that relate to landslides in one language may lose some clarity in translation to another language. The following section reviews some of the leading definitions and presents a classification scheme by Cruden and Varnes (1996) that has been accepted throughout the literature.

2.1 TERMINOLOGY

The first important distinction to be made is the difference between slope instability and a movement of the earth. Many authors use the phrase *slope instability* to describe an active process of movement; however, the phrase *slope instability* more appropriately refers to the predisposition or propensity of a slope to an active movement (i.e. the conditions leading to the event) (Crozier, 1984; 1986). One phrase used frequently as a general heading for movement is *mass movement*. This is defined as the "outward or downward gravitational movement of earth material without the aid of running water as a transportational agent" (Crozier, 1986). This heading includes acts of subsidence (Crozier, 1986) and will therefore not be used here to define hazard zonation. A more apt heading might be the use of *slope movement* as a general category because, as Varnes (1978) notes, it implies an exclusion of subsidence and other ground sinkage.

One of the most common terms, *landslide*, is probably the most ambiguous. The majority of works have used the term landslide as a general classification for almost all movements regardless of the presence of actual sliding. The leading definitions of the term landslide are:

1. The perceptible downward sliding or falling of a relatively dry mass of earth, rock, or mixture of the two (Sharpe, 1938).
2. Downward and outward movement of slope-forming materials composed of natural rock, soils, artificial fills, or combinations of these materials (Varnes, 1958).
3. Rapid movements of sliding rocks, separated from the underlying stationary part of the slope by a definite plane of separation (Zaruba and Mencl, 1982).

4. The movement of a mass of rock, debris or earth down a slope (Cruden, 1991).

Although likely to be used for years to come, the term is a bit misleading in that landslides can refer to an individual process as well as a broad classification that may include some events that include little or no sliding actions (Crozier, 1986; Varnes, 1978; 1984). In the definitions listed above, only Zaruba and Mencl (1982) require the strict sliding of materials over a plane. Reference has also been made to the additional confusion that exists when referring to the movement of slope material versus the actual landslide deposit (Cruden, 1991). Attempts at clarifications of this term have been made (Varnes, 1978); however, the term has a strong presence when referring to all movements. There is, however, some general agreement among some of the leading authors about what constitutes a landslide. In 1977, Coates summarized these primary points as shown below:

1. Landslides represent one category of phenomena included under the general heading of mass movements.
2. Gravity is the principal force involved.
3. Movement must be moderately rapid, because creep is too slow to be included as landsliding.
4. Movement may include falling, sliding and flowing.
5. The plane or zone of movement is not identical with a fault.
6. Movement should be down and out with a free face, thus excluding subsidence.
7. The displaced material has well-defined boundaries and usually involves only limited portions of the hillside.
8. The displaced material may include parts of the regolith and (or) bedrock.
9. Frozen ground phenomena are usually excluded as landslides (Hutchinson, 1968; Varnes, 1958), although Zaruba and Mencl (1982) devoted nearly a page to discussion of solifluction.

Based on the above principles, this paper will use the term landslide as a general heading for all movements as well as a specific process.

The classification presented in Table 1 is a widely accepted scheme suggested in Cruden and Varnes (1996) which is a slightly modified version of the scheme presented by Varnes in the 1978 Transportation Research Board's Special Report 176: *Slope Movement Types and Processes*. The classification is based primarily on the type of movement and secondarily on the type of material. Five main groups including *falls, topples, slides, lateral spreads and flows* constitute the types of movements. Type of material is divided into *rock, debris and earth* while movements of snow and ice are excluded from the classification. For a detailed description of the types and processes, the reader is referred to Cruden and Varnes (1996).

Table 1. Abbreviated classification of slope movements

TYPE OF MOVEMENT	TYPE OF MATERIAL		
	BEDROCK	ENGINEERING SOILS	
		Predominantly coarse	Predominantly fine
FALLS	Rock fall	Debris fall	Earth fall
TOPPLES	Rock topple	Debris topple	Earth topple
SLIDES	Rock slide	Debris slide	Earth slide
LATERAL SPREADS	Rock spread	Debris spread	Earth spread
FLOWS	Rock flow	Debris flow	Earth flow

Reprinted with permission from "Landslides: Investigation and Mitigation" by the National Academy of Sciences, courtesy of the National Academy Press, Washington, D.C. (see Cruden and Varnes, 1996)

When referring to natural hazards, an active process such as a landslide becomes a hazard when people, properties or social well-beings are endangered. Landslide *hazard* is defined as the "probability of occurrence within a specified period of time and within a given area of a potentially damaging phenomenon" (Varnes, 1984). This definition incorporates both a spatial and a temporal scale. The *zonation* of this hazard refers to the "division of the land surface into areas and the ranking of these areas according to degrees of actual or potential hazard from landslides or other mass movements on slopes" (Varnes, 1984). Because landslides, on a regional scale, are triggered by the recurrence of external factors (e.g. earthquakes, antecedent rainfall) whose timings are difficult to relate to the spatial geomorphic or geologic features causing landslides, most hazard studies have focused on the areal zonation of relative hazard degree (Carrara *et al.*, 1995a; Soeters and van Westen, 1996). There are, however, some attempts to develop a complete landslide hazard map which include a temporal component (Glade, 2001). This approach necessitates the need for historical landslide data as well as recurrence intervals for seismic events and antecedent rainfall conditions.

The final map of landslide hazard zonation shows the spatial distribution of relative landslide hazard and is often termed a *susceptibility map* (Brabb, 1984; Hansen, 1984). Susceptibility maps essentially indicate those areas that contain conditions that are more or less likely to lead to landslides. In light of this, and because landslide hazard zonation incorporates a temporal scale, the term *slope instability zonation* is proposed here to refer to delineation of the spatial distribution of those slopes with a propensity to landsliding without regard to a prediction of recurrence. The use of this final product can aid in the strategic planning phase of forest harvesting.

2.2 CAUSAL FACTORS

In any slope instability analysis, it is essential to have a good knowledge of the mechanisms of landslides in order to identify the main factors for the analysis. The initiation of landslides is due to a wide and diverse set of factors interacting in complex ways. Because the processes involved happen in a continuous manner from cause to effect (Varnes, 1978), it is likely that no one cause is the single factor in landsliding. There is, however, a distinction between the inherent conditions that affect the stability of

a slope (causal factors) and the processes that act upon those conditions (triggering factors).

Following this approach, Varnes (1984) lists four factors or conditions that affect stability: *geologic, geomorphic, hydrologic and vegetation* (Figure 1). Some authors include other factors such as *soil properties* and *seismicity* (Sidle *et al.*, 1985). Seismicity, however, is more appropriately grouped as a triggering factor as described later. As noted before, these factors interact in various complex ways and to give distinct groupings is often difficult. A complete review of the conditions and causes of landslides is beyond the scope of this paper; therefore, only a brief discussion is presented below to identify the main factors needed for slope instability zonation and the processes that may alter them.

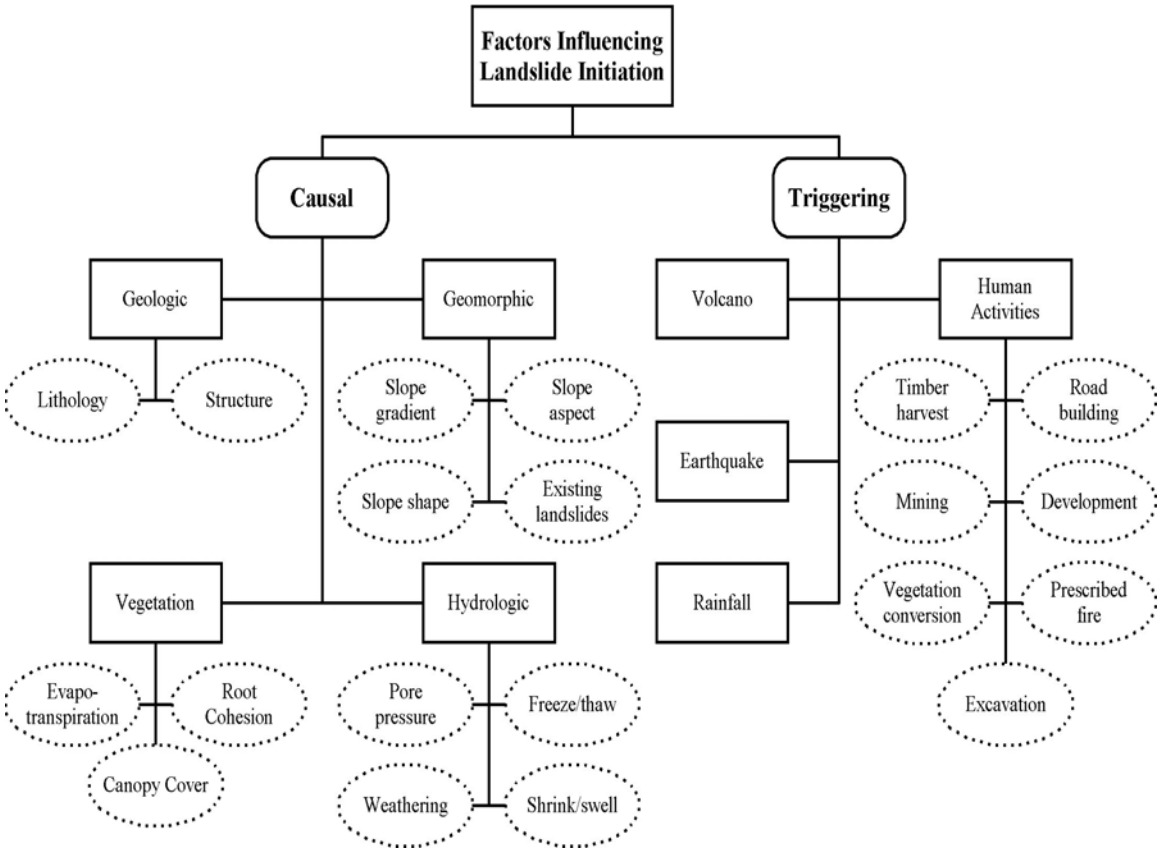

Figure 1. Overview of the various factors influencing landslide initiation including subclasses of each causal or triggering factor (Varnes, 1984; Wieczorek, 1996).

Landslides occur when the inherent conditions of a slope are changed by certain processes or forces. These processes are grouped into two basic categories: those that *increase the shearing stress* and those that *reduce the shearing strength* (Crozier, 1986; Cruden and Varnes, 1996; Hansen, 1984; Varnes, 1978; 1984). These have been described by Terzaghi (1950) as external and internal controls, respectively. When the shearing stresses equal or exceed the shearing strength, a landslide occurs (Bolt *et al.*, 1975; Crozier, 1986). This approach to instability assessment is called "limiting equilibrium analysis" and is generally expressed as

$$FS = \frac{shear\ strength}{shear\ stress}$$

where the higher the Factor of Safety (FS) the more stable the slope (Crozier, 1986). Shearing stresses can be increased through the removal of the lateral or underlying support, imposition of surcharges (e.g. excessive loads), transitory stresses or uplift and tilting (Cruden and Varnes, 1996; Varnes, 1978).

Shearing strengths can be regarded as initially low or reduced by certain processes. Those factors that lead to an initially low strength are the inherent conditions such as the lithology and structure as described below (Cruden and Varnes, 1996; Varnes, 1978). Shearing strength can be reduced through the removal of root reinforcement (Sidle *et al.*, 1985), weathering of the materials and by the increase in pore pressures (Bolt *et al.*, 1975; Cruden and Varnes, 1996). When pore pressures are raised, frictional resistance within the soil or rock decreases.

2.2.1 Geologic

Geologic conditions are divided into lithology and structure, both of which are critically important components of a regional zonation of slope instability. Because geology influences the formation of soils, the types of vegetation and the hydrologic conditions, it is an important factor for slope instability. *Lithology* refers to the composition of the underlying rock and the characteristics that influence the decomposition of those rocks (Varnes, 1984). Weathering has a large effect on the soil physical properties that control landsliding such as texture, porosity and shrink-swell properties. Weathering processes that decompose the rock act as internal controls that decrease the rock's shearing strength and contribute to a low and/or reduced strength. *Structure* refers to the "inhomogeneity and discontinuity" of the rocks and soils such as faults and folds (Varnes, 1984). The existence of bedding planes, faults, folds and the attitude of the underlying rocks may give rise to instabilities by creating a weakness in the rock or soil, thereby contributing to a low strength.

2.2.2 Geomorphic

Geology is an important factor in slope instabilities; however, because most landslides are shallow (Varnes, 1984), other variables such as geomorphology might be more important in a forest management context. Geomorphic factors include slope shape, aspect, gradient and the existence of previous landslides. The major driving force that affects the shearing stresses in a slope, gravity, is highly correlated to slope gradient. When the slope gradient increases, the gravity and shearing stresses increase as well. Shearing strength can also be affected by the geomorphologic conditions when water collects in the valley bottoms. This creates higher pore water pressures, as described above, and can reduce strength. As discussed in the section on GIS and landslides, these factors are becoming increasingly more accessible and, therefore, are prime factors for slope instability zonation.

2.2.3 Hydrologic

Regional climate conditions and the associated hydrologic conditions are often underrepresented as a factor in the zonation of slope instabilities. Because the conditions are often not well documented in rainfall records or because the spatial distribution of hydrologic conditions is unknown, these factors are often omitted in landslide studies. However, they play an important role in the processes involved in initiating landslides. Hydrologic processes can act upon the other factors by both reducing shearing strength (e.g. increased pore water pressure and weathering) and increasing shearing stress (e.g. freeze-thaw and shrink-swell).

More and more studies are examining the role of hydrology and incorporating that factor into zonation models. Some studies have used past rainfall records in the zonation of instability (Guzzetti *et al.*, 1999) while others use hydrologic models in individual slope stability analyses (Gritzner *et al.*, 2001). The latter are most often associated with deterministic methods as discussed later. In Virginia, Wieczorek *et al*. (2000) developed a rainfall threshold for triggering debris flows in Central Virginia. Although the rainfall events that trigger debris flows in a single area (at least in the Blue Ridge of Virginia) may have a long recurrence interval, the same magnitude event can occur elsewhere in a region every few years. This is important because it may be possible to predict the locations of debris flows in areas not yet affected.

2.2.4 Vegetation

The presence or absence of vegetation on a slope has a number of effects on slope stability. The primary ways vegetation affects stability is through the modification of the soil moisture regime by evapotranspiration and by adding cohesion through root reinforcement (Sidle *et al.*, 1985; Sidle and Wu, 2001). Both of these effects increase the shearing strength of the soil. Other ways vegetation can affect the stability of a slope is through the effects of forest cover. Examples include the interception of climatic agents such as wind and rain that may induce instability, reducing the amount of water hitting the slope surface and contributing to the immobilization of water through the forest floor (Kleim and Skaugset, 2003; Prandini *et al.*, 1977). However, not all vegetation effects are positive. Large trees can apply an enormous amount of surficial weight to a slope and, therefore, increase shearing stresses. In addition, tree roots often penetrate rocks, resulting in fragmented rock pieces that can detach from a slope. To adequately address the issue of slope instability zonation, a comprehensive list of all the factors needs to be utilized; however, rarely are the needed data available at all scales for all locations. Where studies use less than the optimal amount of data, the limitations should be noted and, as always, should be followed by field investigations.

Humans have a profound impact on some of the inherent conditions and processes involved in landslides. In the context of forest management, the primary impacts are timber harvesting and road building. Both of these activities affect each of the inherent conditions in variable ways changing those conditions to increase shearing stresses or reducing shearing strength. Because of their importance, the effects of forest management and landslides are discussed later in this paper.

2.3 TRIGGERING FACTORS

The number of causes and processes affecting slope stability is large; however, there is usually only one triggering factor. A triggering factor is an "external stimulus…that causes near-immediate response in the form of a landslide by rapidly increasing the stresses or by reducing the strength of slope materials" (Wieczorek, 1996). These may include such natural phenomena as earthquakes, volcanic eruptions, intense rainfall or rapid snowmelt and human activities such as excavation for roads (Figure 1). The intensity of a triggering factor is dependent upon how close the processes acting upon the inherent conditions have brought the slope to a state of instability. A small earthquake may trigger a landslide on 'unstable' ground just as easily as a large earthquake triggers a landslide on 'stable' ground. Sometimes, a triggering factor is not needed for a landslide to occur (Wieczorek, 1996).

2.4 FOREST MANAGEMENT AND SLOPE INSTABILITY

Land management activities have been studied widely in the past for their impacts on slope stability in many areas of the world (Glade, 2003; Guthrie, 2002; Jakob, 2000; Montgomery *et al.*, 2000; Sidle, 1992; Sidle and Wu, 2001; Tang *et al.*, 1997; Veblen, 1982). Land management affects slope stability through vegetation conversion, residential development, mining activities, road construction, prescribed fire and timber harvesting (Sidle *et al.*, 1985). Forest management, however, affects slope stability primarily through timber harvesting and road-building. The effects of these activities are usually not seen immediately and are therefore not considered triggering mechanisms; however, they can affect the inherent conditions and bring a stable slope to instability.

Shallow debris slide-avalanche-flow combinations associated with high precipitation are the most frequent landslide types in most steep forested terrains throughout the world (Guthrie, 2002; Jakob, 2000; Montgomery and Dietrich, 1994; Sidle *et al.*, 1985; Sidle, 1992; Sidle and Wu, 2001). Because the focus here is on forest management and its effects, attention will be paid primarily to the shallow landslides that are induced by heavy rainfall and affected by the construction of roads and the removal of vegetation. In south-central Chile, however, seismic vibrations and volcanoes are also frequent causes of more deep-seated landslides (Wright and Mella, 1963).

2.4.1 Roads

Roads and their construction, believed to be the major source of sedimentation from erosion in forest management, are primary factors in the instability of forested terrain. Sidle *et al*. (1985) describes how road construction in forested terrain changes the shearing stresses and strengths associated with instability by "1) adding weight to the slope in the embankment fill, 2) steepening the slope on both cut and fill surfaces, 3) removing support of the cutslope, and 4) rerouting and concentrating road drainage water".

Several studies have noted an increased frequency of landslides related to roads, particularly in the Pacific Northwest of the U.S. On Vancouver Island, Guthrie (2002) found that the relative concentration of road-related landslides increased from 12 to 94

percent for three watersheds over about forty years. Jakob (2000) found that the area affected by road-related debris flows was four times as high as debris flows in natural terrain and six times as high for debris slides. For large transportation routes, engineering techniques can be applied to prevent landslides from occurring; however, these techniques are expensive and may not be feasible for forest managers (Sidle *et al.*, 1985) Therefore, identifying the spatial location of probable failure sites before construction is extremely important to forest managers.

2.4.2 Timber Harvesting

As discussed previously, the primary influences of the removal of vegetation from hillslopes is through the modification of the moisture regime and through the loss of root reinforcement. When vegetation is removed, evapotranspiration is reduced and soil moisture is increased. This is important in dry seasons because the increase in pore water pressures can drastically reduce the shearing strength of the soil; however, during wet seasons this effect in minimized and the primary influence is through the removal of root reinforcement (Sidle and Wu, 2001).

2.5 SLOPE INSTABILITY ZONATION

As noted earlier, there are several approaches to modeling slope instability using GIS that differ in a variety of ways. However, the applications of these modeling approaches are based on fundamental principles that are widely accepted. Moreover, each approach considers some basic modeling issues that are common to all approaches. This section introduces the basic principles and considerations involved in slope instability zonation as well as the various GIS modeling approaches.

2.5.1 Principles

Varnes (1984) has identified at least three principles that are the basis for slope instability studies today. It should be noted that these principles are assumptions based on previous work or taken from other fields such as geology. The first principle is that "*the past and present are the keys to the future*". Under this assumption, landslides in the future are likely to be in the same geologic, geomorphic and hydrologic conditions as those that led to landslides in the past. Varnes (1984) cautions that this assumption may not be applicable if human activities change the landscape and increase the occurrence of landslides, conditions are not identifiable or if the conditions in the future change and their effects cannot be evaluated. It is also important to recognize that the conditions that lead to landsliding in one locale may be completely different from conditions in another locale.

The second principle stems from the first and states that those *conditions that lead to landsliding are relatively well known and can be identified* and most can be mapped. These conditions can then be used to determine the likelihood of future landslide occurrence. The conditions are varied and related in different ways; however, if the processes involved can be understood, then extrapolation from point/site information is possible to wider regions.

The final principle states that the *degrees of hazard can be estimated* or given some qualitative or semi-quantitative measure and weighted according to relative contribution. This allows for the zonation of slope instability through different heuristic, statistic or deterministic methods into varying probabilities (Guzzetti *et al.*, 1999). It is important to note again that these principles are merely assumptions that have gained acceptance in the field of slope instability zonation. As several authors have noted, a major shortcoming in this field is the lack of accuracy evaluation (Brabb, 1984; Carrara *et al.*, 1995a; 1995b; Varnes, 1984) and, as such, the final zonation is always only a preliminary assessment of landsliding and further field investigation should be pursued.

2.5.2 General Considerations

In any slope instability zonation, a few broad aspects must be considered before any analysis of instability is to begin. Consideration of these aspects will influence the area to be studied as well as the methods to be utilized. The first consideration is the scale of the analysis. Generally, three scales are recognized for slope instability analyses: regional, medium and large scales. A review of these scales and their appropriate usage can be found in Soeters and van Westen (1996) and van Westen (1994). Regional scales (i.e. maps at scales < 1:100,000) are used primarily for reconnaissance investigations preceding further study and cover large areas of 1000 km^2 or more. Medium scales (1:25,000 – 1:50,000) cover a few hundred square kilometers or more. They are particularly suited for large engineering works that require some detail about the likelihood of landsliding. Large-scale studies (1:5,000 – 1:15,000) are aimed at site-specific investigations that include the design phase of engineering works and may cover up to tens of square kilometers.

The second general consideration is that of the mapping or sampling unit. The mapping unit is the basis of evaluation and is somewhat dependent upon the method to be utilized. Hansen (1984) defines the mapping unit as a set of ground conditions that differ from the adjacent units across definable boundaries. Mapping units are ideally homogenous within the unit and heterogeneous between units. Guzzetti *et al*. (1999) review the five main groups of mapping units: *grid cells, terrain units, unique-condition units* (UCU), *slope units* and *topographic units*.

Grid cells are squares of predefined size and are the typical unit in a raster-based analysis environment. For each grid cell a value is assigned based upon the various input factors. The *terrain unit* is the geomorphological approach that separates the land into areas of similar material, form or process. The *unique-condition unit*, described in Chung *et al*. (1995), is an approach that is aimed at minimizing the number of mapping units used in many statistical analyses. UCU's utilize the overlay functions of a GIS to assign a unique combination of factors to a single grid cell. Each UCU is a homogenous domain of several different input factors. *Slope units* are hydrological regions between drainage and divide lines. The sub-basins of an area are determined from the divides of the area with two slope units per sub-basin (right and left side of sub-basin). Slope units are subdivided into *topographic units* based on the intersection of contour lines and flow tube boundaries orthogonal to the contours. The advantage of the topographic unit is that the contributing area of upslope elements can be calculated.

One of the most important considerations in the assessment of slope instability is the availability of data such as elevation, soils or vegetation for a particular study area. The amount of data needed can vary drastically ranging from a simple map of landslides to several input factors with several subclasses per factor. Data can be found through previous studies of similar sites, existing maps, remote sensing, field surveys and laboratory tests (Hansen, 1984). While the analysis of slope instability is data-driven, much of the data needed may be too costly for field collection, depending on the amount of time and money available. Moreover, some data parameters, such as soil depth, have such a high spatial variability that collection for any sizable area is essentially impossible. Hence, the availability of existing data is likely the dominant factor in determining the appropriate approach to be used in a slope instability zonation.

2.5.3 GIS Modeling Methods

A number of GIS methods to modeling slope instability have been employed by different investigators throughout the world, all reviewed by a number of comprehensive works outlining the methods (Brabb, 1984; Carrara and Guzzetti, 1995; Guzzetti *et al.*, 1999; Hansen, 1984; Soeters and van Westen, 1996; van Westen, 1994; Varnes, 1984). This section presents a review of the major GIS approaches (Figure 2) and the specific methodologies used throughout the world for slope instability zonation. Each method has its own distinct benefits as well as drawbacks and none have been shown to be the ideal method for all situations; however, the final output for all methods is a map showing relative slope instability as instability classes (e.g. low → high). The type of application as well as the considerations listed before determines the method to be used. Hansen (1984) describes two general approaches to slope instability zonation: *geomorphologic* and *engineering*.

2.5.3.1 Geomorphological Approach

The geomorphological approach is an overall approach to mapping instability that displays the spatial variability of slope instability through either direct or indirect mapping. Direct mapping methods are those that identify the spatial distribution of instability directly from existing landslides and/or specific knowledge of areas of potential instability. Indirect mapping methods are those that use factors relevant to landsliding to estimate potential instability. The geomorphological approach may use any of several different mapping methods that include distribution analyses, heuristic analyses or statistical analyses. The specific geomorphological mapping methods, whether direct or indirect, can be either qualitative or quantitative in nature.

A. DISTRIBUTION ANALYSES

Distribution analyses provide information only for those locations that have been subjected to previous landsliding. A landslide inventory/distribution map provides spatial information on instability directly from the mapping of previous landslides. The analysis of this distribution can lead to the extrapolation to other areas of possible future instabilities and classification into a final instability map (Guzzetti *et al.*, 1999). The

locations of the landslides are usually determined through the interpretation of aerial photographs and/or field surveys, and then digitized directly into an instability map using a GIS. In a GIS, landslide inventories can be accompanied by a table showing different attributes of the landslide such as type of movement, type of material, activity, depth (Soeters and van Westen, 1996) as well as the certainty of identification and direction of movement (Wieczorek, 1984). Most often, inventory maps are an additional piece of information used as input factors and/or validation assessments for the other methods described later. As straightforward as it is to develop, an inventory map is an invaluable component of any slope instability zonation.

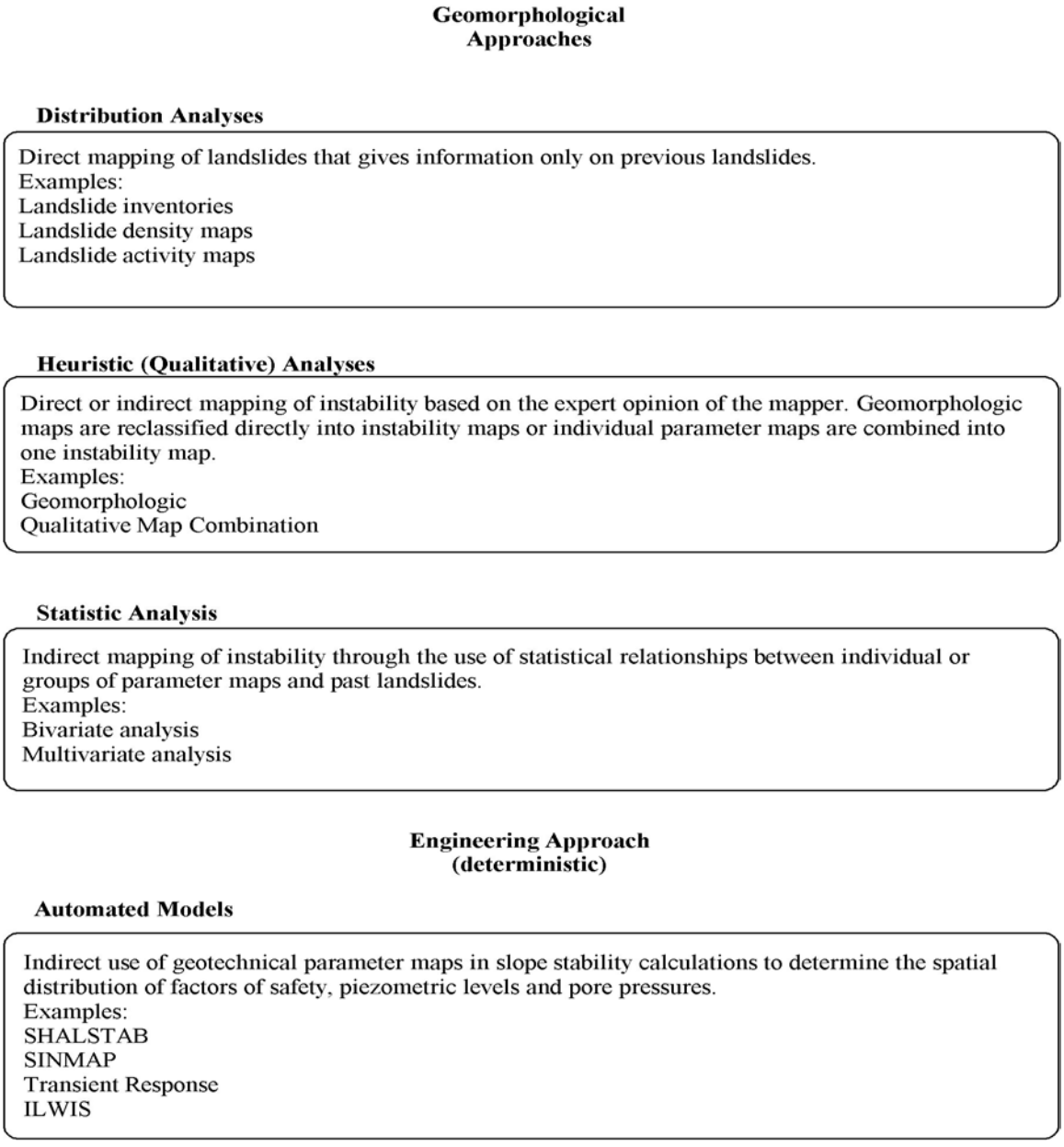

Figure 2. Overview of GIS modeling approaches to slope instability zonation.

An inventory map can also be useful for the development of a landslide density map which depicts the number or percentage of landslides in an area (i.e. the mapping unit). With this method, GIS utilizes overlay functions to allow for rapid calculation of landslide densities within each mapping unit. A special type of landslide density map is the isopleth map in which contours of equal landslide densities are displayed (van Westen, 1994). Another type of inventory map is the landslide activity map. This map is developed with the use of multi-temporal aerial photographs that allow for the analysis of such time-sensitive variables as land use (van Westen, 1994). All of these maps can be used to create instability maps. Because landslide inventories can be time-consuming to conduct and difficult to obtain for large areas, the inventory map is best for medium and large scale projects.

B. HEURISTIC ANALYSES

Heuristic analysis of slope instability can be a direct or indirect qualitative mapping method in which expert opinions, whether the mapper is the expert or the mapper references an expert, are used to develop estimates of slope instability. Heuristic analyses rely heavily on the *a priori* knowledge of landslides and their processes in a region; they can be carried out with either the direct *geomorphologic* mapping method or the indirect *qualitative map combination* method.

A highly qualitative, direct mapping method, geomorphologic mapping uses the expert opinion of the mapper to relate landslide occurrences with landslide processes and associated landforms to evaluate the slope instability. A leader in the development of this method was Kienholz who worked with his colleagues mainly in the Nepal Himalayas. The use of "silent witnesses" (*Stumme Zeugen*), indications of prior morpho-dynamic processes, are used to assess current instabilities (Kienholz, 1977; Kienholz *et al.*, 1984). The method is essentially a site-by-site investigation where the mapper evaluates the potential instability for each site based upon previous experience and various decision rules. The final instability map can be drawn directly in the field or with the display functions of a GIS.

The qualitative map combination (QMC) is a very common indirect method in which the combination of various factor maps is used to obtain one map of slope instability. Each of the factor maps is weighted and then divided into subclasses and weightings are assigned to each subclass. The overlay of the different weighted factor maps and subclass weightings allows for the summation of a relative instability score for each map unit that can then be assigned into different instability classes. In Tasmania, Stevenson (1977) developed an empirical rating system based on his knowledge of the causal factors of landslides. Other rating systems have also been developed in other regions (Saha *et al.*, 2002; Sarkar and Kanungo, 2004). The qualitative map combination has become a very popular method of slope instability zonation due to its ease of use and lack of fieldwork needed to develop a required landslide inventory. The distinction of this method is that a landslide inventory is not needed because the weightings are assigned based on the field knowledge of an experienced geomorphologist. The drawback is that the assignment of weightings is often based upon insufficient field knowledge (van Westen, 1994). The use of GIS for the weighting assignments and overlays has made this method fast and easy to use provided the needed data are available.

Many of the early examples of this method are from the Himalayas where geology and tectonic activity are such that landslides are large, destructive and common. In the Kathgodam-Nainital area of India, Anbalagan (1992) used what is called the *landslide hazard evaluation factor* (LHEF) to assign weightings to factor subclasses. The LHEF weights each subclass with a value, in this case either 0 to 1, or 0 to 2, which automatically weights each factor map as well as the subclass. In the Kumaun Himalaya of India, Anbalagan and Singh (1996) adjusted their model to incorporate a *risk assessment matrix* into their map combination to show potential damage if a landslide does occur. This concept of risk is difficult because of the many indirect and often non-monetary damages associated with landslides. However, the model can provide valuable information in land-use planning. Other studies have also used this concept of risk in slope instability zonation (Carrara *et al.*, 1991; Espizua and Bengochea, 2002).

C. Statistical Analyses

Statistical approaches attempt to use quantitative relationships between past landslides and the environmental conditions that led to them to indirectly predict future landslides in areas with similar environmental conditions under the assumption that the "past and present are the keys to the future" (Soeters and van Westen, 1996). This indirect, quantitative method provides a probability for landslide occurrence, although time is still a factor often omitted. Statistical analyses are popular because they provide a more quantitative analysis of slope instability and have the ability to examine the various effects of each factor on an individual basis. Statistical analyses of slope instability can include bivariate and multivariate methods.

The bivariate methods, as termed by van Westen (1994), are a modified form of the qualitative map combination with the exception that weightings are assigned based upon statistical relationships between past landslides and various factor maps; alternatively, those statistics can be used to develop decision rules (van Westen, 1994). Individual factor maps (independent variable) or combinations of factor maps (e.g. *unique-condition unit*) are overlaid with a landslide map (dependent variable) to develop cross tabulations for each factor and subclass. From this data, weights or decision rules are developed to be applied to each factor subclass. To use weights, normalized values are calculated and summed for a relative instability score that can then be classified much like the QMC. To use decision rules, specific combinations of factors are classified using a matrix of instability classes. An example of the use of decision rules is the *Slope Morphology Model* (SMORPH) which uses only two factors, slope gradient and slope form, to determine instability risks (Shaw and Johnson, 1995). This model was developed to help foresters in the Pacific Northwest develop timber sales on state-trust lands using a single Digital Elevation Model (DEM) as the input.

The main difference among the specific bivariate methods is the manner in which the weights are produced. Conditional analysis, based on Bayes theorem (Morgan, 1968), allows the use of landslide frequency or density data for specific combinations of factors (i.e. *unique-condition unit*) to establish weights. The formal probability is given by

$$LF = P\,(L|UCU) = \text{landslide area/UCU area}$$

where the landslide frequency (LF) within a UCU is equal to the probability of the occurrence of a landslide within that unit. Comparing these probabilities with the average probability within the entire study area allows for the classification of the area into instability classes (Carrara *et al.*, 1995a). Bonham-Carter *et al.* (1990) used conditional analysis to develop the *'weights of evidence'* method for use in mineral exploration. Weights are assigned to the factor subclasses using conditional analysis and "added to the log of the odds of the prior probability, giving the log of the odds of the posterior probability" (van Westen, 1994). The output is once again a relative instability map that can be classified. Clerici *et al.* (2002) used conditional analysis to write a shell script in the GIS GRASS (Geographical Research Analysis Support System) for the quick and repeatable analysis of slope instability. This ability to quickly repeat instability analyses is of particular use in evaluating a variety of factor combinations.

Similar to these methods are the *'information value method'* (Jade and Sarkar, 1993; Yin and Yan, 1988) and *'landslide index method'* (van Westen, 1997b) which use logarithms of the landslide density per factor subclass divided by the landslide density of the entire map as the weight. The weights are then added sequentially for a total hazard score. Gupta and Joshi (1990) also used density data to develop a *landslide nominal risk factor* (LNRF) to define subclass weightings for each of four factors for a catchment in northern India: lithology, land-use, slope aspect and distance from major shear zones. The LNRF was calculated as the ratio of landslide incidences in a subclass to the average incidence in the factor map. Similar numeric weighting factors have been used for other parts of the Himalayas. Other studies simply use the frequency of landslide events per factor subclass to assign a relative weight (Temesgen *et al.*, 2001) while others have used regression and frequency of landslides to assign weightings (Pachauri and Pant, 1992; Pachauri *et al.*, 1998).

Most of the early examples of slope instability zonation using multivariate statistical methods come from Italia, where Carrara and his team used examples from mineral and oil explorations as a template for zonation (Carrara, 1983). Carrara (1983) used both discriminant and regression analysis techniques for the evaluation of stable and unstable grid cells. Subsequent work introduced GIS techniques and, using slope units as the mapping unit, reduced the number of mapping units for a more meaningful inference (Carrara *et al.*, 1991). For each sample unit, whether grid cell, slope unit or the later used *unique-condition unit*, the environmental conditions at that location are crossed with landslide occurrences through the use of GIS then exported to an outside statistical package where the regression is performed. Bringing in the developed equations from the regression to the GIS allows for the calculation of relative instability at each sample unit and the classification into instability classes.

Because a model always fits the sample from which it was developed better than the population, a "learning" set was divided from the population to estimate the model, while a "target" set was used for testing and validation purposes (Carrara *et al.*, 1991). Obviously, for this statistical approach to be effective, enough data on the relevant factors and landslide occurrences needs to be available. This statistical approach is often considered a data-driven method and for the model to work in other regions requires similar geologic and geomorphologic characteristics. Similar studies have used these same techniques in other parts of the world such as the Himalayas (Jade and Sarkar, 1993; Rowbotham and Dudycha, 1998), Spain (Baeza and Corominas, 2001), China (Dai

and Lee, 2002a; 2002b), the United States (Ohlmacher and Davis, 2003) and parts of Italy (Luzi and Pergalani, 1996).

2.5.3.2 Engineering Approach

The second general approach is deterministic and based on the use of "limiting equilibrium analysis" to develop models that determine the distribution of factors of safety, piezometric levels and pore pressures for a given region (Terlien *et al.*, 1995). This is often done by coupling hydrologic models with the various geotechnical parameters necessary to determine the factor of safety (i.e. bulk density, soil depth, etc.). Within a GIS, the model calculates for a certain mapping unit a factor of safety or, in some cases, a threshold needed to reach a factor of safety equal to one (i.e. the point at which a landslide occurs). The output can again be interpreted as a relative indication of instability. Ideally, the geomorphologic approach is done on a regional scale that is then followed up by a detailed engineering approach. Neither of these general approaches is a final assessment of the stability of a slope, rather an indication of the relative instability for use in prioritizing areas for further field study.

Deterministic models calculate slope instability in one, two or three dimensions (Terlien *et al.*, 1995). In one-dimensional models, the infinite slope model (Bolt *et al.*, 1975) is used to calculate instability at individual pixels. Slope profiles are analyzed in two-dimensional models and the entire landslide body is analyzed in three-dimensional models. Hydrological models can also be one, two or three dimension models; however, problems exist for both slope instability and hydrological models when using three dimensions in the conventional two-dimensional GIS (Terlien *et al.*, 1995). For two and three-dimensional instability models, the problem is often the complexity of the calculations whereas the hydrological models have problems converting three-dimensional output maps into forms usable in GIS calculations.

As noted in some studies (Gao, 1993; Shaw and Johnson, 1995) the dominant controls on shallow landsliding in most of the U.S are topographic factors such as slope gradient and slope form (i.e. concave, convex and planar). Based upon this knowledge, Montgomery and Dietrich (1994) developed a model that combined a hydrologic model (O'Loughlin, 1986) with an infinite slope stability equation, the Mohr-Coulomb failure law (Bolt *et al.*, 1975), for the prediction of slope instabilities based upon the minimum amount of steady-state rainfall required to trigger landsliding. With this model, referred to as *Shallow Landsliding Stability Model* (SHALSTAB), the required inputs are obtained from a Digital Elevation Model (DEM) that is widely available within the U.S. and a few representative values of geotechnical parameters such as soil bulk density, internal angle of friction and water table depth. This model calculates pore pressures for steady-state saturated water flow parallel to the slope plane. Another model based upon these same principles is the *Stability Index Mapping* (SINMAP) model developed by Pack *et al*. (1998). The main difference between these two models is that SHALSTAB assumes zero soil cohesion because of the spatial and temporal heterogeneity of soil cohesion (and therefore the difficulty in obtaining values) and because assuming a zero cohesion value results in the most conservative estimate of slope instability (Dietrich *et al.*, 2001). However, new versions of the model do allow for the inclusion of soil cohesion.

Other existing models include the *Transient Response Model* developed by Iverson (2000) that uses unsaturated flow to calculate pore pressures for vertical flow. The International Institute for Aerospace Survey and Earth Sciences (ITC) has developed a GIS called the *Integrated Land and Water Information System* (ILWIS) that has modules incorporated in the GIS for deterministic instability zonation (van Westen, 1997a). The *Level I Stability Analysis* (LISA) prepared for the U.S. Forest Service by Hammond et al. (1992) uses average estimates for geotechnical parameters in their model; however, this model is not spatially explicit.

The previous models were developed in existing GIS packages (i.e. ESRI's ArcView or ILWIS); however, many users may still develop their own zonation models based upon whatever equations or parameters they feel are necessary. For example, van Westen (1994) performed a study in Columbia that utilized the mentioned theories and practices for that specific locale. Here, the equations and parameters are manually input into the GIS to develop instability maps, whereas the existing packages have user-friendly interfaces that automatically develop the maps with only minor input from the user. Either manual or automatic determination of instability with these models will work; however, automation enables more users to access the models.

Some possibilities for the future application of these approaches, whether geomorphological or deterministic, are to use GIS along with a Decision Support System (DSS) to automatically make a decision regarding some aspect of mountain harvesting. In the Northeastern part of the U.S., Davis and Reisinger (1990) developed a model using GIS to evaluate the ability of forest terrain to support harvesting equipment. They incorporated slope angle, soil strength and surface roughness to assign a terrain classification to an area of land. They then used equipment operability criteria to delineate areas appropriate for each harvesting system. This map was then integrated with a DSS to help allocate resources. Decision Support Systems incorporated with GIS are becoming widely used because of the objectivity of automated decisions and the ability to automatically document the entire decision process.

Similar to this model, Visser and Adams (2002) developed a model using GIS to support a DSS in deciding on optimal harvesting equipment allocations when considering debris slide hazard (Shaw and Johnson, 1995), soil compaction and soil erosion hazard. The model, called *Steep Terrain Harvesting Risk Assessment Model* (STHRAM), uses the State Soil Geographic Database (STATSGO) or the Soil Survey Geographic Database (SSURGO) along with DEMs. STHRAM is programmed within the Visual Basic environment of ArcMap™ with a user-friendly interface to make model use as easy as possible. Another GIS/DSS in development is the CONES model conceptualized in Europe. This model uses factors such as harvesting productivity, residual stand damage and stability of the residual stand to decide upon a certain combination of decision alternatives, namely type of harvesting system, location of trails, and silvicultural prescription (Stampfer *et al.*, 2001).

2.6 ERROR AND UNCERTAINTY IN SLOPE INSTABILITY ZONATION

Although many models exist for the zonation of slope instability and studies have been performed throughout the world, little literature exists on the validation of these

studies in terms of the effects of potential GIS uncertainty and error. A GIS is often viewed as a tool that, because of its automation, must be more accurate and better overall as an absolute measure of defining spatial distributions than manual work. Although more consistent, GIS always have uncertainty and error associated with them that make any output prone to a variety of errors. Because GIS deal with the transformation of reality into computer models, uncertainty and error is inherent. The most extensive validation studies have been for the SHALSTAB model (Dietrich *et al.*, 2001; Montgomery *et al.*, 1998) in which accuracy and input data uncertainties are a primary focus. These studies have examined the model for verification of its ability primarily in the Northwest. However, none of these studies has focused on other GIS uncertainties such as algorithm and/or model errors. Studies of algorithmic and modeling errors have compared models of the same method (Carrara *et al.*, 1995a; Morrissey *et al.*, 2001a) or between two different methods (Vaugeois and Shaw, 2000), respectively, for evaluation of accuracy in identifying mountain risk. However, despite these exceptions there have been no other examinations of GIS uncertainty and error for slope instability models.

In the world of academia (particularly in GIS), uncertainty is a common field of study; however, there is a gap between academic research and the application of models to real-world situations. Despite the few acknowledgements of potential error in the previous validation studies, there remains a lack of sensitivity analyses for the models. These sensitivity analyses differ from validation studies in that they focus on "what-if" scenarios of potential GIS error and not just output accuracy. The concept of data models (i.e. the reduction in dimensionality) introduces issues of classification error, varying spatial resolution and geometric representation that typical mountain risk models fail to recognize. Most GIS model users will specify that the output of the model is intended only for preliminary planning and that field work is essential; however, the combination of GIS academic research and forestry field applications have yet to meet in the same arena.

For any mountain harvesting risk assessment there is the great potential for the use of GIS as a preliminary decision-support planning tool. Although the validation studies have included mention of potential error in there analyses, a more in-depth look at the actual error should accompany the model outputs. The goal of any of these models is to assist in real-world applications and, although that goal is ideal, consideration of the potential effects of a wrong decision (i.e. risk) should be included with the models. Aside from including "what-if" scenarios, these models should also be evaluated against other potentially useful models that use differing approaches. Although some general comparisons have been made regarding overall aspects of different approaches, little has been done regarding the output comparison of different approaches. This current study is an attempt at a systematic comparison of the model output from various zonation methods and a general examination of the effects of potential GIS uncertainty and error.

CHAPTER 3. METHODS AND MATERIALS

The main objective of this study is to evaluate the effectiveness of various slope instability zonation methods for use in forest management in the central Appalachian Mountains. The overall procedure is to develop topographically-driven slope instability models using three different methods (Qualitative Map Combination, Bivariate Statistical Analysis and a Deterministic Analysis) for a study area in Madison County, Virginia followed by validation step for a location in Nelson County, Virginia. A subsequent comparison of the three models and their outputs (i.e. instability maps) will be made and analyzed for use in other areas of the Blue Ridge Mountains in Virginia. The first two models will be manually developed in ESRI's[2] ArcGIS 8.3 environment while the third will use the existing automated approach of SHALSTAB (ArcView 3.2). The key issue is the development of a standardized method of comparison for the various models. Sensitivity analyses will also be performed that examine the effects of varying source data on model output.

3.1 STUDY AREA

Virginia has historically been subjected to numerous landslides, in particular debris slides and flows, from the Blue Ridge Mountains to the Alleghenies. Debris flows have occurred in western Virginia (Hack and Goodlett, 1960) and throughout the Blue Ridge including debris flows in Nelson County (Williams and Guy, 1973), Madison County and within the Shenandoah National Park (Morgan and Wieczorek, 1996). On June 27, 1995, a severe storm swept across a portion of Madison County, Virginia, initiating widespread debris flows and floods which caused one fatality and damaged property and the environment (Morgan *et al.*, 1997; Wieczorek *et al.*, 1996). Similarly, Nelson County, Virginia was affected by Hurricane Camille in 1969 that also caused widespread damage and the loss of 150 lives (Wieczorek *et al.*, 2004). A recent assessment of the regional debris flow distribution throughout Virginia and North Carolina shows the most severe event occurring in Nelson County (Wieczorek *et al.*, 2004). These Virginia areas are representative of the type and location of landslides prevalent in the state of Virginia (i.e. shallow debris flows occurring mainly in steep "hollows").

The area of study for the development of the models, about 270 km^2, is situated in the northwest portion of Madison and Greene Counties, Virginia (Figure 3). The area is characteristic of the Blue Ridge of Central Virginia with steep, dissected ridges ranging from 0 to 150 percent in slope and with elevations ranging from about 149 to 1174 meters above mean sea level. The area is primarily rural with most of the landcover consisting of mixed hardwood forest stands. Although the area includes many broad alluvial valleys where farms are situated, the region was logged extensively from 1880 to around 1920 (Wieczorek *et al.*, 2000). This site has also been the focus of extensive fieldwork in recent years and landslide inventories have been developed and used in the development of slope instability zonation maps (Campbell and Chirico, 1999; Morgan *et al.*, 1999b; Morrissey *et al.*, 2001a). However, these evaluations have used only a single method (e.g.

[2] Environmental Systems Research Institute, Redlands, CA

deterministic) to assess instability. Therefore, the Madison County area affected (Figure 3) is used as a study area to develop and evaluate various slope instability zonation methods that can be evaluated for application in other areas of similar geomorphologic characteristics. The validation site will be the area in Nelson County affected by Hurricane Camille (Figure 3). This site is similar to the Madison County site in terms of topographic features.

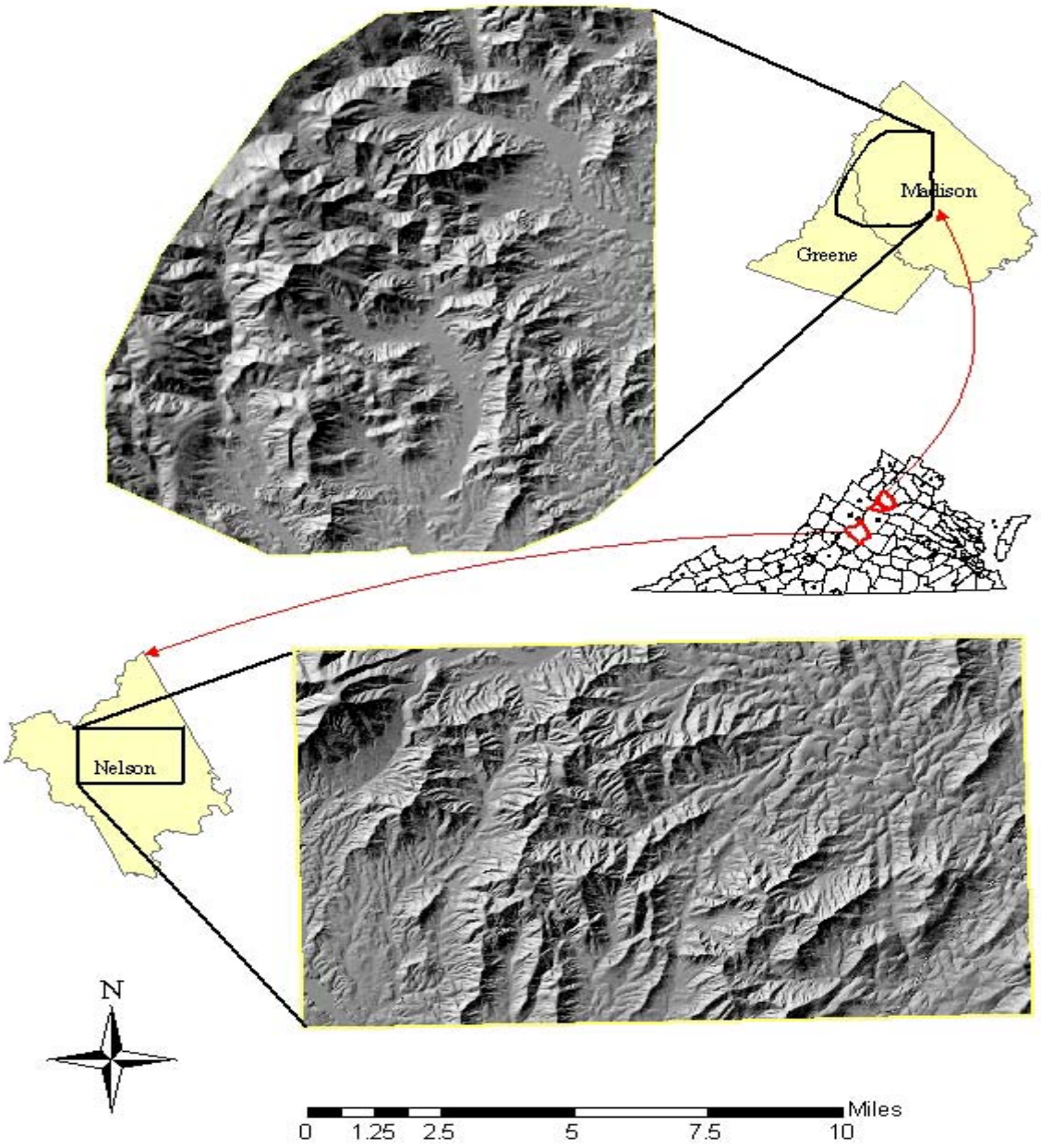

Figure 3. Location of study areas within Madison and Nelson Counties, Virginia (shown with shaded relief maps)

3.2 DATA

For this project, the data used were selected based on three key attributes: *relevance*, *availability* and *scale*. If land managers are to efficiently develop management plans that include attention to slope instability, relevant factors that are readily available are necessary to minimize the time and effort required to develop a slope instability map. Moreover, the scale of analysis needed to identify specific areas for further investigation is an important consideration. The data used in this study are the debris flow inventory prepared by Morgan *et al*. (1999c), the geotechnical data obtained from Morrissey *et al.* (2001b), elevation, soils and roads maps that can be easily downloaded from the Internet or obtained through local agencies. Derivatives from the elevation layer include a slope gradient map, an aspect map and a planform curvature (concave, convex, planar) map.

The analyses are performed in a raster environment (i.e. grid cells) because of the simplicity and ease of use of grid cells in a functional analysis such as overlay. In addition, the comparison of models is made easier with evenly sized grid cells. Moreover, the elevation derivatives are all already in a raster data structure and form a bulk of the factors. Therefore, all vector data will be rasterized to a resolution of 10 meters, the highest resolution of the raster layers. One common factor often used in slope instability analyses, vegetation, will not be used in these models primarily because of the small scale of most common vegetation data. However, the use of vegetation could easily be incorporated into the models as an additional factor with the knowledge that interpretations would be limited to the smallest scale. A primary goal of this study is the creation of medium-scale models and using data at such a small scale as most vegetation data limits the interpretation of the models to that scale.

3.2.1 Elevation Data

Both 10- and 30-meter elevation data are used for this study. The 10-meter elevation layer was compiled from six U.S. Geological Survey (USGS) Digital Elevation Model (DEM) 7.5-minute quadrangles: Big Meadows, Old Rag Mountain, Fletcher, Madison, Stanardsville and Rochelle. These layers are mapped at a scale of 1:24,000. The 30-meter data for Madison County come from the USGS National Elevation Data (NED) also mapped at a scale of 1:24,000. For the purpose of this project, both resolutions will be used to show the effects of uncertainty in digital data representation. All elevation layers are in the Universal Transverse Mercator (UTM) projection using the North American Datum 1927 (NAD27). The six quadrangles were mosaicked together to form one elevation layer. For the validation site in Nelson County, the 10-meter elevation data is comprised of two 7.5-minute quadrangles, Horseshoe Mountain and Lovingston. The 30-meter data for Nelson County is also from NED like the Madison County site.

3.2.2 Soils Data

The decision to use soils data instead of geologic data to model slope instability is largely due to the availability of digital data and the scale of the analysis. For the site in Madison County, digital geologic data at a scale of 1:24,000 exist for only one of six quadrangles encompassing the area (Bailey *et al.*, 2003). Another source of geologic data is a recent publication completed by Morgan *et al.* (2003) characterizing the geology of

the Blue Ridge region of Shenandoah National Park. This report consists of digital geologic data of the entire study area; however, the scale of this data is 1:100,000 and would be inappropriate for a medium scale analysis. Therefore, because of data availability and scale issues, the analyses presented here will be based upon soils data.

There are two primary digital soils databases for states and counties in the U.S.: *STATSGO* and *SSURGO*. These two databases are maintained by what is now known as the U.S. Department of Agriculture's Natural Resources Conservation Service, formerly the Soil Conservation Service. The State Soil Geographic (STATSGO) database covers the entire state but has a scale similar to the geology data by Morgan *et al.* (2003). The Soil Survey Geographic (SSURGO) database contains digital representations of county soil survey maps. The paper survey for Madison County was created in 1975 and mapped at an initial scale of 1:15,840. Madison County SSURGO data were digitized at a scale of 1:24,000. The SSURGO database is available for most counties in a state, including Nelson County, and has varying scales dependent upon the initial mapping of the soil survey. The data for the two counties contain differing soil series and will therefore only be used for the Qualitative Map Combination. This is caused by the problems inherent in the statistical analyses in which statistical relationships for use in instability zonation are dependent upon the existence of the same data existing in both the development and testing areas.

However, because of its almost complete coverage of U.S. counties and its large scale, the SSURGO database will be utilized in the analyses for both Madison and Nelson Counties for the Qualitative Map Combination. Unfortunately, SSURGO data for Greene County is not available and the analyses will not include the part of Greene County where SSURGO is not available. The Nelson County study site is covered entirely by SSURGO data. The data are in ESRI's shapefile format and come in the Albers Conical Equal Area NAD27 projection. They were subsequently re-projected to the UTM NAD27 projection to match the previous datasets. In addition to the shapefiles, the SSURGO database is contained in a Microsoft Access file consisting of the various tables of information associated with the soils.

3.2.3 Roads Data

The road layers for this study come from the USGS Digital Line Graphs (DLG) containing transportation and are mapped at a scale of 1:24,000. The roads in Madison were compiled from the same six 7.5-minute quadrangles as the elevation layer. These layers were developed from the corresponding topographic quadrangles and come in the UTM NAD27 projection. The six quadrangles were first converted from ArcInfo export files (.e00) to ESRI's coverage format then merged together and converted to shapefile format. Finally, to approximate the actual width of a road, the layer was buffered with a distance of 2.5 meters on either side of the line for a total road width of 5 meters. The same procedure is used for the two Nelson County quadrangles.

3.2.4 Debris Flow Inventory

The inventory by Morgan *et al.* (1997; 1999c) was created as an ArcInfo export file (.e00) showing the locations of debris flows and their run-out paths as well as flood

effects from the storm event of 1995 (Figure 4). An additional layer showing the points of debris flow origin was also included. Over 600 debris flow origins have been identified by the highest point of a debris flow polygon. These layers were developed at a scale of 1:24,000 by interpretation of aerial photographs taken approximately 2 months after the storm with subsequent field checks for verification (Morgan et al., 1997; Wieczorek et al., 1996). Both of these layers were converted to ArcInfo coverage format with their original UTM Clarke 1866[3] projections.

The layer showing debris flows and flood effects was queried to identify only debris flows and subsequently exported to a new ESRI shapefile with a UTM NAD27 projection. The point coverage was also exported as an ESRI shapefile with a UTM NAD 27 projection. The result is one layer showing only debris flow polygons and one layer showing debris flow origins.

The inventory for Nelson County (Figure 4) was also created as two export files (.e00) (Morgan et al., 1999a) but came with an existing UTM NAD27 projection so re-projection was unnecessary. They were developed from interpretation of aerial photographs taken in August of 1969 and April of 1971. The two study areas were mapped for debris flows in two different manners. Whereas the Madison County inventory came as one polygon and one point file, the Nelson County inventory consists of a polygon file and an arc file. The polygon file displays the entire debris flow source, path and accumulation zone as one polygon for both counties. The arc file depicts debris flow tracks on the aerial photo too narrow to delineate with an area measurement such as a polygon.

3.2.5 Geotechnical Data

The geotechnical data from Morrissey *et al.* (2001b) that were used in this study include soil properties such as cohesion (N/m^2), internal angle of friction (^{o}), depth to failure plane (m) and bulk density (kg/m^3). These properties were approximated from two colluvial samples located at debris flow origins in the Madison County area and are shown in Table 2 along with the default SHALSTAB values (Morrissey *et al.*, 2001b). Properties for Nelson County are comparable to Madison County as indicated by Morrissey *et al.* (2001b) and Auer (1989) and will therefore be used for both sites. Because geotechnical properties may not be available for all locations, SHALSTAB will also be run with default parameters. SHALSTAB uses these properties along with an elevation layer in its analysis.

Table 2. Soil properties for use in SHALSTAB.

	Madison/Nelson County values	SHALSTAB default values
Friction angle (^{o})	35	35
Bulk Density (kg/m^3)	1200	1700
Cohesion (N/m^2)	1300	2000
Depth (m)	2	1

[3] Clarke 1866 is the ellipsoid upon which the NAD27 is based.

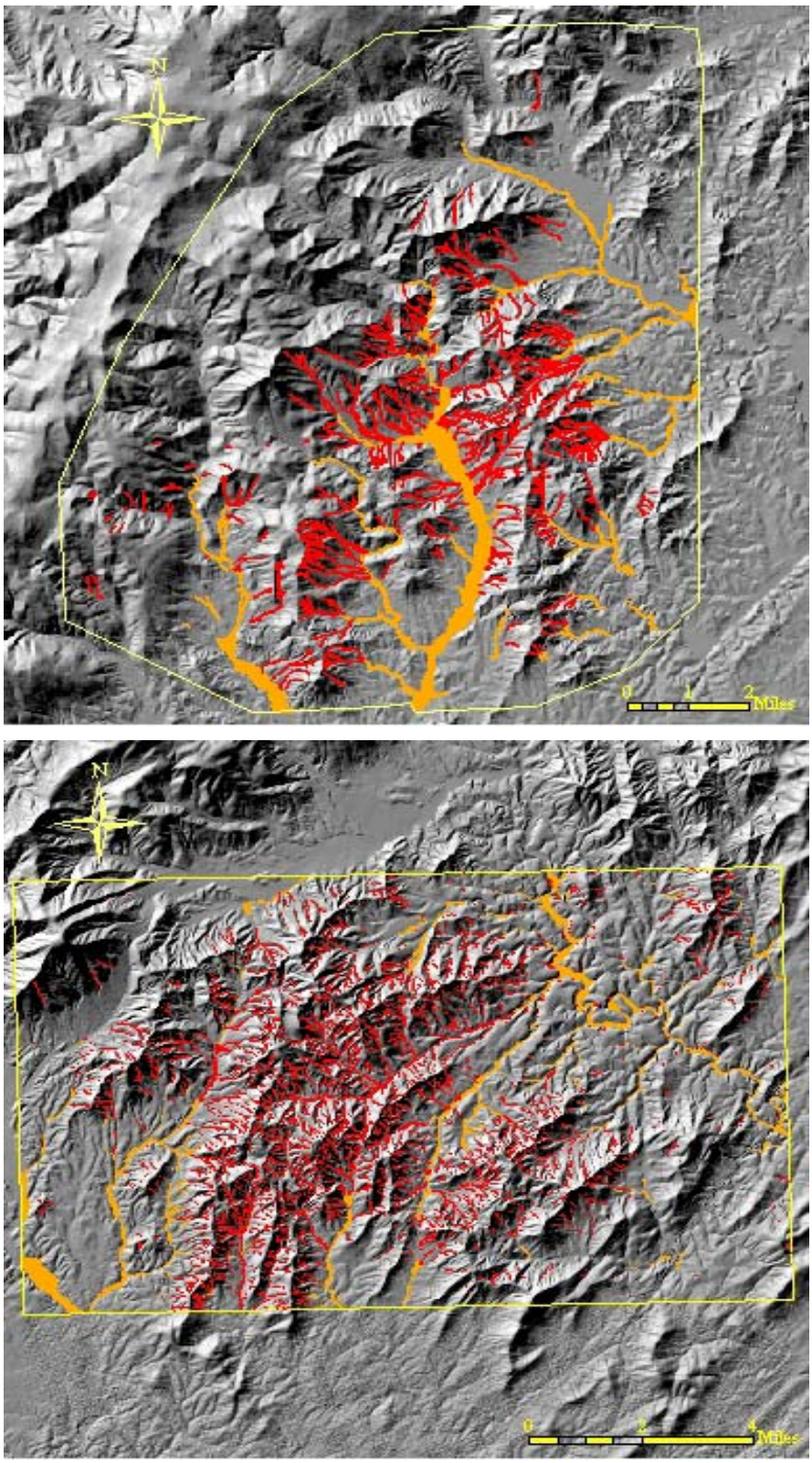

Figure 4. Debris flows and flooding in Madison and Nelson Counties (debris flows in red and flooding in orange).

3.2.6 Hydrography

Water features such as lakes, ponds and large rivers were obtained for this study for the creation of a mask so that certain cells can be excluded from the analyses. Because debris flows do not occur within these large, flat water features they are excluded to avoid any mapping errors such as a debris flow origins being located within a river or lake. The hydrography of both Madison and Nelson Counties were obtained from Digital Line Graphs (DLG) for the same quadrangles as the elevation and roads layers. The format and projection of the hydrography layers are the same as the roads layers. Large streams and other smaller intermittent streams are not included with the hydrography layers, only the large flat features such as lakes and ponds.

3.3 MODEL DEVELOPMENT

This section will outline the procedures used to develop the models, standardize the model outputs and develop management classifications of instability. The primary goal of model development in Madison County is to derive the thresholds that define instability classifications. In addition, weightings for the Bivariate Statistical model are developed for use in Nelson County as well as other areas. All of the models will be developed at a scale of 1:24,000 and will use the grid cell as the mapping unit.

3.3.1 Development of factor maps

The various factors and factor maps used as input to the models are shown in Table 3. The Qualitative Map Combination (QMC) uses elevation, soil and road data to create the factor maps. The Bivariate Statistical Analysis (BVS) will use the elevation and road datasets as well as the landslide inventory. SHALSTAB uses only one input dataset and is discussed separately from the first two models. From four to five factor maps and the landslide inventory are created (three from the elevation layer) for use in the QMC and BVS overlays.

Table 3. Factor maps used as input to the various model runs.

	Model Run					
Input factors	QMC Run 1	QMC Run2	QMC Run3	BVS Run 1	SHALSTAB Run 1	SHALSTAB Run 2
Slope	✓	✓	✓	✓	✓	✓
Aspect	✓	✓	✓	✓		
Curvature	✓	✓	✓	✓		
Distance to roads	✓	✓	✓	✓		
Soils	✓	✓				
Upslope Contributing Area					✓	✓
Geotechnical Data					✓	✓

Using the ArcGIS Spatial Analyst extension, slope gradient, slope aspect and slope planform curvature are created from the elevation layer. While slope and aspect are programmed functions in ArcGIS, planform curvature is created using the Raster Calculator and the following syntax: *curvature([elevation], #, plancurv)*. Two of these factors are perhaps the most important layers in the analyses because of the many published reports suggesting that slope gradient and curvature are the primary factors involved in rainfall-induced landsliding in this region (Sidle *et al.*, 1985). The importance of aspect in slope instability may be linked to the increased soil moisture levels on certain slopes (Gao, 1993).

Because these layers consist of continuous data, they will need to be reclassified into discrete subclasses. These subclasses are somewhat subjective but are based upon previous studies in the area and are shown in Table 4. The subjectivity of subclass division is always present and will continue to be the most subjective aspect of most slope instability zonation projects. However, using some consistency in different study areas may help reduce the effects of subjectivity. Both the QMC and BVS analyses will use the same subclasses for consistency. Slope output is measured in degrees and divided into five subclasses while slope curvature is measured in 1/100 z units and divided into three subclasses. The slope subclasses used for this analysis follow the subclasses used by Campbell and Chirico (1999) in Madison County. According to ESRI, a positive curvature output indicates an upwardly convex slope and a negative output indicates concavity. A curvature of zero is interpreted as planar. Aspect is also measured in degrees and divided into eight default ESRI subclasses with an additional subclass for flat areas.

Table 4. Subclass breakdowns for DEM derivatives.

Slope (degrees)	**Slope Subclass and number**	**Aspect degree**	**Aspect Subclass and number**	**Curvature**	**Curvature Subclass and number**
0 - 14	Flat (1)	-1	Flat (1)	< 0	Concave (1)
14.01 - 26	Gentle (2)	337.5 - 22.5	N (2)	0	Planar (2)
26.01 – 34	Moderate (3)	22.5 - 67.5	NE (3)	> 0	Convex (3)
34.01 - 45	Steep (4)	67.5 - 112.5	E (4)		
> 45.01	Very Steep (5)	112.5 - 157.5	SE (5)		
		157.5 - 202.5	S (6)		
		202.5 - 247.5	SW (7)		
		247.5 - 292.5	W (8)		
		292.5 - 337.5	NW (9)		

Because debris flows often originate from or near roads, a raster layer containing the Euclidian distance to each road was created using the SA extension with the same cell size as the elevation (10m). This fourth factor map was reclassified into two discrete subclasses, less than or equal to 50 meters and greater than 50 meters. Again, it should be noted that the subdivision of factor maps is subjective and the subclass designations can be altered. An automated version of the QMC is being developed that allows for the manipulation of factor subclasses.

The fifth factor map, soil type, is derived from the SSURGO shapefiles which show the spatial distribution of individual phases of a soil series. Each phase is represented as a set of polygon features referred to as map units and accompanied by an attribute table.

The table contains each map unit's identifying code and symbol named 'MUKEY' and 'MUSYM', respectively. The SSURGO data was first clipped to the boundary of the study area (which is only the Madison County portion) and then dissolved into new map units based upon the first two letters of the 'MUSYM' code. This essentially aggregates map units that have the same phase but different slope classes into one new map unit. For example, the *'Elioak loam, 2 to 7 percent slopes, eroded'* map unit and *'Elioak loam, 7 to 15 percent slopes, eroded'* map unit have symbols *'EmB2'* and *'EmC2'*, respectively. By aggregating the map unit based upon the first two letters of the 'MUSYM', the result is a grouping of all the map units of an *'Elioak loam'* soil into one new map unit (i.e. *'Elioak loam' or 'Em"*). This new map unit contains all the slope classes of a particular phase. The purpose of this step is to eliminate the use of a slope factor twice in the models. These five factor maps along with the landslide inventory discussed below will be the input to the models.

The major issue concerning the use of the landslide inventory is the style in which the mapping was done. For example, one polygon in the coverage represents a debris flow source area, run-out path and depositional area as being grouped together. Because the inventory is the only such dataset for the area this issue cannot be avoided. Therefore, since there is no way to separate the source area from the rest of the debris flow tract and depositional area, the point coverage of origins will be used to represent debris flow source areas for the analysis. However, because points are being used to represent a source 'area' (typically the highest elevation in a debris flow polygon), the analysis will use a raster layer showing all cells within a specified distance of the point (15 meters) to account for using points to represent polygons.

There are two potential methods for including cells within a specified distance of the points. The first method involves creating a buffer with a specified radius around the points and then converting the vector circle to a raster layer (Figure 5). The second method would be to run a distance function using the points as a source and then reclassifying all resulting raster cells within the specified distance to a unique value (Figure 5). The two methods will produce different results concerning the number of cells affected by debris flow activity and, thus, different validation results. When converting the buffer layer (15m) to a raster layer, the number of cells affected by a debris flow point ranges from 4 to 9 with an average of about 7 (7 10-meter grid cells = .173 acres). When running the distance function and reclassifying the result, the number of cells affected by a debris flow point is 9 (9 10-meter grid cells = .222 acres). Therefore, to most closely approximate the actual area within 15 m. of a point (≈ .17 acres), the first method will be used.

Unfortunately, the Nelson county debris flow inventory does not consist of a point layer that can be used to represent source areas. Therefore, the validation of the models in Nelson County will use the polygon layer and a buffered arc layer. The buffer will use the same distance as the Madison County point layer. The use of the polygon layer and buffered arc layer for validation of the models is a limitation to any interpretation of the models but is the best available data. Until standard methods of mapping debris flows are used universally, these limitations will continue to exist.

Finally, a mask layer is created to identify the study area to be included in the analyses. This layer is essentially a raster layer of the study area with the exclusion of hydrography cells that are large, flat expanses of water. In addition, the study area for

Madison County encompasses a portion of Greene County that is not included in the SSURGO data. Therefore, the Madison County study area will only include the portion that contains SSURGO data for use in the Qualitative Map Combination. The Bivariate Statistical Analysis and SHALSTAB could use the entire Madison/Greene study area but, for consistency, will only use the Madison County portion. For Nelson County, the mask will include the entire study area of both quadrangles. The study area is simply the boundary of the quadrangles. The mask for Nelson County is created in the same manner as that for Madison County.

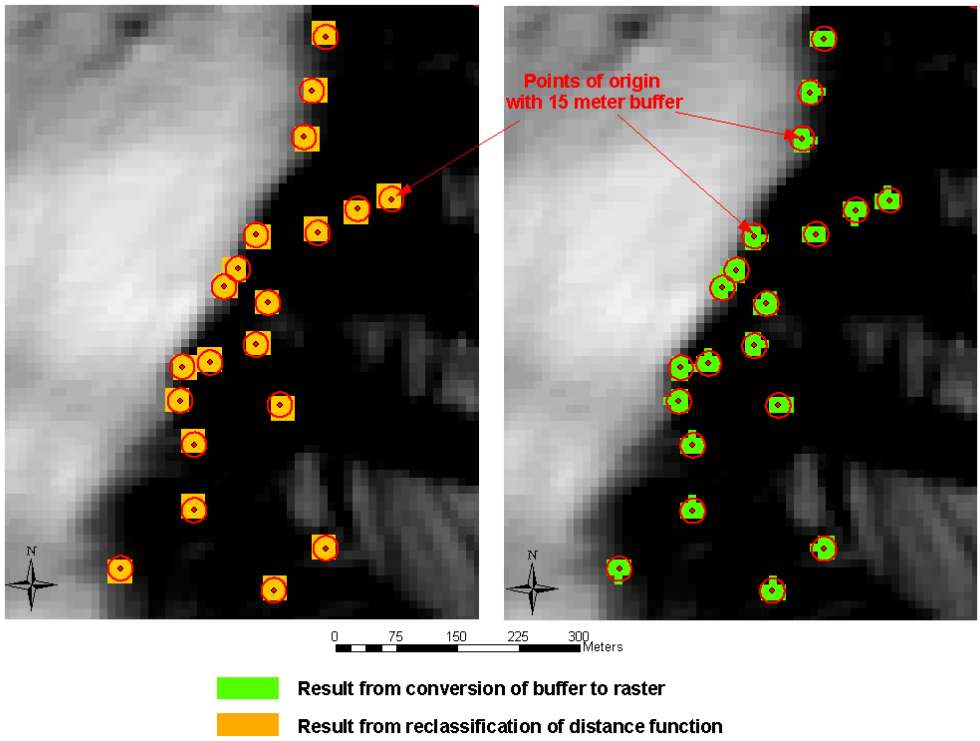

Figure 5. Buffer conversion of debris flow origins.

First, the study areas are converted to raster layers with a 10-meter resolution. This layer shows a value of '1' within the boundaries and a value of 'NoData' outside the boundaries. The hydrography DLGs are then converted to a raster layer with a 10-meter resolution. This layer shows a value of '1' where a water feature occurs and a value of 'NoData' elsewhere. The values were subsequently reversed to show a 'NoData' value where these water features occur. This new layer is then crossed with the study area for a final mask.

3.3.2 Qualitative Map Combination (QMC)

Once the factor maps are created, the method for qualitative map combination is very straightforward and can be applied easily to anywhere in the state as long as a good knowledge of the influence of the various factors are known. The mapping unit for this

method will be the grid cell. The basic steps of this model are 1) classification of each factor map into discrete categorical subclasses (already done), 2) weight each factor subclass (e.g. on as scale of 1 to 10), 3) weight the overall factors, and 4) overlay the various weighted maps using addition for a numeric map of instability (van Westen, 1994). The final product will have, for each grid cell, a score that will have a range based upon the weights assigned. An overview of the procedure is given in Figure 6. An important note about this model is that no debris flow inventory is needed for analysis. The inventory will, however, be used for development of instability classifications.

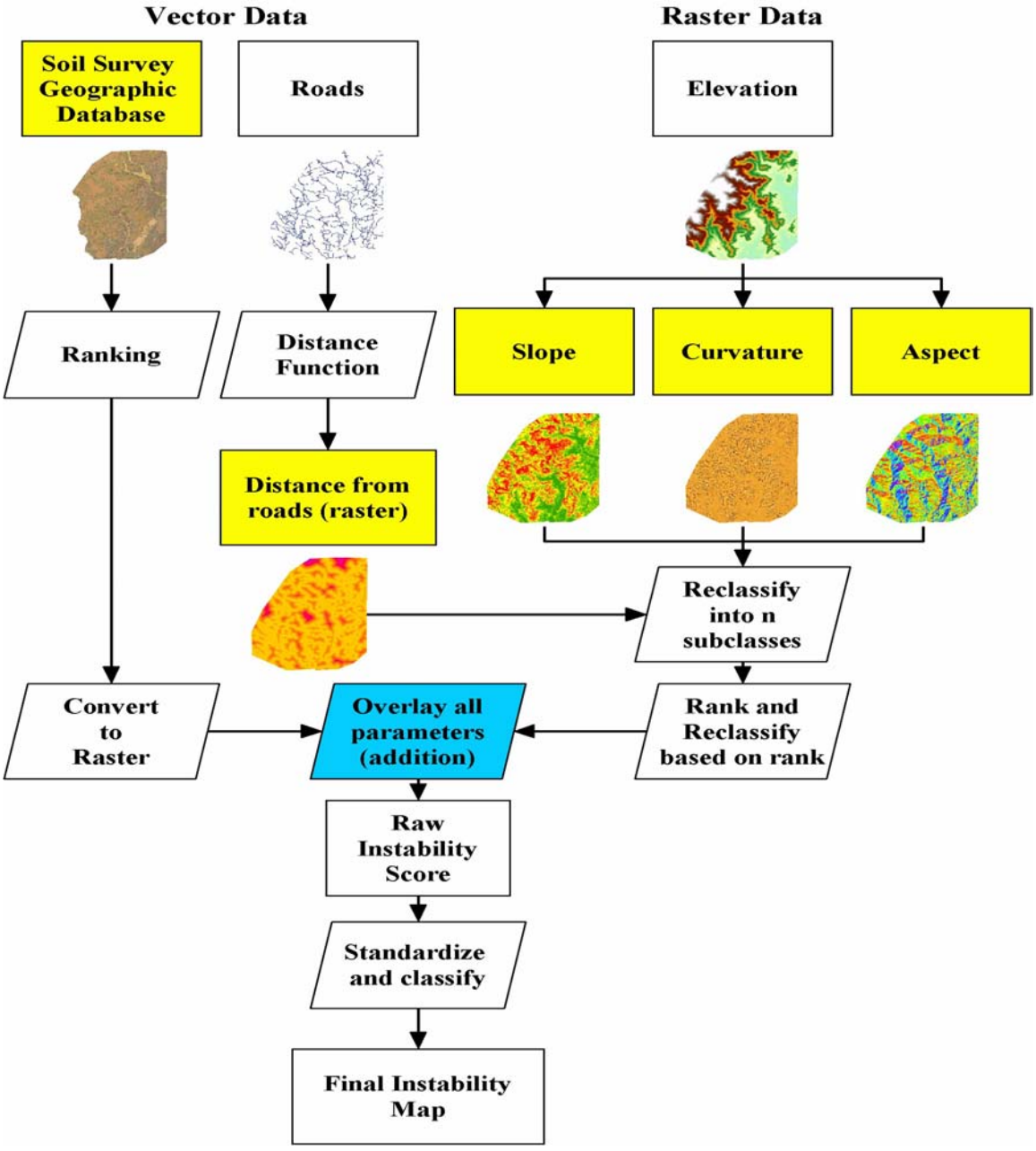

Figure 6. Overview of the Qualitative Map Combination analysis (factors shown in yellow boxes).

For this method, research on the various factors comprises the bulk of the work for the assignment of weights to the various subclasses. The weights used for the slope, aspect, curvature, SSURGO and roads factor maps are shown in Table 5. The basis for these weights is from a study done using the Nelson County 1969 landslide event (Gao, 1993), studies of road effects on debris flow initiation (Guthrie, 2002; Jakob, 2000) and basic knowledge of debris flow initiation in forested landscapes. An important aspect of this analysis is that these weights, although based upon previous studies that may have developed statistics for the debris flows, are subjective in nature because they are derived from empirical studies of the causal factors.

Table 5. Weights for the qualitative map combination (Weights in parenthesis were used in a second run of the model).

Factor Map	Subclasses	Factor Weight	Subclass Weight
Slope	1. 0^o - 14^o	2	2
	2. 14.01^o - 26^o		4
	3. 26.01^o - 34^o		10 (6)
	4. 34.01^o - 45^o		8 (10)
	5. > 45.01^o		6 (8)
Curvature	1. Concave	2	10
	2. Planar		5 (4)
	3. Convex		4 (5)
Aspect	1. Flat	1	0
	2. North		7
	3. Northeast		8
	4. East		2
	5. Southeast		3
	6. South		4
	7. Southwest		2
	8. West		8
	9. Northwest		10
Dist. To Road	1. < 50 m	1	5
	2. > 50 m		1
SSURGO[a]	1. GW, GP, GM, SW, SP, SM	1	10
	2. SC-SM, GC-GM		7
	3. GC, SC, ML, OH, OL, Pt		5
	4. CL-ML		3
	5. MH, CL, CH		1

[a]Weights for individual soils are shown in Appendices A and B; also see Table 6 for explanation of groups.

There are two important concepts concerning the weighting of the slope and aspect factor subclasses. First, the fifth slope class has been assigned a lower weight than the fourth subclass. This is due to the fact that on such steep slopes there is often little soil material and therefore there is little to no debris flow material. Second, aspect in this region influences soil moisture and subsequently pore pressures such that wetter slopes have higher instability. On south and southwestern slopes there is more solar heat and therefore less soil moisture. However, the fact that the Blue Ridge Mountains have a

general NE-SW ridgeline may influence the importance of these aspect classes in such a way as to indicate more instability on western and eastern slopes because there are fewer northern and southern slopes.

The weighting for SSURGO data involves querying the MS Access databases for the Unified Classification Group (UCG) used to represent the lowest soil horizon above bedrock. The Unified Soil Classification system is a system used to classify mineral and organo-mineral soils for engineering purposes based on particle-size distribution, liquid limit and plasticity index (ASTM, 2001; U.S. Dept of Agriculture, 2003). The use of this system to weight soil map units in this study is due to the lack of information in the SSURGO database relating to landslide initiation. Mobilization of debris flows occur in loose, contractive soils such as coarse-grained colluvial soils with low clay content (Ellen and Fleming, 1987; Wieczorek *et al.*, 2000). Based upon this knowledge, those soil map units having a more coarse-grained texture and a low liquid limit (i.e. the moisture content when a soil flows like a liquid) in the soil horizon just above bedrock are assumed to be more susceptible to debris flow initiation. The Unified groups are shown in Table 6. Those Unified groups that contain two different groups (e.g. SC-SM) consist of soils with properties of both groups.

This model will be performed three times using various combinations of weights in Madison County. An overview of the model runs are given later in Chapter 3.3.5. The factor weights will be the same on all three runs; however, the second run will use different subclass weights and the third run will use the subclass weights of Run 2 with the exclusion of SSURGO data. The raw instability scores range from 14 to 65 for the first two model runs and from 13 to 55 for the third run. These factors will also be used in the same three model runs using 30-meter elevation data in Madison County. However, only the elevation data will consist of 30-meter data because the roads and soil vector maps are rasterized with the highest resolution. The 30-meter elevation data is the actual source data and will, therefore, create only the slope, aspect and curvature factor maps with that resolution. There will be a total of six model runs using the QMC approach.

The query for the Unified Classification Group for SSURGO weighting involves joining various tables from the database to acquire a representative value of the UCG. The SSURGO spatial features are in the form of map units as described earlier. These map units are composed of one or more ‘components’ that are then made up of several ‘layers’ corresponding to soil horizons. Several UCGs are assigned to each ‘layer’; however, one UCG is considered representative of the layer. In order to assign one representative value to each map unit it is necessary to work from the layer up to the map unit. First, the bottom horizon is identified and the representative value for that layer is obtained. If no value for the bottom horizon is identified then the horizon directly above bedrock is used. The value for this horizon is assigned to the component to which it belongs and subsequently weighted based upon Table 5.

Since there can be multiple components in a map unit, the most conservative estimate is given by assigning the most susceptible value from the various components to an individual map unit. Once this is complete, a manual check of the weights compared to the description of each map unit is performed to eliminate unrealistic weights. For instance, many of the soils occurring in stream bottoms or terraces have very coarse textures deep in the soil profile. These soils are often assigned a coarse-textured Unified Group (e.g. GW). However, assuming that debris flows will not occur in valley bottoms

(because of flat slopes) the weights given to stream bottom soils are adjusted to a lower weight (i.e. '1'). The weightings assigned to each soil map unit are given in Appendices A and B.

Table 6. Unified Classification Groups (ASTM, 2001; U.S. Dept of Agriculture, 2003)

Criteria				**Soil Classification**	
Major Divisions				**Group Symbol and Weight**	**Group Name**
Coarse-grained soils; more than 50% retained on No. 200 sieve	Gravel; more than 50% of coarse fraction retained on No. 4 sieve	Clean gravel; less than 5% fines	Well graded	GW (10)	Well-graded gravel
			Poorly graded	GP (10)	Poorly graded gravel
		Dirty gravel; more than 12% fines	Non-plastic fines	GM (10)	Silty gravel
		More than 12% fines	Plastic fines	GC (5)	Clayey gravel
	Sands; 50% or more of coarse fraction passes thru No. 4 sieve	Clean sands; less than 5% fines	Well graded	SW (10)	Well-graded sand
			Poorly graded	SP (10)	Poorly graded sand
		Dirty sands; more than 12% fines	Non-plastic fines	SM (10)	Silty sand
			Plastic fines	SC (5)	Clayey sands
Fine-grained soils; 50% or more passes the No. 200 sieve	Silts and clays; Liquid Limit less than 50%	Inorganic	Medium Plasticity	CL (1)	Lean clay
			Low plasticity	ML (5)	Silt
		Organic	Low plasticity	OL (5)	Organic silts and clays
	Silts and clays; Liquid Limit greater than or equal to 50%	Inorganic	High plasticity	CH (1)	Fat clay
			Medium Plasticity	MH (1)	Elastic silt
		Organic	Medium to high plasticity	OH (5)	Organic silts and clays
Highly organic soils				PT (5)	Peat

Once the weights have been identified, the data layers are reclassified into new layers based upon the subclass weight to which each grid cell belongs. For SSURGO data, this involves converting the vector maps to raster maps based upon the weighting.

Finally, using the Raster Calculator, the reclassified data layers will be crossed using arithmetic overlays and the raw instability score, *Y*, will be calculated for each grid cell. For each grid cell, *k*, having a particular combination of factor subclasses, the instability score, Y_{ijk}, at that cell is calculated as

$$y_{ijk} = \sum_{i=0}^{i} factor\ weight_i \times subclass\ weight_{ij}$$

where *i* is a factor map and *ij* is a subclass of factor *i*.

3.3.3 Bivariate Statistical Analysis (BVS)

This analysis will use the *'landslide index method'* as described by van Westen (1997b). The bivariate analysis follows the same basic steps as the qualitative map combination with the exception that subclass weightings are assigned through statistical relationships with previous debris flows and factors are equally weighted with a value of '1'. The major assumption for this model is that debris flows are most likely to occur where debris flows have occurred in the past (Principle #1). The debris flow densities within certain factor subclasses are related to the overall debris flow density of the study area. Taking a logarithm of the ratio allows for the negative weighting of densities lower than normal and positive weightings where densities are above normal. The formal weightings for each factor subclass are defined by the following equation

$$ln\,W_i = ln\left(\frac{Densclas}{Densmap}\right) = ln\left(\frac{\frac{Npix(Si)}{Npix(Ni)}}{\frac{\sum Npix(Si)}{\sum Npix(Ni)}}\right)$$

where W_i is the weight given to a certain factor subclass, *Densclas* is the landslide density of a certain subclass, *Densmap* is the landslide density of the entire map, *Npix(Si)* is the number of pixels containing debris flow origins in a subclass and *Npix(Ni)* is the total number of pixels in a subclass. This method is essentially the same as the *'information value method'* proposed by Yin and Yan (1988) with the exception that the formula uses a natural logarithm as opposed to the base 10 logarithm. Once each subclass has a weighting assigned, the factor subclasses are reclassified based upon the weight and added sequentially for a total instability score as in the qualitative map combination. A general overview of the procedure is given in Figure 7.

To perform this analysis within the ArcGIS environment, the buffered debris flow origins (raster) are first reclassified with a value of '1' where debris flows occur and a value of 'NoData' elsewhere. Once the four factor maps (SSURGO excluded) are classified into subclasses the debris flow raster is multiplied by the reclassified factor maps. This results in a new debris flow map with values of the factor subclasses at each debris flow grid cell and 'NoData' values elsewhere. The attribute tables, containing the count of cells in each subclass, of each of the factor maps as well as the overlain debris flow/subclass maps are exported to a spreadsheet where the densities can be calculated.

In the situation where no debris flow cell occurs within a subclass, the *'densclas'/'densmap'* ratio is given a value just lower than the lowest ratio value (van Westen, 1997b). This is due to the fact that a logarithm cannot be taken of a zero value. The new weightings can then be used to reclassify the factor maps which are then overlain, using addition, for a raw instability score, *Y*.

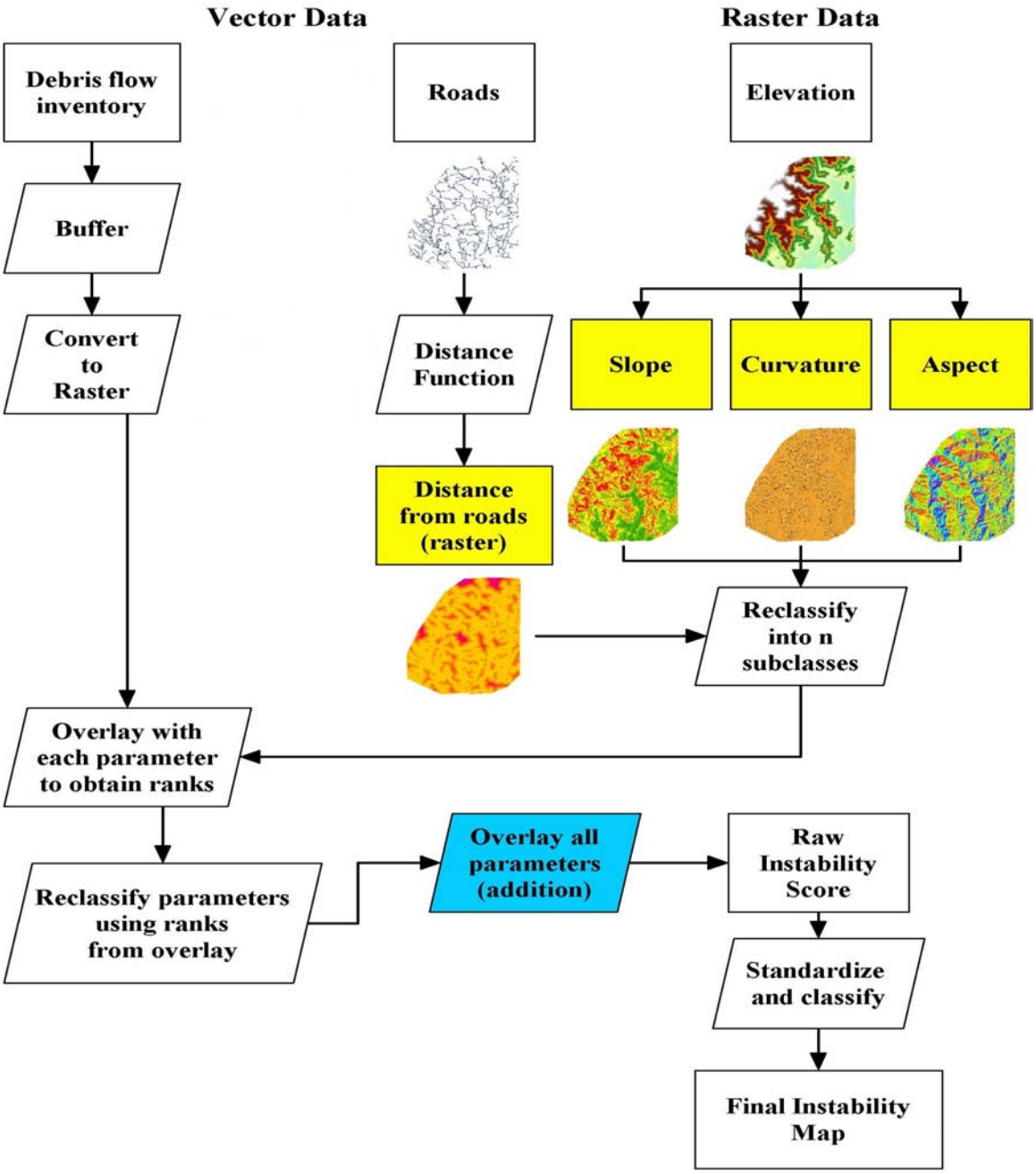

Figure 7. Overview of the Landslide Index Method (factors shown in yellow boxes).

This procedure is done for the Madison County site using both 10-meter and 30-meter elevation data for a total of two model runs. However, the debris flow origins will

remain at a resolution of 10-meters because it would be unjustifiable to increase the area affected by debris flows simply because of a variation in other source data. Therefore, weightings for both 10-meter and 30-meter data are developed from the Madison County debris flows and will be applied to the Nelson County site.

3.3.4 Shallow Landsliding Stability Model (SHALSTAB)

As previously mentioned, the SHALSTAB model estimates the minimum amount of steady-state rainfall necessary to trigger debris flows. It couples a hydrologic model (O'Loughlin, 1986) with an infinite slope form of the Mohr-Coulomb failure law (Bolt *et al.*, 1975; Dietrich *et al.*, 2001) for the spatial prediction of relative slope instability. The model is topographically driven and makes several simplifications that make the model more transportable. Key assumptions of the model used in this study include the lack of lateral root support along a failure surface, steady-state rainfall, parallel subsurface flow and spatially constant soil properties (Dietrich *et al.*, 2001). The combined hydrologic-instability equation at slope failure takes the form

$$Q_c = \frac{T \sin\theta}{(a/b)}\left[\frac{C'}{\rho_w g z \cos^2\theta \tan\phi} + \frac{\rho_s}{\rho_w}\left(1 - \frac{\tan\theta}{\tan\phi}\right)\right]$$

where Q_c is the critical steady-state rainfall necessary to initiate failure, T is the transmissivity of the soil, θ is surface slope, ϕ is the internal angle of friction, C' is cohesion, ρ_w and ρ_s are the density of water and soil bulk density, respectively, g is gravitational acceleration, a is the upslope contributing area and b is the length of the outflow boundary (Dietrich *et al.*, 2001; Montgomery *et al.*, 1998). This same model has been applied to the Madison County study area by Morrissey *et al.* (2001a) in a comparison of deterministic models.

The use of this model in this study is due to its portability and ease of use (Dietrich *et al.*, 2001) as well as the nature of its output[4]. The output of SHALSTAB is given as the logarithm of the hydrologic ratio, Q_c/T, where Q_c is the effective precipitation at failure and T is the transmissivity, or the subsurface ability to convey water downslope (Dietrich *et al.*, 2001). The output ranges from unconditionally unstable (value = -10) to unconditionally stable (value = 10); a grid cell gets an unconditionally stable value at slopes under approximately 20 degrees (dependent upon input parameters) whereas a grid cell gets an unconditionally unstable value at slopes over approximately 45 degrees (dependent upon input parameters).

Unconditionally stable cells are essentially those areas where the height of the water table can become greater than the thickness of the soil. Likewise, unconditionally unstable cells are those areas where the water table can become zero, usually corresponding to bedrock outcrops (Dietrich *et al.*, 2001). The values of '-10' and '10' do not represent actual values. Rather, they simply represent a class of instability. For a more detailed explanation of the unconditionally unstable and unconditionally stable values, please see Montgomery and Dietrich (1994). Between these two values, the

[4] The SHALSTAB model is automated within ESRI's ArcView 3.2 software environment and is available at http://socrates.berkeley.edu/~geomorph/shalstab/

SHALSTAB output represents a relative indication of potential instability where the lower the *log* (*Q/T*) value, the higher the chance of landsliding (i.e. the lower the amount of rainfall needed to induce landsliding) (Dietrich *et al.*, 2001). This value equates to the relative instability score, *Y*, of the QMC and BVS models. Because this output is not pre-classified into instability classes (e.g. SINMAP), the standardization of SHALSTAB values with the values of the other models becomes possible.

The primary input factor needed for this model is the elevation layer. In addition, the geotechnical parameters already mentioned, soil cohesion, internal angle of friction, soil depth and soil bulk density will be used. As discovered by Morrissey *et al*. (2001a), the geotechnical parameters necessary for this evaluation are similar to the parameters measured in debris flow areas in Nelson County (Auer, 1989). Subsequent field studies have given representative values of these parameters for Madison County (Morrissey *et al.*, 2001b). The values are similar (Table 2) and will be used for SHALSTAB runs in Madison County using both 10-meter and 30-meter elevation data. The SHALSTAB model will also be run with default values (Table 2) using 10-meter and 30-meter elevation data for a total of four model runs. Factor maps are not created for input into the SHALSTAB model because the model automates the creation of a slope factor. In addition to the slope factor, SHALSTAB creates a 'contributing area' factor map indicating the upslope area contributing to a grid cell's water flow. These two maps are then used in the equation along with the geotechnical parameters to derive the logarithm of the Q_c/T ratio. An important note about this model is that the elevation layer used does not have its sinks[5] filled, contrary to the authors' recommendations. This is due to the presence of lakes in the Madison County area. The effects of not filling the sinks, however, are probably minimal when comparing relative model performances.

3.3.5 Standardization of Model Output

Once all of the models, shown in Table 7, have been run in Madison County (12 total), the outputs need to be standardized to the same scale. This standardization allows for a better comparison among the models. The raw instability scores, *Y*, are transformed into standardized scores, Y_s, where the new scale ranges from a minimum of '0' to a maximum of '1'. To achieve this, a linear scaling will be applied to the raw instability scores of each of the models:

$$Y_s = (Y_i - Y_{min})/(Y_{max} - Y_{min})$$

This will divide the difference between the raw instability score (Y_i) at a given cell and the minimum raw instability score by the range of raw instability scores, giving a standardized instability score (Y_s). Because the models indicate relative slope instability, this standardization is possible as it relates a grid cell's score to other grid cells surrounding it. Grid cells of the same value are assumed to be of equal instability.

[5] Sinks are cells of an elevation layer where all surrounding cells are higher in elevation and there is no outflow. Sinks can be natural, such as large lakes, or they can be errors in mapping.

Table 7. Overview of the various model runs.

Model Run	Model Description
QMC Run 1 & 2	Model runs with slope and curvature weighted double the rest of the factors and subclass weights that vary only in slope subclasses 3-5 and curvature subclasses 2-3.
QMC Run 3	Model run using QMC Run 2 subclass weighting but without the use of SSURGO data.
BVS Run 1	Equally weighted factors and statistically developed subclass weights without the use of SSURGO data.
SHALSTAB Run 1	Model run using site-specific geotechnical parameters from Madison and Nelson Counties.
SHALSTAB Run 2	Model run using default geotechnical parameters provided by SHALSTAB.

The standardization procedure for the QMC and BVS models are identical in which the equation above is applied directly to the raw instability outputs; however, the procedure used to develop the SHALSTAB standardization is quite different. Because the unconditionally stable and unconditionally unstable values that SHALSTAB uses do not represent an actual instability value (they are more of a cutoff), the linear standardization equation used on the QMC and BVS models is not valid on the raw output. Although SHALSTAB uses the same standardization equation, the raw output from the model requires a number of processing steps before it can be input into the equation. In addition, the relative indication of instability is reversed in SHALSTAB. Instead of the maximum output value representing the highest potential for instability, SHALSTAB's minimum value represents the highest potential for instability. In the absence of a developed method to standardize SHALSTAB output, the following method was developed and applied.

The method has a 6-step reclassification process that takes the raw instability map from SHALSTAB and creates a new raw instability map. The goal of this process is to assign the minimum and maximum values of the raw SHALSTAB output (excluding the unconditional values) to the classes of unconditionally unstable and unconditionally stable, respectively. Assuming that the unconditionally unstable/stable grid cells are the most unstable/stable areas, respectively, these areas will be reclassified to the lowest or highest actual Q_e/T values. Once the unconditional values are reclassified with the minimums and maximums, the SHALSTAB output can be input to the standardization equation with one minor change. Because of the reversal of instability values, the equation for SHALSTAB takes a new form:

$$Y_s = 1 - \left(\left(Y_i - Y_{min} \right) / \left(Y_{max} - Y_{min} \right) \right)$$

where Y_s is the standardized instability score, Y_i is the raw instability score at a given cell, Y_{max} and Y_{min} are the maximum and minimum instability scores in the map, respectively.

The steps to this process involve several reclassifications (Table 8) and overlay steps. The steps are as follows:

1) Reclassify raw SHALSTAB output using reclassification #1
2) Reclassify the result from step 1 using reclassification #2
3) Multiply the result from step 2 by the raw SHALSTAB output (this step provides the minimum and maximum values)

4) Reclassify the result from step 1 using reclassification #3
5) Divide the raw SHALSTAB output by the result of step 1
6) Multiply the result from step 5 by the result from step 4

Table 8. Reclassification steps used to standardize the SHALSTAB output.

Reclassification #1			
Old Value	-10	Q_c/T value	10
New Value	-10	1	10

Reclassification #2 (from Reclass 1)			
Old Value	-10	1	10
New Value	NoData	1	NoData

Reclassification #3 (from Reclass 1)			
Old Value	-10	1	10
New Value	SHALSTAB min	1	SHALSTAB max

The final step in this standardization produces a map with Q_c/T values at all grid cells including those unconditional grid cells. The values at grid cells other than the unconditional cells are the same as the original values. This new map can then be standardized using the modified linear equation given above. All scaled values will be masked with the hydrography mask developed earlier.

3.3.6 Development of Instability Classifications

With all of the model runs (12 total) being standardized to the same scale, the outputs will be overlain with the debris flow origins of Madison County to determine the threshold values to be used in classifying the maps into instability classes (e.g. very low → very high). These classes are identified with a value of '1' for 'Very Low' to '5' for 'Very High'. The approach used for this follows the recommendations of the SHALSTAB authors in interpreting model output for management purposes (Dietrich *et al.*, 2001). None of the model outputs, although standardized to the same scale, give an indication of how to interpret the output in terms of what is 'very high' instability, 'high' instability, etc. Therefore, each debris flow origin buffer from Madison County will be assigned an instability value between '0' and '1' based on the zonal statistics of the buffer and summarized through a frequency table. The frequency table is then used to develop the threshold values that will be used to reclassify the standardized model outputs into final instability maps.

The assignment of an instability value to each debris flow buffer follows recommendations by Dietrich *et al.* (2001) and uses the most unstable value/score within the buffer. The use of a single instability value to characterize a buffer polygon may underestimate the area of high instability because many debris flow buffers may contain instability scores that are more stable than the score assigned to the buffer (Dietrich *et al.*,

2001). This use of the most unstable score does create some bias in the results because the debris flow values are skewed to the unstable side where a debris flow may contain a lower average or median score. Dietrich *et al. (2001)* explain that this may negate the effects of excluding the steeper and more convergent topography of the actual terrain that is often omitted when using digital elevation data. Therefore, the use of the single, most unstable score may present a balanced manner in which to view slope instability, a positive aspect for forest management and hazard studies in general.

When assigning instability scores from the 30-meter data to the debris flows some instability scores that fall within the zone of a debris flow are not accounted for because of the large grid cell size. When ArcGIS takes zonal statistics, if a grid cell's center point does not fall within the zone the value is not reflected in the output even though a large portion of the grid cell does fall within the zone. To more accurately depict the actual areas of each value that fall within a debris flow the 30-meter instability scores are converted into 10-meter data. This process does not change the values of the grid cells but allows a better comparison of the debris flow instability scores. The use of 30-meter data in this study is to show the effects of source elevation data variations in the creation of instability values; this process highlights those effects rather than the effects of the way ArcGIS computes zonal statistics.

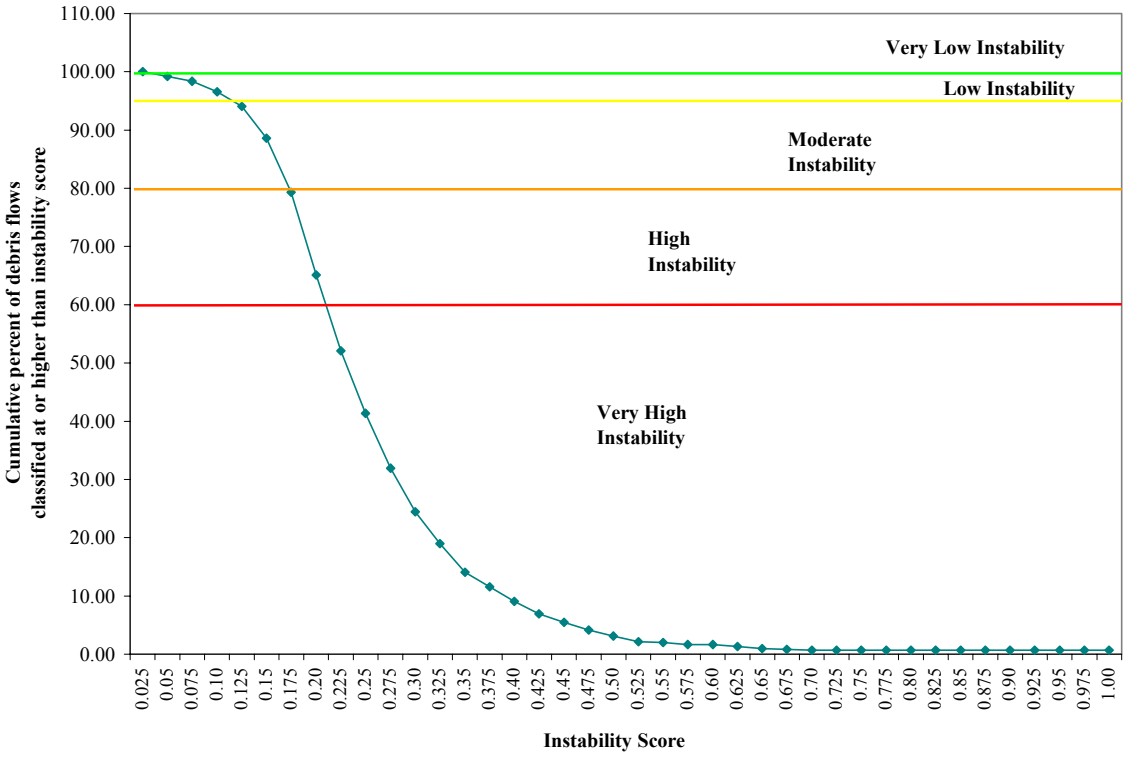

Figure 8. Generic example of the thresholds for instability classifications.

Once the debris flow buffers have been assigned an instability score and a frequency table has been created, the cumulative percent of debris flows assigned an instability score or higher is calculated. The percentage at a specific instability score represents the fraction of debris flows with an instability score equal to or greater than that instability

score (Figure 8). Ideally, the models should capture most of the debris flows at a high instability score. For the purpose of this study, four arbitrary threshold percentages representing the fraction of debris flows assigned an instability score or higher will be used to identify five instability classes. These percentages are 60, 80, 95 and 100 for 'Very High', 'High', 'Moderate' and 'Low' classes, respectively. In other words, sixty percent of the debris flows should be in the 'Very High' class, the next twenty percent should fall in the 'High' class, the next fifteen percent should be in the 'Moderate' class and only five percent of the debris flows should be in the 'Low' class. There should be no debris flows classified into the 'Very Low' class (i.e. 100% of the debris flows are classified into a class higher than 'Very Low'). These numbers may be adjusted based upon specific circumstances; however, the majority of debris flows should always be classified into the 'Very High' class. Once the instability scores at the given threshold percentages are identified, the standardized instability maps are then reclassified based upon those scores for final instability classifications.

3.4 MODEL VALIDATION

To assess model performance, the models that have been developed in Madison County using certain weighting schemes and instability threshold scores for classification are applied to the area in Nelson County. The Nelson county model runs (12 total) will use the same methods applied to the Madison County models applying both 10-meter and 30-meter elevation data. The instability scores for each of the given threshold percentages developed in Madison County will be used to develop final instability maps for the Nelson county site. In addition, the BVS weightings developed in Madison County will be applied to the Nelson County BVS model. Although the QMC and SHALSTAB models can be altered to fit the Nelson County area best no changes are needed for this study. This allows for a more systematic comparison among models. Moreover, the physiographic and geotechnical characteristics of both areas are very similar.

The Nelson County models will be evaluated for both Type I and Type II errors using the final reclassified instability maps where Type I errors are assumed the worst type of error. Type I errors are "omission errors" in which areas classified into low instability categories have had debris flows occur. These errors may lead to management activities in a hazardous area. Type I errors (i.e. incorrectly classified debris flows) will be identified as those debris flow polygons (including buffered arcs) that consist of entirely 'Very Low' and 'Low' grid cells. Correctly classified debris flows are those polygons/arc buffers containing at least one grid cell of 'Moderate', 'High' or 'Very High' instability. This follows the approach used by Vaugeois and Shaw (2000) in assessing model performances. Type I errors will be expressed as the percentage of incorrectly classified debris flows compared to the total number of debris flows.

Type II errors are "false positives" where areas classified into high instability categories have not had debris flows occur. These types of errors can lead to over-caution in management decisions but does not necessarily imply that there is no instability in an area; rather the area may be of concern for future instability. Type II errors will be identified as those grid cells having an instability class of 'Moderate', 'High' or 'Very High' that do not occur within an existing debris flow. All other cells will be assumed as classified correctly. To assess Type II errors the debris flow arcs/polygons (not origins)

are converted to a raster format with values of '1' at grid cells overlapping debris flows and values of '0' elsewhere. These values are then reclassified to show '-1' values at debris flows and values of '1' elsewhere. This new map is then overlaid with the final instability maps to determine the number of grid cells classified into each instability class at areas that have not been subjected to landsliding. The evaluation of Type I and Type II errors will be performed for both 10- and 30-meter model runs. As in the assignment of instability scores to debris flows in Section 3.3.6, using 30-meter data in this overlay with 10-meter data necessitates the increase in resolution of the 30-meter data to more accurately depict the actual areas of various instability classes. This overlay will therefore use the grid cell size of the debris flow raster but does not change the instability scores of the grid cells. This step allows a more systematic comparison between 10- and 30-meter Type II errors.

Type II errors will be expressed as the percentage of grid cells classified as 'Moderate', 'High' or 'Very High' instability falling outside the extent of landsliding compared to the total number of grid cells in the same three classes. The use of the '-1' value to represent the debris flows will all the comparison of Type II errors of individual instability classes. The percentages of correct and incorrectly classified cells can then be compared across models and between resolutions.

3.5 DEVELOPMENT OF CONTINGENCY TABLES

To assess the sensitivity of resolution on the individual grid cell classifications, a contingency table is used that shows the percentages of grid cells that did not differ in instability class from the 10-meter elevation data to the 30-meter elevation data. This table is created by overlaying the final instability maps from both resolutions and, using the minimum resolution, obtaining the classifications of both resolutions. Essentially, a 30-meter grid cell is divided into nine grid cells that overlay exactly with the 10-meter data. Using the Raster Calculator, the 10-meter values (i.e. 1 to 5) are multiplied by a factor of ten and added to the 30-meter value. This allows for the assessment of the percentage of grid cells classified the same, with a one-class difference and with a two-class difference.

CHAPTER 4. RESULTS

4.1 DEBRIS FLOW ORIGINS

In an effort to characterize the debris flow origins, first summary descriptive statistics were computed for each of the factors at the debris flow origins. These statistics (Table 9) give an indication of the typical geomorphology found at the location of initiation. Debris flows were initiated on a wide variety of slopes including somewhat flat slopes. The average slope gradient at debris flow origins was 26.9% while the average slope shape was a bit concave with a curvature of -.54. Debris flows occurred preferentially on slopes facing SSE (150º) and at distances of almost 300 meters from the nearest road. The average elevation of debris flow initiation was about 460 meters above mean sea level. Statistics were not computed for the SSURGO data because of the categorical nature of the data. However, for the typical soil at a debris flow origin, the vast majority of debris flows (~46%) started in the 'Porters very stony loam' series. The soil with the next highest percentage was "Rock land, Porters and Hazel materials' with about 25% of the debris flows originating on that soil and approximately 10% occurring on 'Rock land, acidic' soils.

Table 9. Descriptive statistics of the various factors at debris flow origins.

	Input Factor				
Statistic	Slope (deg)	Dist. To Roads (m)	Curvature (1/100 z units)	Aspect (deg)	Elevation (m)
Min	4.045	0	-7.353	The majority (≈45%) of debris flow origins occurred on East and Southeastern slopes	184
Max	45.784	1179.915	2.911		916
Range	41.739	1179.915	10.264		732
Mean	26.853	293.479	-0.542		460.893
St. Dev.	6.613	230.025	1.395		122.287

4.2 BVS WEIGHTINGS

The results of the Landslide Index Method are shown in Table 10. These weightings, developed from the Madison County data were applied to the factor maps in Nelson County for development of instability maps. The range of weighting values from the Landslide Index Method is much smaller than the QMC weightings (see Table 5, p.55) with a minimum of -2.467 and a maximum of 1.805 for the 10-meter elevation data and a minimum of -2.880 and a maximum of 1.483 for the 30-meter data. Of particular interest are the 'distance to roads' weights where higher weights are given to those areas farther away from roads for both 10-meter and 30-meter elevation data. This is the opposite of the QMC weighting scheme. Also, the weightings for the fifth slope subclass are consistently lower than the third and fourth slope subclasses. East-facing slopes also receive high weightings.

The likely reason for the lower weightings of slope subclass five is that slopes with such a steep gradient usually do not have a lot of soil that can develop into debris flows.

These areas are typically bedrock outcrops. However, these steep slopes may be more inclined to other types of landslides such as rock falls. As for the weights for the distance to roads, the 50-meter threshold may not be high enough to capture an adequate amount of debris flows. As shown in Table 9, the average distance of a debris flow to the nearest road is almost 300 meters. A better factor map using roads may be road density where the higher the number of roads per unit area may indicate more unstable areas.

Table 10. Weighting for the Landslide Index Method using both 10-meter and 30-meter elevation data.

10-meter elevation data

Factor Map	Subclasses	Factor Weight	Subclass Weight
Slope	1. 0^o - 14^o	1	-2.467
	2. 14.01^o - 26^o		-0.052
	3. 26.01^o - 34^o		1.193
	4. 34.01^o - 45^o		1.805
	5. > 45.01^o		1.010
Curvature	1. Concave	1	0.450
	2. Planar		-1.074
	3. Convex		-0.153
Aspect	1. Flat	1	-1.832
	2. North		-0.038
	3. Northeast		-0.056
	4. East		0.418
	5. Southeast		0.378
	6. South		-0.127
	7. Southwest		-0.801
	8. West		-0.380
	9. Northwest		0.119
Distance To Road	1. < 50 m	1	-0.431
	2. > 50 m		0.067

30-meter elevation data

Factor Map	Subclasses	Factor Weight	Subclass Weight
Slope	1. 0^o - 14^o	1	-2.077
	2. 14.01^o - 26^o		0.405
	3. 26.01^o - 34^o		1.483
	4. 34.01^o - 45^o		1.265
	5. > 45.01^o		-2.880
Curvature	1. Concave	1	0.197
	2. Planar		-0.577
	3. Convex		-0.224
Aspect	1. Flat	1	-1.088
	2. North		-0.161
	3. Northeast		0.078
	4. East		0.373
	5. Southeast		0.287
	6. South		-0.330
	7. Southwest		-0.984
	8. West		-0.397
	9. Northwest		0.384
Distance To Road	1. < 50 m	1	-0.431
	2. > 50 m		0.067

4.3 RAW INSTABILITY SCORES

The raw instability scores, *Y*, shown in Table 11 vary in their minimums and maximums as well as their ranges. The range of the QMC model scores is the highest with a minimum and maximum of 13 and 65, respectively, while the BVS and SHALSTAB models have much smaller ranges that include negative values as well as positive values. However, considering the fact that the SHALSTAB raw instability scores indicate instability in a manner that is opposite the other models (i.e. lower scores indicate higher instability), the raw instability scores of the models cannot be directly compared. Moreover, the SHALSTAB model statistics include the unconditional classes with the minimums and maximums and therefore have average standardized values lower than the other models (much of the areas are classified into the unconditional stable class).

The differences between the average raw and standardized instability scores as well as the inverse nature of the SHALSTAB scores illustrate the necessity to have a standardized scale. Once standardized, the BVS model has a consistently higher average score than does the QMC models; in contrast, the average raw instability score of the QMC models is much higher than the BVS. In addition, the mean raw instability scores of the BVS and SHALSTAB models may indicate that the models behave in a similar fashion where these two models are actually the most different in terms of average standardized score.

Table 11. Raw instability scores for 10- and 30-meter model runs in Madison County.

10 meter

	Raw Instability					Standardized Instability	
Model Run	**Min**	**Max**	**Range**	**Stdev**	**Mean**	**Stdev**	**Mean**
QMC1	14	65	51	9.9084	35.1615	0.1943	0.4149
QMC2	13	65	52	8.8523	34.5334	0.1702	0.4141
QMC3	13	55	42	7.4016	26.6747	0.1762	0.3256
BVS	-5.8	2.74	8.54	1.853	-1.1305	0.217	0.5468
SHALSTAB1[a]	-6.5224	-1.6313	4.8911	0.7071	-2.4397	0.1446	0.1653
SHALSTAB2[a]	-6.6766	-1.4045	5.2721	0.5231	-1.6722	0.0992	0.0508

30 meter

	Raw Instability					Standardized Instability	
Model Run	**Min**	**Max**	**Range**	**Stdev**	**Mean**	**Stdev**	**Mean**
QMC1	15	65	50	8.7734	34.9185	0.1755	0.3984
QMC2	15	63	48	7.3881	35.441	0.1539	0.4259
QMC3	15	53	38	6.3512	27.5831	0.1671	0.3311
BVS	-4.07	2.13	6.2	1.4646	-0.9043	0.2362	0.5106
SHALSTAB1[a]	-5.9054	-2.1593	3.7461	0.5603	-2.7311	0.1496	0.1526
SHALSTAB2[a]	-4.7653	-1.9319	2.8334	0.2845	-2.038	0.1004	0.0375

[a]SHALSTAB statistics include the cutoff values classified with the minimums and maximums.
Values are for entire study area

4.4 INSTABILITY CLASSIFICATION THRESHOLDS

The instability score thresholds (i.e. upper limit of instability class) developed in Madison County used for classification of the standardized maps in Nelson County vary widely in their ranges (Table 12). However, the threshold scores are consistent among the various model runs using both resolutions of elevation data. The BVS model captures most debris flows with the highest instability scores followed by the QMC models and then SHALSTAB. The instability scores for the 'Very High', 'High', 'Moderate', 'Low', and 'Very Low' classes using 10-meter data range from .2375 to .88, .1875 to .8125, .0375 to .725, .0375 to .725, and .025 to .425, respectively. Instability scores for the same classes using 30-meter data range from .15 to .82, .0375 to .75, .03 to .6375, and .025 to .25. These ranges vary consistently between the 10-meter and 30-meter model runs with the 30-meter runs capturing the debris flows at lower instability scores.

Table 12. Instability score thresholds used to classify the standardized maps into instability classes.

Instability Class Cutoff Score
10-meter elevation data

	Percent of debris flows desirable for instability class				
	0	5	15	20	60
Model Run	Very Low	Low	Moderate	High	Very High
QMC1	0.325	0.56	0.66	0.7875	1
QMC2	0.35	0.525	0.625	0.675	1
QMC3	0.2	0.46	0.53	0.58	1
BVS1	0.425	0.725	0.8125	0.88	1
SHALSTAB1	0.025	0.18	0.25	0.295	1
SHALSTAB2	0.025	0.0375	0.1875	0.2375	1

Instability Class Cutoff Score
30-meter elevation data

	Percent of debris flows desirable for instability class				
	0	5	15	20	60
Model Run	Very Low	Low	Moderate	High	Very High
QMC1	0.2	0.318	0.525	0.5675	1
QMC2	0.25	0.38	0.4875	0.575	1
QMC3	0.075	0.21	0.3375	0.46	1
BVS1	0.25	0.6375	0.75	0.82	1
SHALSTAB1	0.025	0.12	0.1725	0.217	1
SHALSTAB2	0.025	0.03	0.0375	0.15	1

Threshold scores indicate the upper limit to a instability class

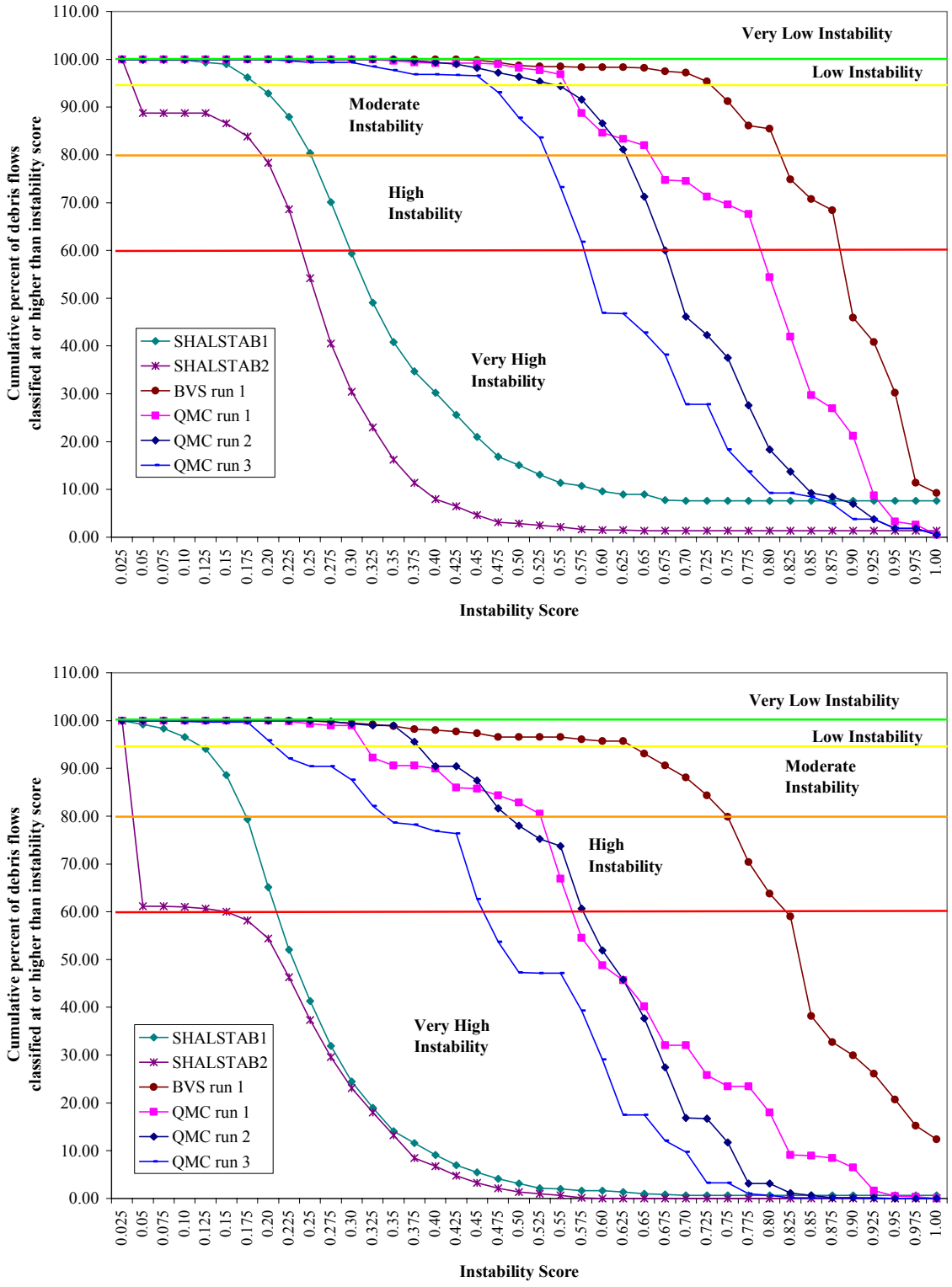

Figure 9. Threshold curves used to classify the standardized instability maps into instability classes using 10-meter (top) and 30-meter (bottom) elevation data.

For the QMC and BVS models, the instability thresholds drop drastically near the threshold score between 'Low' and 'Moderate' classes (Figure 9). The SHALSTAB model follows an inverse S-curve with the threshold score dropping rapidly between the 'Low' and 'Moderate' classes and leveling out around .4 to .5 (Figure 9). The SHALSTAB model captures most debris flows with very low instability scores. The QMC model runs 1 and 2 have threshold curves that are intertwined throughout the range of instability classes. QMC model run 1 captures most debris flows at a higher instability score than the second model run using 10-meter data; however, the second QMC model run captures most debris flows at a higher instability score using 30-meter data. The QMC model run 3 captures the majority of debris flows at instability scores lower than both QMC model runs 1 and 2 but higher than both SHALSTAB model runs. Overall, the differences between the threshold values of 10-meter and 30-meter resolutions are consistent in that the 10-meter thresholds are higher than the 30-meter thresholds.

These scores are related to the average instability scores of the entire study area shown in Table 11. The distribution of instability scores within an area are therefore the driving force for the development of instability thresholds used to capture the debris flows in Madison County. Using these threshold values, the standardized instability maps in Nelson County are classified into instability classes. Because the Madison County site is the development area for the models, the validation procedure for Type I and Type II errors are described only for the Nelson County site.

4.5 INSTABILITY CLASS DISTRIBUTIONS

The distribution of instability within Nelson County is skewed mostly to the lower instability classes for the 10-meter meter elevation runs on all models with decreasing amounts of unstable land area in the 'Moderate', 'High' and 'Very High' classes (Figure 10). Both SHALSTAB runs using 10-meter data classify about 80% of the grid cells into the 'Very Low' class while the second SHALSTAB run classifies 0% of the grid cells into the 'Low class. SHALSTAB Run 2 classifies approximately 5% of the area into 'Moderate', 'High' and 'Very High' classes while SHALSTAB Run 1 puts about 7% into the 'Moderate' class and 2-3% into the 'High' and 'Very High' classes. The QMC models 1 and 2 classify about 45% of the total area into the 'Very Low' class and about 35% of the area into the 'Low' class. These two models classify about 10% into the 'Moderate' class and about 4-5% into both the 'High' and 'Very High' classes. Both the QMC run 3 and BVS run 1 classify more area into the 'Low' class, about 54% and 47%, respectively, than the 'Very Low' class, about 20% and 28%.

The 30-meter data gives a much more evenly distributed classification of instability among the five classes with the exception of the second run of SHALSTAB which puts almost 85% of the grid cells into the 'Very Low' class. This second run of SHALSTAB puts the remainder of grid cells into the 'Very High' class with 0% in the middle three classes. Of particular interest is the increasing amount of grid cells classified into higher instability classes using the third run of the QMC. The remaining model runs classify a slightly decreasing amount of the land area into progressively higher instability classes. Figure 11 through Figure 16 shows the distribution of instability within Nelson County at a scale of 1:24,000 while small-scale instability maps are shown in Appendix C.

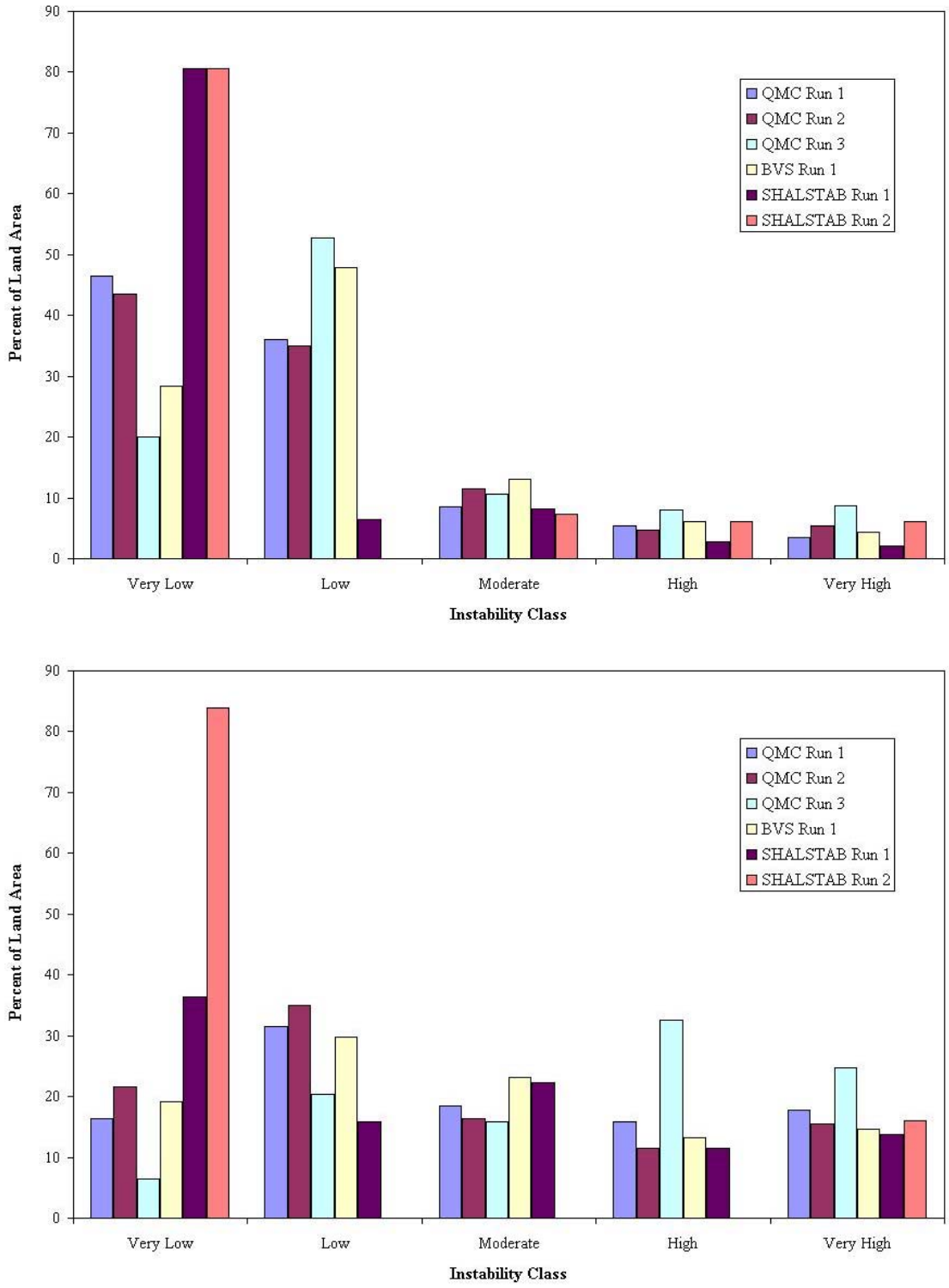

Figure 10. Distribution of total land area into instability classes for Nelson County with 10-meter (top) and 30-meter (bottom) elevation data.

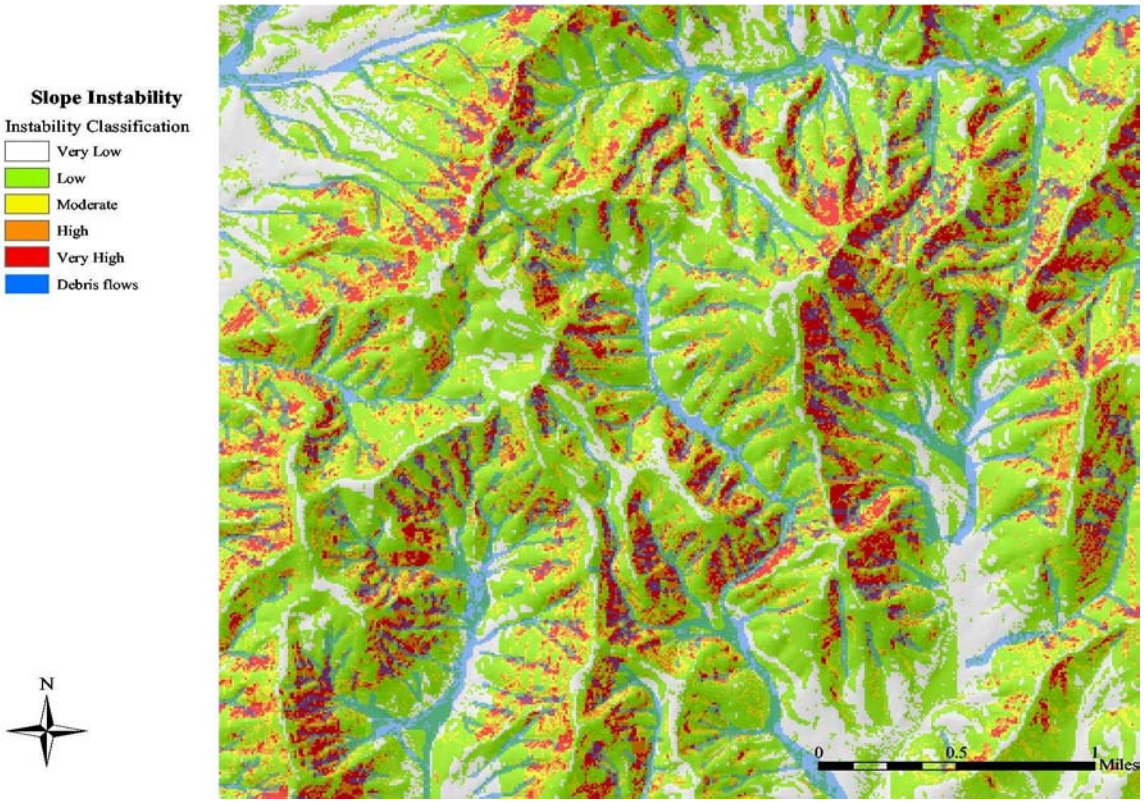

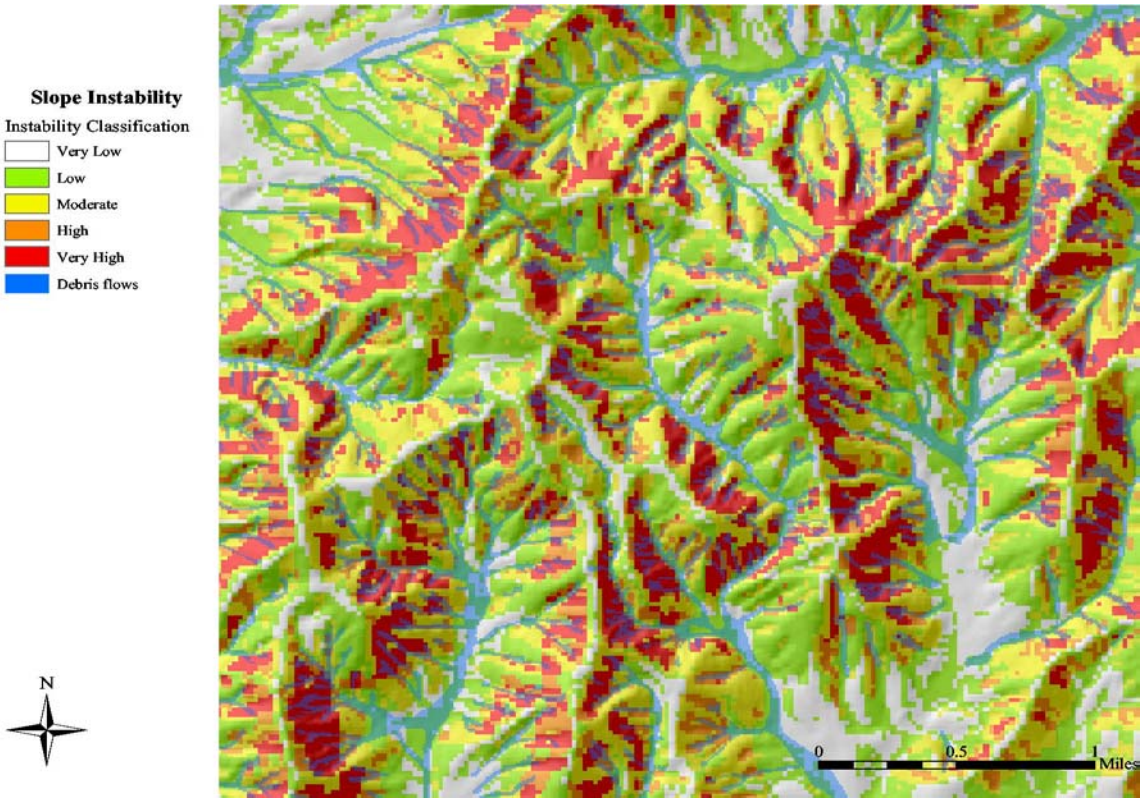

Figure 11. Instability maps created using the Bivariate Statistical Analysis in Nelson County using 10-meter (top) and 30-meter (bottom) elevation data.

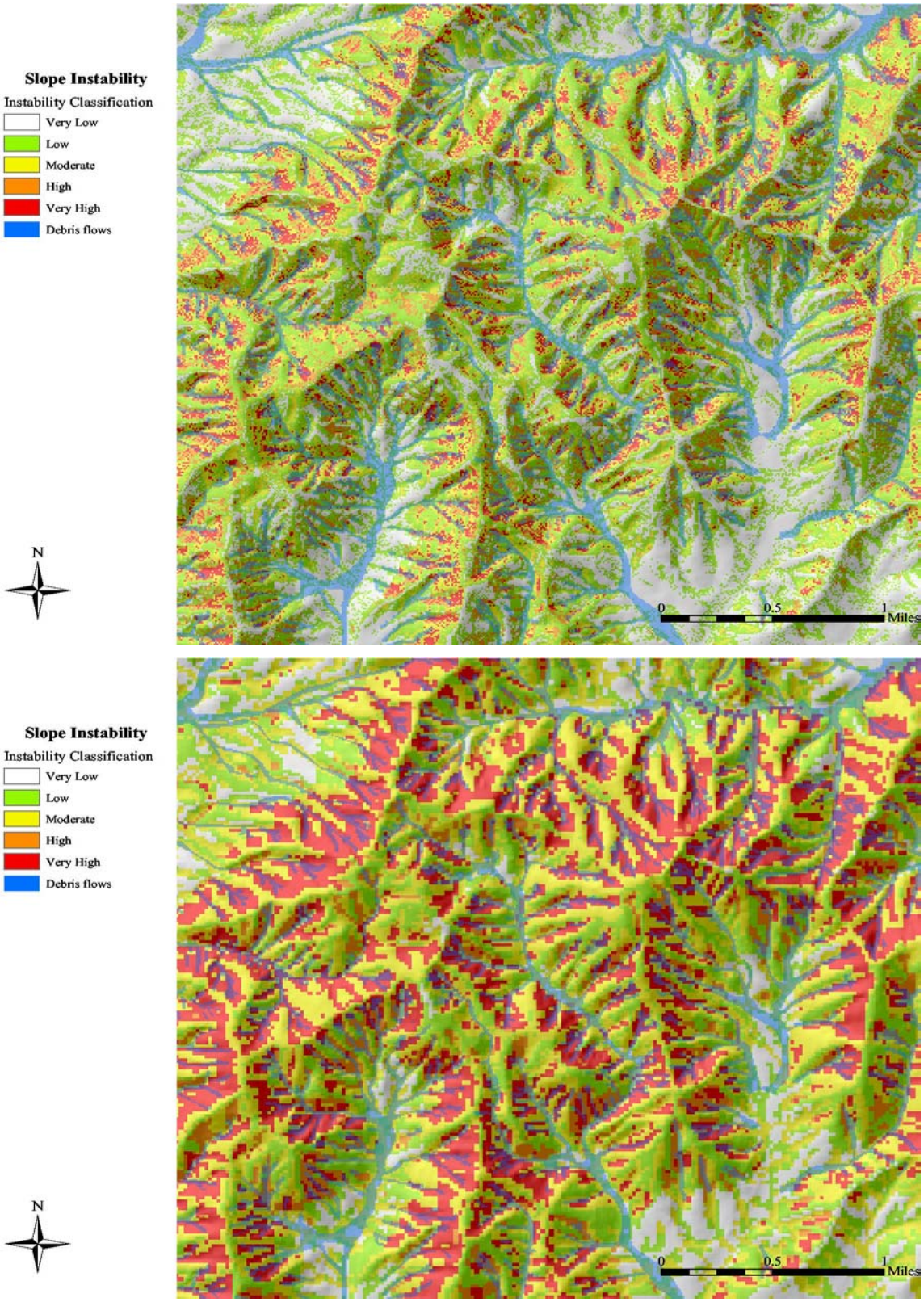

Figure 12. Instability maps created using Qualitative Map Combination Run 1 in Nelson County with 10-meter (top) and 30-meter (bottom) elevation data.

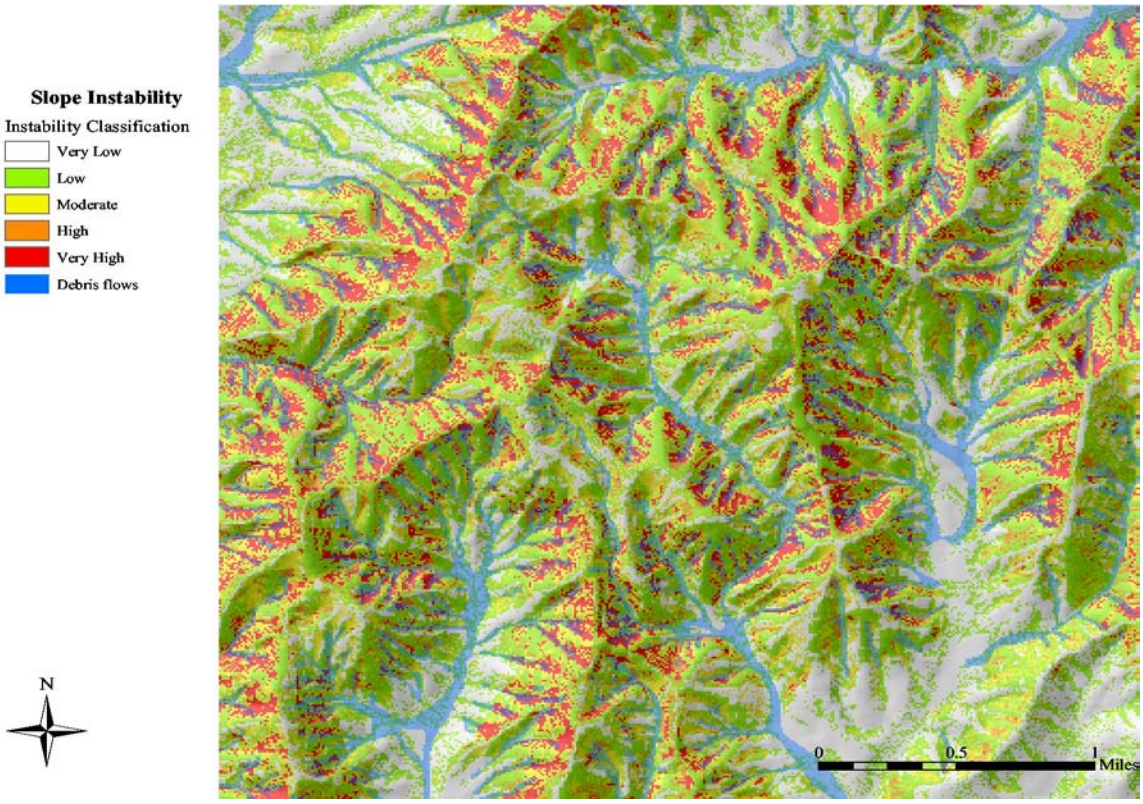

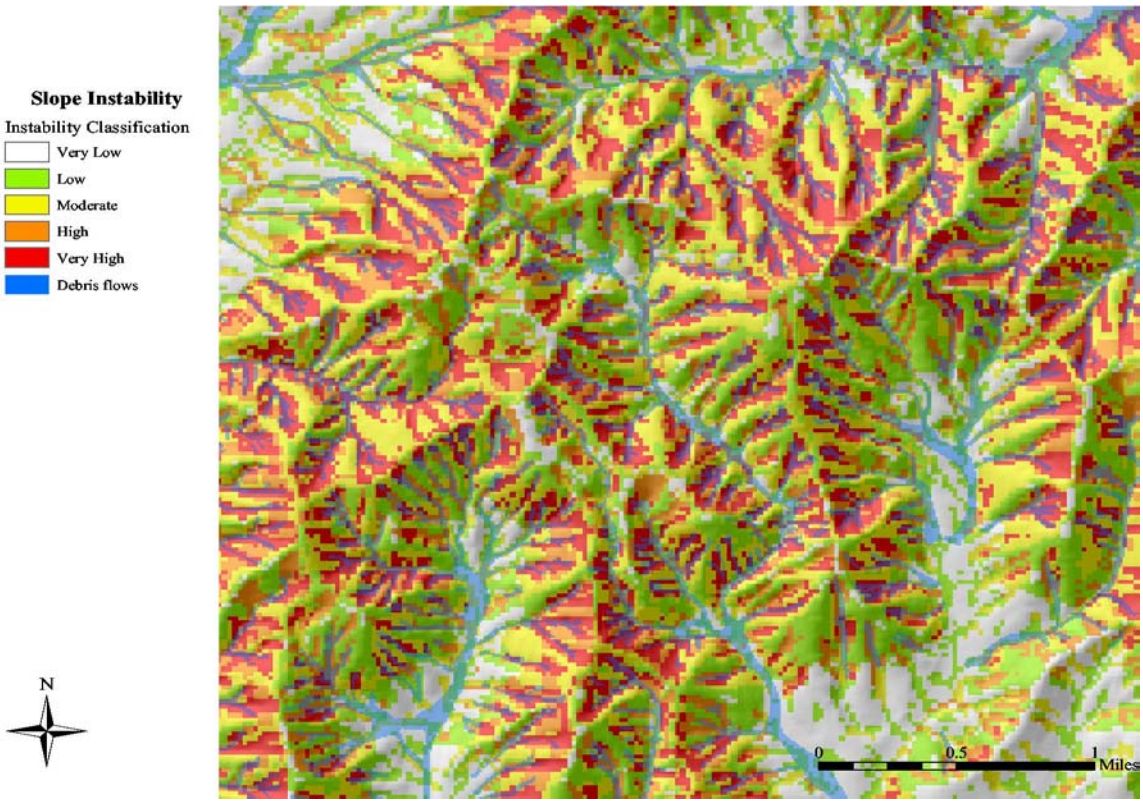

Figure 13. Instability maps created using Qualitative Map Combination Run 2 in Nelson County with 10-meter (top) and 30-meter (bottom) elevation data.

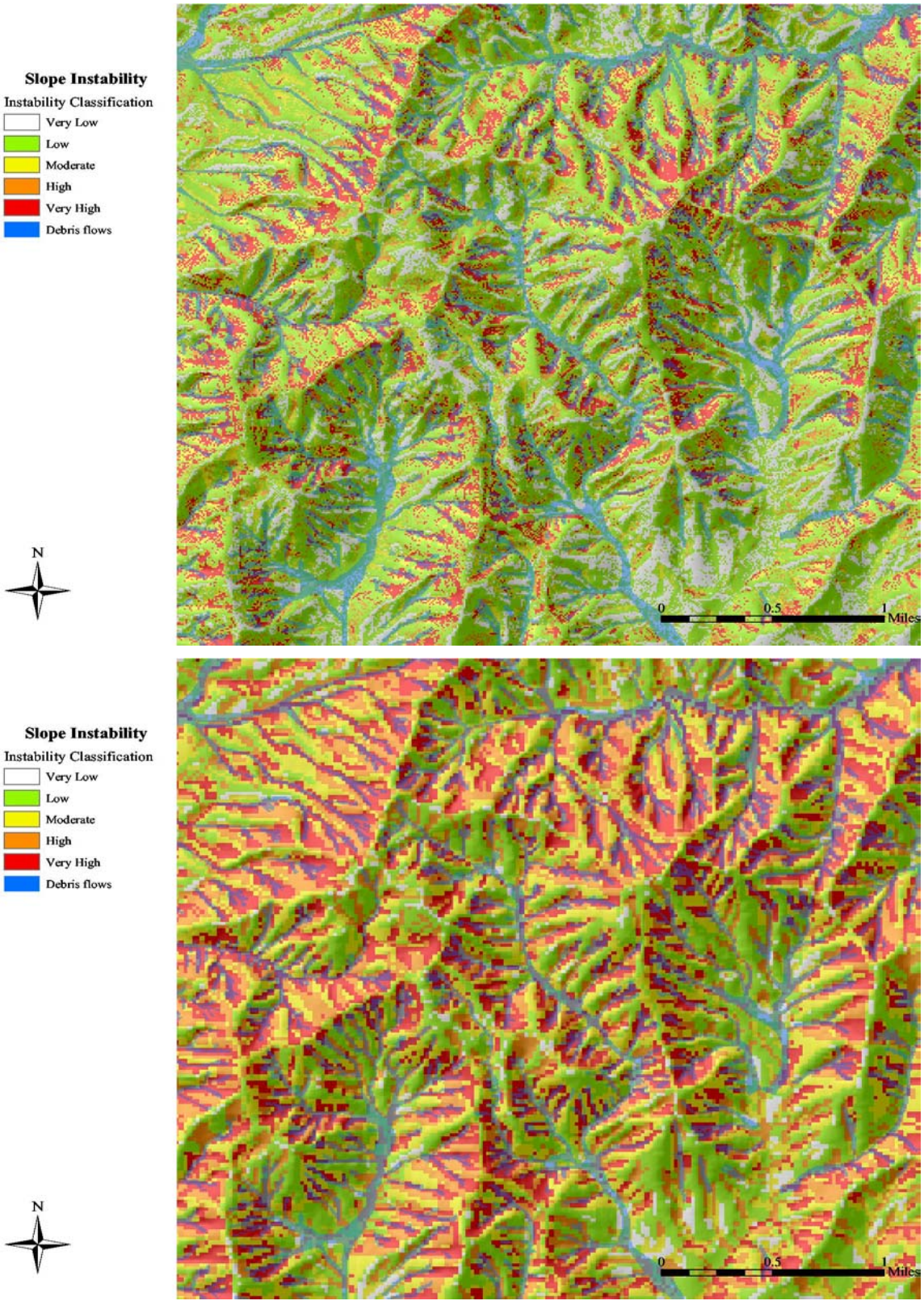

Figure 14. Instability maps created using Qualitative Map Combination Run 3 in Nelson County with 10-meter (top) and 30-meter (bottom) elevation data.

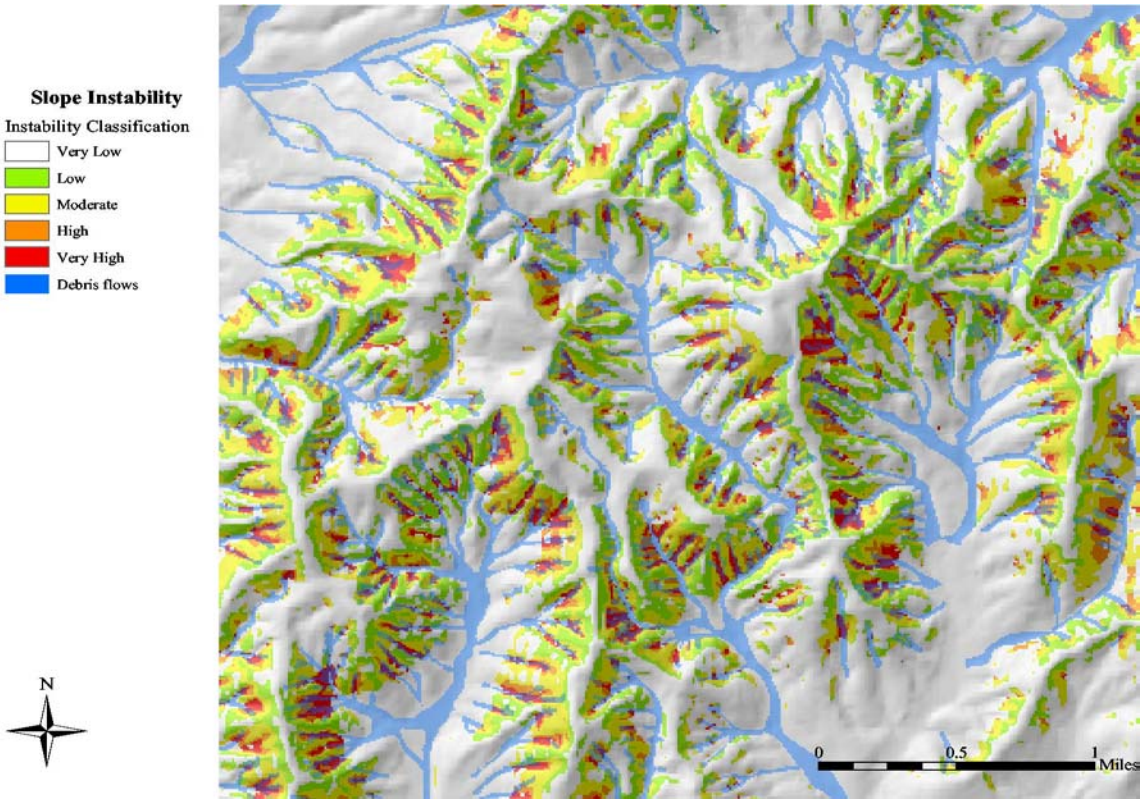

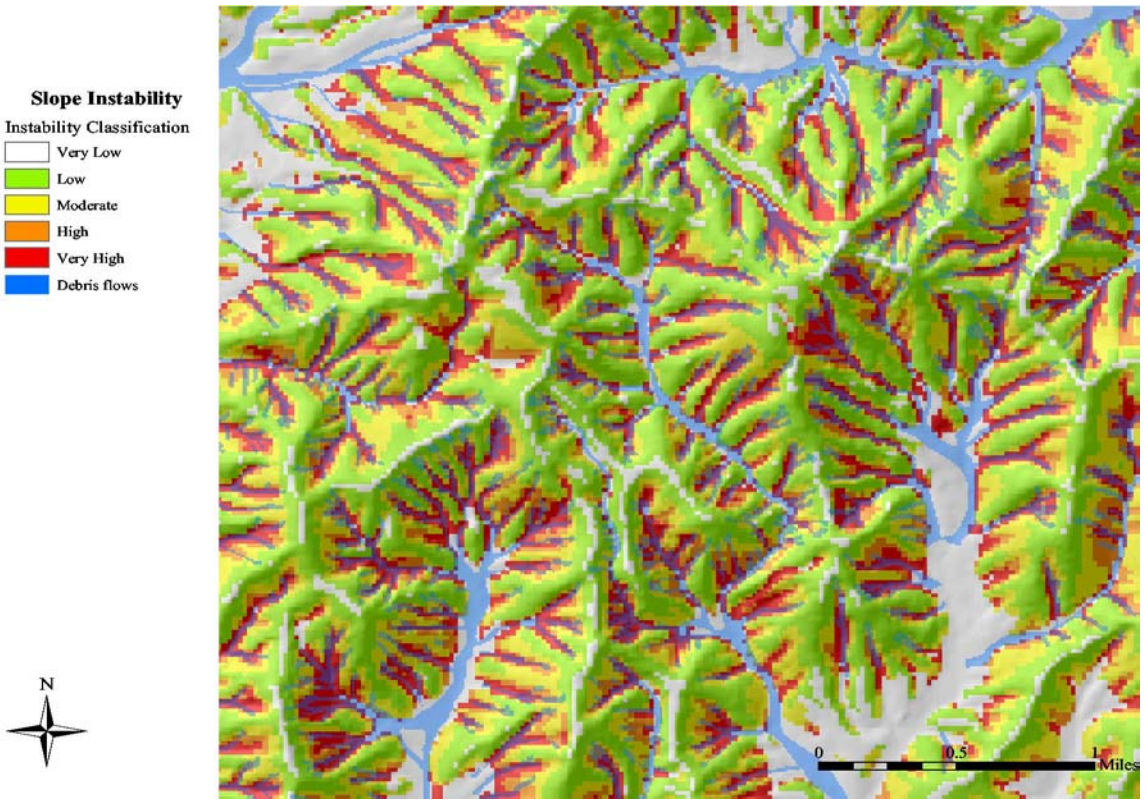

Figure 15. Instability maps created using SHALSTAB Run 1 in Nelson County with 10-meter (top) and 30-meter (bottom) elevation data.

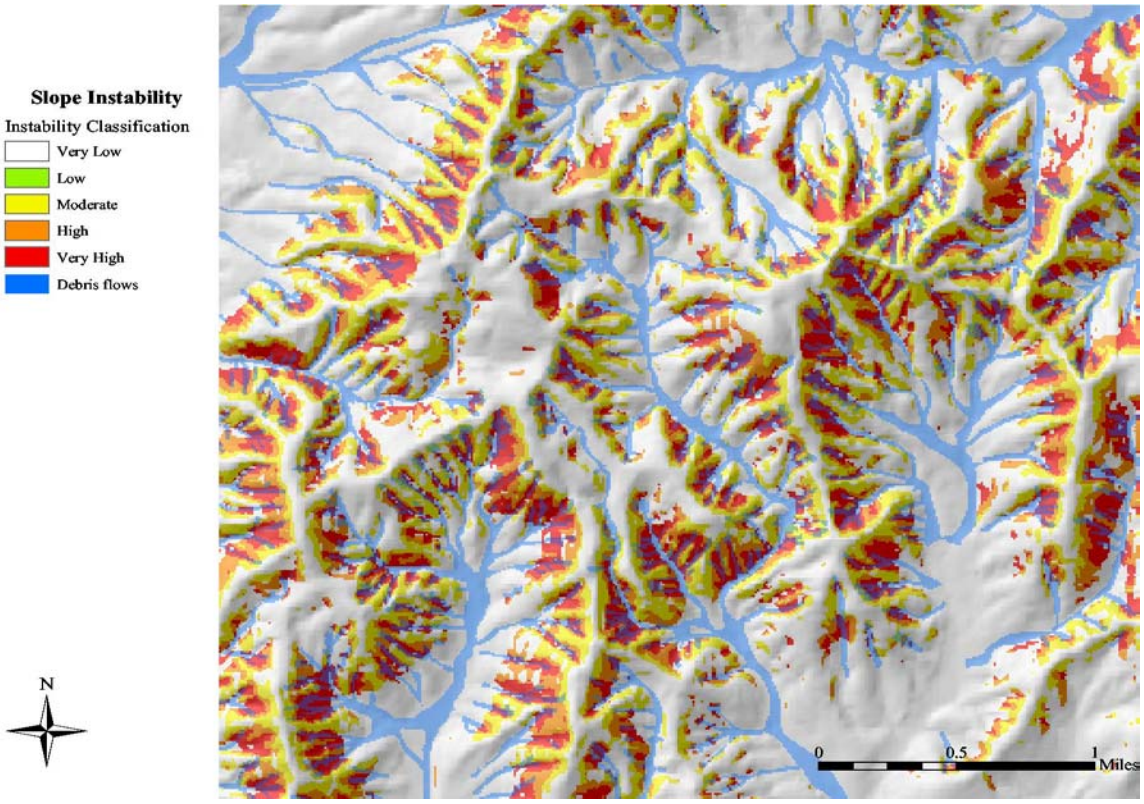

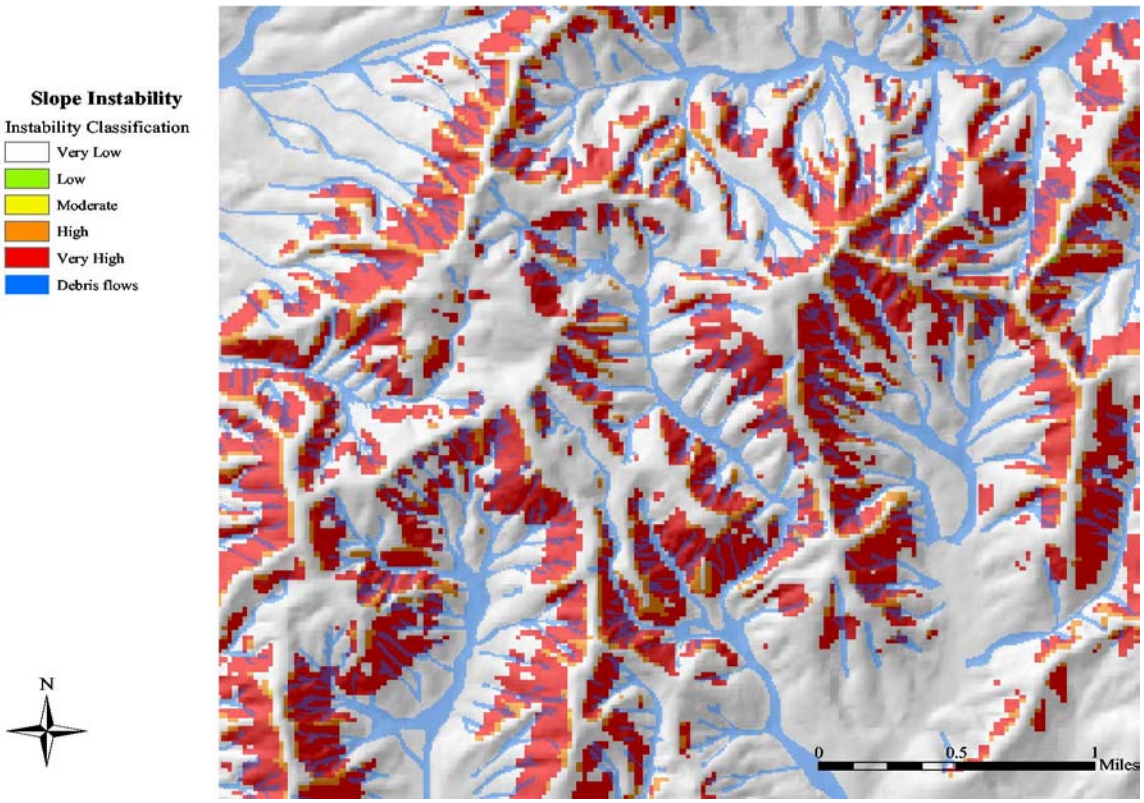

Figure 16. Instability maps created using SHALSTAB Run 2 in Nelson County with 10-meter (top) and 30-meter (bottom) elevation data.

4.6 TYPE I AND TYPE II ERRORS

The numbers of Type I errors (i.e. prediction of low instability where there have been debris flows) in Nelson County for both 10-meter and 30-meter elevation data are shown in Table 13. Overall, the Type I error percentage using 30-meter data is lower, 9.9%, than the Type I error percentage using 10-meter data, 15%. However, two individual model runs using 10-meter data have lower percentages than the same model runs using 30-meter data. These two model runs, BVS and SHALSTAB Run 2, misidentified 8% and 24% of the debris flows using 10-meter data and 11% and 35% of the debris flows using 30-meter data. The QMC model runs using 30-meter data misidentified fewer debris flows than the same model runs using 10-meter data. The most significant difference of these three model runs was in the first run where the 10-meter data misidentified 14% of the debris flows while the 30-meter data misidentified less than 2% of the debris flows. Both of the SHALSTAB model runs produced the highest percentage of misidentified debris flows with the exception of the first 30-meter run in which SHALSTAB misidentified only 6% of the debris flows.

Table 13. Type I error percentages for model runs in Nelson County.

10 meter

		# of debris flows	# of incorrectly identified debris flows	Type I error
Model Run	BVS Run 1	4502	375	0.083
	QMC Run 1	4502	645	0.143
	QMC Run2	4502	493	0.110
	QMC Run3	4502	238	0.053
	SHALSTAB Run 1	4502	1233	0.274
	SHALSTAB Run 2	4502	1084	0.241
			Average	**0.1506**

30 meter

		# of debris flows	# of incorrectly identified debris flows	Type I error
Model Run	BVS Run 1	4502	488	0.108
	QMC Run 1	4502	87	0.019
	QMC Run2	4502	227	0.050
	QMC Run3	4502	41	0.009
	SHALSTAB Run 1	4502	272	0.060
	SHALSTAB Run 2	4502	1578	0.351
			Average	**0.0997**

Within the 10-meter model runs the SHALSTAB Run 1 produced the highest number of errors (27%) followed by the second SHALSTAB run (24%), then the QMC run 1 (14%), then QMC run 2 (11%), followed by the BVS run (8%) and the QMC Run 3 (5%) had the lowest errors. Of the 30-meter model runs, the second SHALSTAB run had

the highest number of errors (35%) followed by the BVS model (11%), then the first SHALSTAB run (6%), the second QMC run (5%), the first QMC run (2%) and again the third QMC run had the lowest number of errors (.01%). The two consistent model runs are the second SHALSTAB run and the third QMC model run.

The frequency of debris flows within each instability class also gives an indication of the predictive capacity of the models. The histogram of debris flow frequencies within each instability class (Figure 17) shows that most of the debris flows are captured within the 'Very High' instability class, a positive indication for the models. However, as discussed above concerning Type I error percentages using SHALSTAB, Figure 17 shows that a large percentage of debris flows fall in the 'Very Low' and 'Low' instability classes. These graphs also show how one large error percentage (SHALSTAB run 2), can increase the overall error percentage of the 10-meter data to greater than that of the 30-meter model runs. Looking at these graphs indicates that the 10-meter model runs may actually give fewer Type I errors.

Type II errors for Nelson County are numerous and encompass large portions of the Nelson County area. These errors, described in Table 14 and Table 15, show the overall percentages of Type II errors for each model run with both resolutions of elevation data. In addition, the percentage of Type II errors within the 'Moderate', 'High' and 'Very High' classes are shown.

The overall Type II error percentage using 10-meter elevation data is about 88.4%. This means that about 88% of the grid cells in the 'Moderate' to 'Very High' instability classes are outside the extent of any debris flows. The QMC model Run 2 has the least Type II error percentage with 86.7%, followed by the QMC model Run 1 with 87.2%, the SHALSTAB Run 1 (87.4%), the BVS (88.8%), the QMC Run 3 (89.6%) and SHALSTAB Run 2 with the highest percentage of 90.5%. Within the 'Moderate' instability class, SHALSTAB Run 2 has the highest error percentage of all classes and all models with 96%. The 'High' instability class has a maximum error percentage of 92% using SHALSTAB Run 2 and the 'Very High' class has a maximum percentage of 88% using the QMC Run 3. In general, the 'Very High' instability class has the least amount of Type II errors among all the models with increasing amounts of Type II errors in the lower instability classes.

Using 30-meter data, the overall Type II error percentage is about 90.2%. As with the 10-meter data, the least amount of Type II model error is using the second QMC model run, 88.5%. The next highest error percentage is using the first model run of SHALSTAB (89.3%), followed by the first QMC run and the second SHALSTAB run (90.1%), the third QMC run (91.2%) and the BVS with the highest Type II error percentage of 91.9%. The highest Type II error percentage among all models and within all classes is 96.7% in the 'High' instability class using the second SHALSTAB run. The remaining instability classes and model runs have varying degrees of Type II errors that range from 79% in the 'Very High' instability class of SHALSTAB Run 1 to 95% in the 'Moderate' classes of the BVS Run 1 and SHALSTAB Run 1. In general, the 10-meter model runs have a more consistent variation in the Type II error percentages.

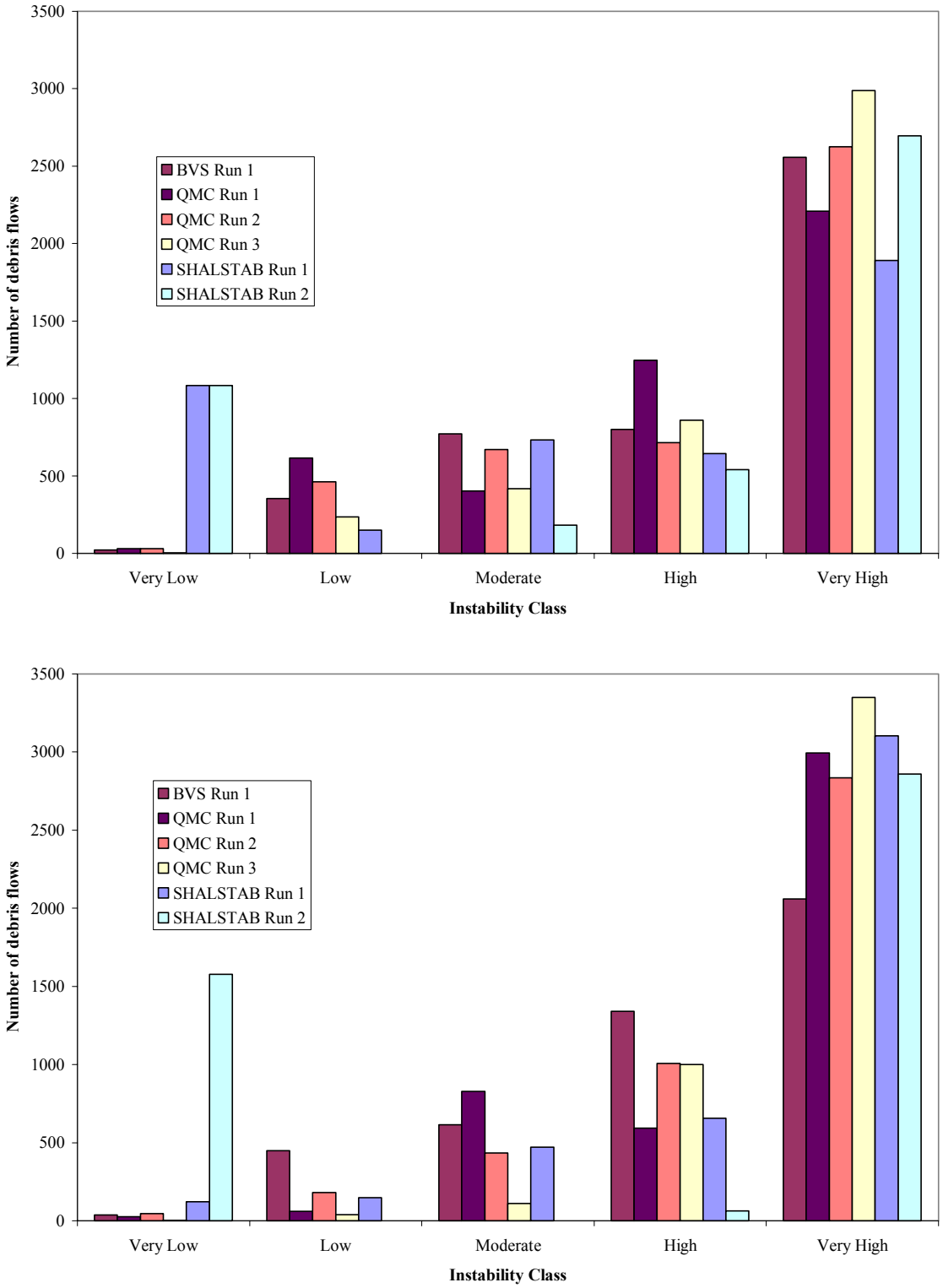

Figure 17. Debris flow frequencies for each model run in Nelson County using 10-meter (top) and 30-meter (bottom) elevation data.

Table 14. Type II error percentages for overall model runs and individual instability classes in Nelson County using 10-meter elevation data.

Instability Class	BVS Run 1 Total cell count	BVS Run 1 Type II cell count	BVS Run 1 Type II error
Very Low	867210	830190	N/A
Low	1461161	1386702	N/A
Moderate	399364	359178	0.899
High	187726	167548	0.893
Very High	132509	112046	0.846
		Total	**0.888**

Instability Class	QMC Run 1 Total cell count	QMC Run 1 Type II cell count	QMC Run 1 Type II error
Very Low	1418816	1372552	N/A
Low	1098465	1020302	N/A
Moderate	258069	228411	0.88507725
High	164970	142535	0.86400558
Very High	107650	91864	0.8533581
		Total	**0.8720927**

Instability Class	QMC Run 2 Total cell count	QMC Run 2 Type II cell count	QMC Run 2 Type II error
Very Low	1326379	1282497	N/A
Low	1065363	1004108	N/A
Moderate	352325	309188	0.8775647
High	141613	121876	0.8606272
Very High	162290	137995	0.8502988
		Total	**0.867167**

Instability Class	QMC Run 3 Total cell count	QMC Run 3 Type II cell count	QMC Run 3 Type II error
Very Low	608336	589817	N/A
Low	1610352	1522732	N/A
Moderate	323132	293544	0.90843371
High	243362	217863	0.89522193
Very High	262788	231708	0.88172976
		Total	**0.8960945**

Instability Class	SHALSTAB Run 1 Total cell count	SHALSTAB Run 1 Type II cell count	SHALSTAB Run 1 Type II error
Very Low	2454186	2318475	N/A
Low	196976	190423	N/A
Moderate	247887	226659	0.9143642
High	83824	70513	0.841203
Very High	65097	49594	0.7618477
		Total	**0.873889**

Instability Class	SHALSTAB Run 2 Total cell count	SHALSTAB Run 2 Type II cell count	SHALSTAB Run 2 Type II error
Very Low	2454186	2318475	N/A
Low	216	215	N/A
Moderate	225254	217039	0.964
High	183452	168225	0.917
Very High	184862	151710	0.821
		Total	**0.905**

Table 15. Type II error percentages for overall model runs and individual instability classes in Nelson County using 30-meter elevation data.

Instability Class	BVS Run 1 Total cell count	BVS Run 1 Type II cell count	BVS Run 1 Type II error	QMC Run 1 Total cell count	QMC Run 1 Type II cell count	QMC Run 1 Type II error
Very Low	689972	663788	N/A	750111	738060	N/A
Low	1236545	1161096	N/A	710543	686990	N/A
Moderate	610554	581912	0.9530885	1041092	963480	0.92545135
High	276676	242696	0.8771849	156427	132990	0.85017292
Very High	229768	201797	0.8782642	385342	329769	0.85578266
		Total	**0.918896**		**Total**	**0.9010513**

Instability Class	QMC Run 2 Total cell count	QMC Run 2 Type II cell count	QMC Run 2 Type II error	QMC Run 3 Total cell count	QMC Run 3 Type II cell count	QMC Run 3 Type II error
Very Low	1054809	1033741	N/A	197445	194296	N/A
Low	817392	780548	N/A	871771	855552	N/A
Moderate	517600	479774	0.9269204	680762	646314	0.94939788
High	364337	317256	0.8707762	761851	692124	0.90847685
Very High	289377	239970	0.8292642	531686	463003	0.87082037
		Total	**0.88533**		**Total**	**0.9124459**

Instability Class	SHALSTAB Run 1 Total cell count	SHALSTAB Run 1 Type II cell count	SHALSTAB Run 1 Type II error	SHALSTAB Run 2 Total cell count	SHALSTAB Run 2 Type II cell count	SHALSTAB Run 2 Type II error
Very Low	1107109	1045505	N/A	2553784	2410209	N/A
Low	841294	827883	N/A	72	67	N/A
Moderate	515616	490835	0.951939	216	192	0.889
High	247717	223835	0.9035916	77649	75089	0.967
Very High	331779	263231	0.7933926	411794	365732	0.888
		Total	**0.892969**		**Total**	**0.901**

4.7 RESOLUTION SENSITIVITY

The previous measures of model performance using various elevation resolutions were aimed at assessing prediction accuracy. In an additional attempt to assess the effects of resolution variability, contingency tables were created to evaluate each model's sensitivity to variations in source data. The contingency tables compare the percentages of grid cells that are classified into the same instability classes. The higher the percentage of cells that are in agreement between the two elevation resolutions the less sensitive the individual models are to variable source resolutions. A summary of the percentages of

cells that are in agreement, have a one class difference, and a two class difference are shown in Table 16.

Table 16. Summary of sensitivity analysis results on the effect of varying resolutions of input elevation data.

Model Run	Percentage of cells in agreement	Percentage of cells with one class difference	Percentage of cells with two class difference
BVS 1	51.4	41.6	6.0
QMC 1	32.7	46.4	16.6
QMC 2	46.3	39.6	10.6
QMC 3	29.0	40.7	21.6
SHALSTAB 1	49.5	26.2	11.5
SHALSTAB 2	84.4	7.0	5.2

The results of the sensitivity analysis indicate that the most sensitive model to variable resolutions is the QMC model run 3 with only 29% of the grid cells classified with the same instability classes in both resolution runs. The least sensitive model is the second SHALSTAB run; however, this is likely due to the fact that most of the grid cells are classified into only two classes overall. The remaining models, in increasing order of sensitivity, are the BVS model (51.4%), SHALSTAB run 1 (49.5%), QMC run 2 (46.3%) and the QMC run 1 (32.7%). The complete contingency tables are listed in Appendix D.

CHAPTER 5. DISCUSSION

The predictive capacity of the instability models is directly dependent upon the physiographic region and distribution of instability within the model development area, Madison County. Therefore, the models developed for this study are only useful in the same topographic settings as Blue Ridge Mountains of Virginia. However, the methodology proposed here allows a means by which a land manager may develop a suitable model. It is important to note that the models used in this study have not been proven to succeed nor fail because no hypothesis has been subjected to testing. However, the SHALSTAB authors have developed a rejectable hypothesis in which random debris flow polygons are compared with actual debris flow polygons. The test was not used in this study because of the inconsistent nature of debris flow mapping standards. This study was more of a comparison of modeling approaches and, as such, focused more on model behavior relative to one another.

The instability thresholds developed are not necessarily indicative of the model's ability to predict debris flows but rather an indication of instability distribution within Madison County. The statistical analysis with the highest instability thresholds was developed from the debris flow inventory and therefore is likely to capture most instability at high values. The distribution of land area with instability scores within the BVS is somewhat bimodal. The SHALSTAB model, on the other hand, assumes that debris flows do not typically occur where there is overland water flow (i.e. water table being higher than the soil depth) and therefore places much of the grid cells into an unconditionally stable class. Because of the large majority of grid cells being classified into the unconditional class, SHALSTAB pushes the instability distribution to the left with lower standardized scores. The SHALSTAB distribution, however, is not typical of a left-skewed curve because there is a large drop-off in instability scores following this large percent to the left. The skew to the left therefore reduces the threshold values so that debris flows can be identified. The distribution of instability scores using the Qualitative Map Combination is the most bell-shaped curve and, as seen in the instability thresholds, falls in the middle between the statistical analysis and SHALSTAB.

Because of the large number of debris flows being captured in the SHALSTAB model at low instability scores the model creates the inverse S-curve where a large drop-off of debris flows occurs low in the scores with few debris flows occurring with high scores. This is the reason for the large amount of Type I errors in both 10- and 30-meter model runs. The threshold curves for both the QMC and the BVS have low numbers of debris flows occurring with low instability scores followed by a large number at higher instability scores, ideal for the purpose of instability zonation. A positive indication that the QMC was designed well is in the strong correlation between the subclass weightings of the QMC and the BVS.

However, the subclass weightings used for the roads factor showed opposite values of instability suggesting that the use of distance to roads may not be a great indication of instability. A better use of a roads layer may be to use road density where the more roads in an area, the more unstable. Moreover, the construction of roads is done with the assumption that roads should be located away from highly unstable areas. Therefore, the use of current road locations may be misleading when assigning weights because roads

are initially located in the safest areas. Despite the roads discrepancies, these two models are very similar in results because of the similarity in other weightings.

The threshold curves developed for these models are dependent upon the desired percentages of debris flows for each instability class. Although this method of assigning threshold values forces the models to act in a similar fashion it does allow a good comparison of model behavior. It is important to note that the percentages used to develop the curves can be altered to fit management objectives. The manipulation of these percentages can help minimize the Type II errors by assigning less area into high instability classes. Adjusting the low instability percentages, though, will result in higher Type I errors. Adjustment of these percentages essentially redistributes the areas assigned to each class. It does not adjust the actual instability values, only the class assignment. However, through various trial runs, the manipulation of threshold percentages can help find the optimal balance between the two types of errors. In addition to the adjustment of threshold percentages, the adjustment of factor subclass designations may have a large effect on the output of the models. Only through many trial runs can these designations be optimized, though and the designations will give varying results depending upon the distribution of factor subclasses within a study area. Therefore, the factor subclass designations used in this study are recommended for future use.

As an alternative to the various factor subclass designations and instability threshold values, an automated form of the QMC and BVS models has been developed using the same factors as this study (excluding SSURGO data) in which the factor subclasses can be manipulated to show the effects of various designations. This essentially equates to the third QMC model run and the only BVS model run. In addition, the weighting system of the QMC may be adjusted for all of the factor subclasses. The BVS automated model uses the factor subclass designations and weightings used in this study for a quick assessment of instability; however, the instability thresholds can be adjusted. The model interface, shown in Figure 18, uses either a 1-step process (BVS) or a 6-step process (QMC) that allows forest managers to quickly assess instability like the SHALSTAB model without spending years on developing the models. The automated model was developed within ArcGIS's Visual Basic for Applications environment.

The distribution of instability classes within Nelson County using 10-meter data gives a clear indication of the relative model behaviors. Both SHALSTAB models tend to classify most of the area into low instability classes. The first and second QMC model runs behave very similarly as do the third QMC model run and the BVS. The similarities between these two pairs of model runs are due to the input factors used in the analyses. The third QMC model run and the BVS both exclude the SSURGO data. With these two model runs placing the most area into the high instability classes, they will be the least likely to have Type I errors. Using 30-meter data, the SHALSTAB default run (#2) tends to classify instability into the extreme classes. This extreme nature of the default SHALSTAB run indicates that the availability of geotechnical data is extremely important in applying SHALSTAB to the Blue Ridge Mountains of Virginia with reduced resolution elevation data. With 30-meter data, the first two QMC model runs are again very similar; however, the BVS Run 1 and the QMC Run 3 give much different results. The QMC run 3 places the most amount of land area into the high instability classes. This result has a pronounced effect on the number of Type I errors. It is clear from the distribution of land area in instability classes that the third QMC run and the BVS run

have the best capability to capture instability because of the percent area assigned to the high classes.

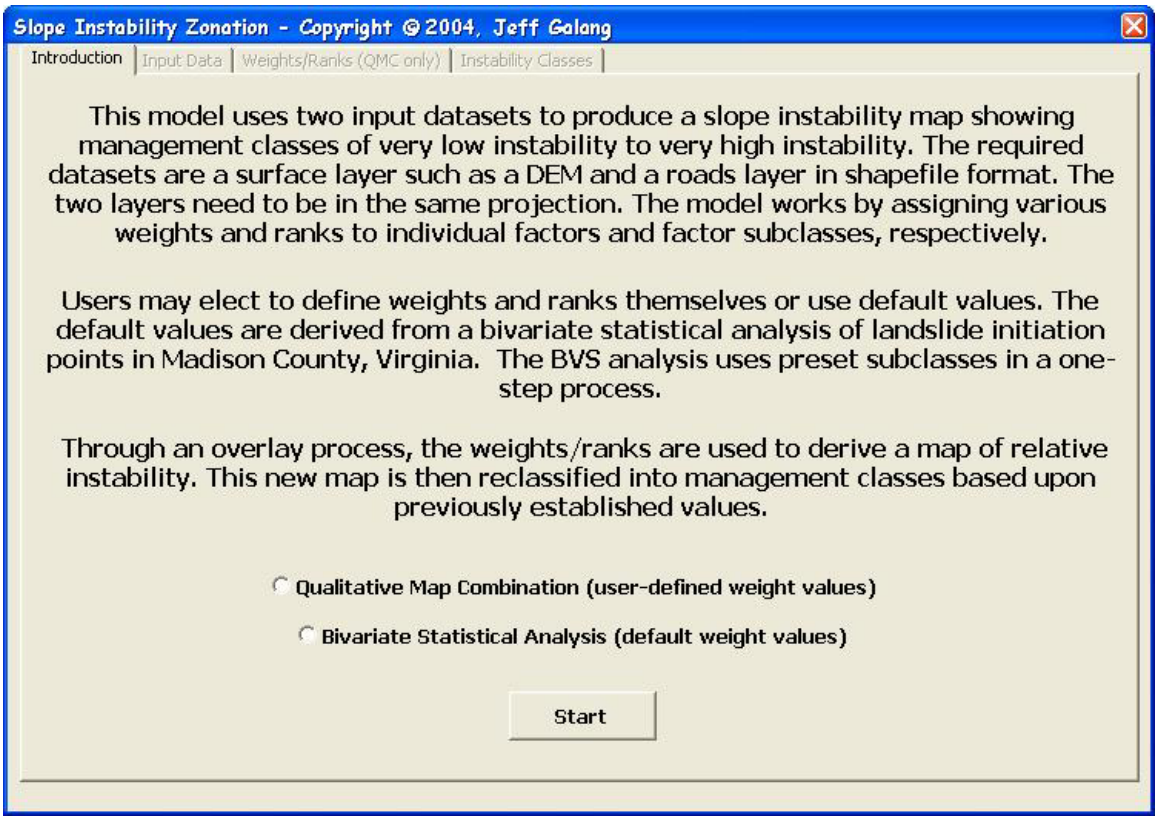

Figure 18. User interface of the automated QMC and BVS models.

When looking at the spatial distribution of instability classes an interesting feature of the first SHALSTAB model is that most of the instability in the area is found in the drainages rather than the slope shoulders. All of the other models predict instability high on the slope including the second SHALSTAB run. One reason for this may be due to the importance that SHALSTAB places on increased pore pressures from water accumulation in drainages. The reason for the second SHALSTAB run placing instability high on the slopes may also be due to the soil depth factor. The first SHALSTAB run uses a constant soil depth that is twice that of the second run. Because of the much more shallow soils in the second run, the model may tend to place instability higher on the slopes where shallow soils have a high chance of mobilizing into debris flows.

The effect of excluding SSURGO data from the third QMC run and the BVS model is that large-scale topographic features of a particular watershed become more pronounced. This is because the weighting system used for the SSURGO data classifies entire mountain regions with high instability weights. This may reduce the importance of local slope and curvature features. By removing the generally high instability weights of entire mountainsides may give more weight to the local topographic features. Without a better weighting scheme for the SSURGO data, the exclusion of soils may give a better indication of instability. This may give more credit to the automated model using only the four remaining factors. The effect of excluding vegetation data is minimal because the

vegetation data for Madison County puts the majority of the mountainsides into forest cover. This is essentially the same effect of the exclusion of SSURGO data except that the vegetation data is at a much smaller scale and can only be interpreted at that scale. Thus, the models become more of a regional analysis as opposed to a medium scale analysis.

The evaluation of Type I and Type II errors gives another indication of relative model behavior; however, because of the nature of debris flow mapping the errors cannot be interpreted as an absolute value. Rather, the errors give only a relative indication of model behavior against one another. The result of the Type I error analysis with 10-meter data clearly indicates the performance of the third QMC run and the BVS run as the best of the six models. As discussed previously, this is due to the distribution of instability classes within the county which is dependent upon the instability thresholds. If a model classifies more area into high instability classes the likelihood of a single grid cell with a high instability class occurring within a debris flow becomes much greater. This may be the cause of the lower Type I error percentages using 30-meter data because the 30-meter model runs classify a consistently higher percentage of land area into high instability classes.

The Type II errors, although numerous, also give relative indications of model behavior. The performance of the models using 30-meter data compared to using 10-meter data reflects the number of Type I errors. Because the 30-meter classifies more area into the high instability classes there are less Type I errors; however, for this same reason, there are more Type II errors using 30-meter data. For individual model runs, both resolutions yield the least amount of Type II errors in the second QMC run. The remainder of the model runs yields little differences in the amounts of Type II errors. Type II error interpretations can be misleading because of the time frame of interpretation. The extent of instability in an area can be misrepresented because of the use of a debris flow inventory from a single event. The actual area of instability is likely to be more than what is represented which would result in fewer Type II errors. Simply because there are many Type II errors does not necessarily imply that there is poor model performance. In fact, these 'errors' may not be actual errors as they simply indicate unstable areas that have yet to fail. Rather, a better interpretation of the Type II errors is that these areas are the likely sources of instability in the future given a certain storm event. Therefore, areas with Type II errors need to be watched carefully in terms of forest management.

As the Type I errors are the more serious of the two errors because they may lead to management activities within a hazardous area, the evaluation of the performance of the models is based primarily on the Type I errors rather than the Type II errors. However, to assess the most 'efficient' or 'optimal' model, the goal would be to minimize both types of errors. Therefore, the ideal model is the one that captures the most debris flows with the least amount of high instability. To better assess this 'efficiency', a summary of the error percentages for each model at both resolutions is presented in Table 17 with the models being sorted from the lowest Type I error percentages to the highest Type I error percentage.

With the concept of 'efficiency' in mind the best performing models using 10-meter data are the third QMC model run, the BVS and QMC Run 2. Of these models, the second QMC run has a relatively low Type I error percentage and the lowest Type II

error percentage. However, both of these models, the second QMC run and the BVS run, are still the most efficient. The first QMC model run performs the next best and both SHALSTAB models perform the worst with the first model run being the worse than the second.

Table 17. Summary of Type I and II errors for comparison of model 'efficiency'.

Resolution					
10-meter elevation data			30-meter elevation data		
Model Run	**Type I error percent**	**Type II error percent**	**Model Run**	**Type I error percent**	**Type II error percent**
QMC Run 3	5.3	89.6	QMC Run 3	0.9	91.2
BVS Run 1	8.3	88.8	QMC Run 1	1.9	90.1
QMC Run 2	11.0	86.7	QMC Run 2	5.0	88.5
QMC Run 1	14.3	87.2	SHALSTAB Run 1	6.0	89.3
SHALSTAB Run 2	24.1	90.5	BVS Run 1	10.8	91.9
SHALSTAB Run 1	27.4	87.4	SHALSTAB Run 2	35.1	90.1
Average	**15.06**	**88.40**	**Average**	**9.97**	**90.20**

Using the 30-meter data the QMC models have the lowest Type I error percentages while the first SHALSTAB run performs much better than the second. Although the third QMC run and the first QMC run have the lowest Type I error percentages, the most efficient model would be the second QMC run with the lowest Type II error percentage a relatively low Type I error percent. The first SHALSTAB run and the second QMC run both perform about the same with the QMC Run 2 performing slightly better. Although the 30-meter model runs produce less Type I errors, the interpretation of their performances is simply that the models tend to over generalize the area into the higher instability classes (as seen in the higher Type II error percentages) therefore producing less Type I errors. However, the 30-meter runs tend to miss the local topographic features apparent in the 10-meter data. Therefore, as an overall generalization of model performance, the 10-meter model runs using the second QMC model and the BVS model seem to best capture the actual instability of the area. When using 30-meter data, however, the first SHALSTAB run seems to be equally capable of capturing instability as the second QMC run while the BVS run decreases dramatically in its performance.

The sensitivities of these models to resolution variability indicate that the SHALSTAB Run 2 is the least sensitive to variations. However, due to the poor predictive capacity of this model the sensitivity makes little difference. The most sensitive model, the QMC Run 3, although more sensitive to variations still has the predictive power to be a useful model. Overall, the second QMC model, with its relatively low sensitivity and high efficiency seems to be the best available model for assessing instability given the option of various resolutions of source data.

CHAPTER 6. CONCLUSIONS

Although the indications of predictive capacities among the various slope instability models do not represent absolute values of the potential for debris flows to occur, the methods and results presented in this study do give a valuable means by which to compare model behaviors. The largest indication of performance is that the use of default values in the Shallow Landsliding Stability (SHALSTAB) model does not yield good results in this area of the country. However, if good geotechnical data are available, the SHALSTAB model can be useful in predicting instability. Generally, among the models the three Qualitative Map Combination (QMC) models all have a high capacity for identifying instability. However, when assessing the best models in terms of efficiency the second QMC model run has the best predictive capabilities when using either 10-meter or 30-meter data. When using only high resolution data, the Bivariate Statistical Analysis (BVS) is an efficient model at predicting instability. However, the BVS is not very good when using 30-meter data. When high resolution elevation data are not available, the SHALSTAB run with site-specific parameters has good predictive abilities for assessing instability and is very efficient. From these findings, it is clear that quantitative and deterministic models are not necessarily indicative of better results.

These models may be used in other parts of the Blue Ridge Mountains without having to develop new weightings or instability classification thresholds. The use of a debris flow inventory is not necessary unless the models are applied to areas outside the Blue Ridge Mountains. In the case of applying these models elsewhere, the debris flow inventory is essential for the BVS model in order to develop new weightings. This is the shortcoming of the statistical approach and the benefit of the other approaches. When applying the heuristic and/or deterministic approaches, such as the QMC and SHALSTAB, respectively, to other areas without the use of a debris flow inventory it necessitates the need to develop another approach to instability classification. One possible method would be to assign individual instability classes based upon the standardized instability distributions. For instance, classifying into the ‘Very High’ class the top 5% of instability scores and into the ‘High’ class the next 10% and so on. Research on this approach may be the next logical step to the comparison of slope instability models.

Various issues have been identified in this study that address methods of debris flow inventory mapping. While inventory methods are becoming more of a subject of interest, there needs to be more effort in accurately identifying the various components of debris flows and landslides in general. Identification of source areas, run-out paths and depositional areas can become increasingly more accurate with the new technologies used to obtain aerial photographs. For example, the Virginia Base Mapping Project (VBMP) has been able to create aerial photographs with resolutions of less than one foot. This type of aerial photography can be invaluable in identifying debris flow outlines therefore allowing better assessments of accuracy. Moreover, the development of better elevation data such as laser altimetry, although not available in many regions, will prove very useful in the accuracies of these models.

Other potentially valuable assessments include the identification of the size and shape of debris flows that initiate from unstable areas as well as the run-out paths of the

debris flow. This could be accomplished by using the amount and type of soil material in areas of high instability to estimate the volumes of future debris flows. Knowing the size of potential debris flows and the location of initiation, the prediction of debris flow depositional areas can be identified. Forest managers and community planners could benefit greatly from this knowledge.

The methods developed for this study have allowed a systematic comparison of various modeling approaches and their behaviors. These various GIS techniques for assessing slope instability have been applied in many regions worldwide; however, the decision as to which model to use seems to still be very subjective for many areas. The standardization techniques used in this study may be applied to almost any instability zonation project allowing a worldwide comparison of instability for certain landslide types. However, the various instability zonation projects still need to be developed for each region and for each landslide type. The standardization techniques proposed in this study simply allow various model outputs to be directly compared. In addition, these techniques have allowed an assessment of the appropriate modeling approach to use in the absence of high resolution data.

For forest management, the use of these modeling approaches can prove useful for initial planning phases for which land owners need to identify the acreage of specific stands susceptible to instability as well as the spatial distribution of instability. This information can then be used to further assess instability in a more detailed fashion with field visits. The automated models (SHALSTAB and the models developed in this study) are especially useful for this because managers can obtain this information quickly instead of spending large amounts of money and time developing the instability maps. This knowledge can be applied to various forestry activities such as timber harvesting, road-building and trail-building. In addition, these models can prove very useful in development projects in which communities need to locate the best locations for building houses, roads and trails. This is extremely important in developing countries where the landscape is such that people are forced to live in marginal lands (i.e. marginalization). Furthermore, developing countries are gaining more access to these technologies and new datasets are being developed for remote parts of the world each year. Other potential benefits from this research could include the use of the instability maps for use in insurance assessments by local agencies as well as by the Federal Emergency Management Agency (FEMA).

Future evaluations of slope instability and modeling comparisons should include differing input factors such as vegetation, road density and geology. However, it is essential that researchers understand the limitations of using various scales of data and the implications for interpreting the outputs. The models described in this study are topographically driven and require a minimum amount of data, an important aspect in developing countries where the availability of data is limited.

REFERENCES

Alexander, D.E. (1995). A Survey of the Field of Natural Hazards and Disaster Studies. In: Carrara, A. and Guzzetti, F. (Eds), Geographical Information Systems in Assessing Natural Hazards. Advances in Natural and Technological Hazards Research. Kluwer Academic Publishers, Vol 5: Dordrecht, 1-19.

Anbalagan, R. (1992). Landslide Hazard Evaluation and Zonation Mapping in Mountainous Terrain. Engineering Geology, 32(4): 269-277.

Anbalagan, R. and Singh, B. (1996). Landslide Hazard and Risk Assessment Mapping of Mountainous Terrains - a Case Study from Kumaun Himalaya, India. Engineering Geology, 43(4): 237-246.

ASTM (2001). D 2487-00 Standard Practice for Classification of Soils for Engineering Purposes (Unified Soil Classification System). In: Annual Book of ASTM Standards Vol 04.08: 246-257.

Auer, K.M. (1989). Geotechnical Investigation of Debris Avalanche Activity Associated with Hurricane Camille in Central Virginia. Master's Thesis, Kent State University, 137 pp.

Baeza, C. and Corominas, J. (2001). Assessment of Shallow Landslide Susceptibility by Means of Multivariate Statistical Techniques. Earth Surface Processes and Landforms, 26(12): 1251-1263.

Bailey, C.M., Berquist, P.J., Mager, S.M., Knight, B.D., Shotwell, N.L. and Gilmer, A.K. (2003). Bedrock Geology of the Madison Quadrangle, Virginia. Virginia Division of Mineral Resources, Publication 157, 22 pp., 1 plate 1:24,000.

Bolstad, P.V. and Smith, J.L. (1992). Errors in GIS: Assessing Spatial Data Accuracy. Journal of Forestry, 90(11): 21-29.

Bolt, B.A., Horn, W.L., Macdonald, G.A. and Scott, R.F. (1975). Geological Hazards. Springer-Verlag, New York. 328 pp.

Bonham-Carter, G.F., Agterberg, F.P. and Wright, D.F. (1990). Weights of Evidence Modelling: A New Approach to Mapping Mineral Potential. In: Agterberg, F.P. and Bonham-Carter, G.F. (Eds), Statistical Applications in the Earth Sciences. Geological Survey of Canada Paper, Vol 89(9): Ottawa, 171-183.

Brabb, E.E. (1984). Innovative Approaches to Landslide Hazard Mapping. In: Proceed. IV Int. Symp. Landslides, Toronto, pp. 307-324.

Brunsden, D. and Prior, D.B. (Editors) (1984). Slope Instability, Vol. John Wiley and Sons, Chichester, U.K., 620 pp.

Burrough, P.A. (1986). Principles of Geographical Information Systems for Land Resources Assessment. Clarendon Press, Oxford. 194 pp.

Campbell, R.H. and Chirico, P. (1999). Geographic Information System (GIS) Procedure for Preliminary Delineation of Debris-Flow Hazard Areas from a Digital Terrain Model, Madison County, Virginia. U.S. Geological Survey, Open-File Report 99-336, 23 pp.

Carrara, A. (1983). Multivariate Models for Landslide Hazard Evaluation. Mathematical Geology, 15: 403-426.

Carrara, A., Cardinali, M., Detti, R., Guzzetti, F., Pasqui, V. and Reichenbach, P. (1991). GIS Techniques and Statistical Models in Evaluating Landslide Hazard. Earth Surface Processes and Landforms, 16(5): 427-445.

Carrara, A., Cardinali, M., Guzzetti, F. and Reichenbach, P. (1995a). GIS Technology in Mapping Landslide Hazard. In: Carrara, A. and Guzzetti, F. (Eds), Geographical Information Systems in Assessing Natural Hazards. Advances in Natural and Technological Hazards Research. Kluwer Academic Publishers, Vol 5: Dordrecht, 135-175.

Carrara, A., Cardinali, M., Guzzetti, F. and Reichenbach, P. (1995b). GIS-Based Techniques for Mapping Landslide Hazard. Available at http://deis158.deis.unibo.it/ April 16 2004.

Carrara, A. and Guzzetti, F. (Editors) (1995). Geographical Information Systems in Assessing Natural Hazards. Advances in Natural and Technological Hazards Research, Vol. 5. Kluwer Academic Publishers, Dordrecht, 353 pp.

Carro, M., De Amicis, M., Luzi, L. and Marzorati, S. (2003). The Application of Predictive Modeling Techniques to Landslides Induced by Earthquakes: The Case Study of the 26 September 1997 Umbria-Marche Earthquake (Italy). Engineering Geology, 69(1-2): 139-159.

Chen, B. (1990). Landslide Prediction Using Landsat TM-Images and Terrain Information. Master of Science, University of Alaska Fairbanks, Fairbanks, 90 pp.

Chung, C.-J.F., Fabbri, A.G. and van Westen, C.J. (1995). Multivariate Regression Analysis for Landslide Hazard Zonation. In: Carrara, A. and Guzzetti, F. (Eds), Geographical Information Systems in Assessing Natural Hazards. Advances in Natural and Technological Hazards Research. Kluwer Academic Publishers, Vol 5: Dordrecht, 107-133.

Clerici, A., Perego, S., Tellini, C. and Vescovi, P. (2002). A Procedure for Landslide Susceptibility Zonation by the Conditional Analysis Method. Geomorphology, 48(1): 349-364.

Crozier, M.J. (1984). Field Assessment of Slope Instability. In: Prior, D.B. (Ed), Slope Instability. John Wiley & Sons, Vol Chichester, U.K., 103-142.

Crozier, M.J. (1986). Landslides: Causes, Consequences and Environment. Croom Helm, London. 251 pp.

Cruden, D.M. (1991). A Simple Definition of a Landslide. Bulletin of the International Association of Engineering Geology, 43: 27-29.

Cruden, D.M. and Varnes, D.J. (1996). Landslide Types and Processes. In: Turner, A.K. and Schuster, R.L. (Eds), Landslides: Investigation and Mitigation. Transportation Research Board Special Report. National Academy Press, Vol 247: Washington D.C., 36-75.

Dai, F.C. and Lee, C.F. (2002a). Landslides on Natural Terrain: Physical Characteristics and Susceptibility Mapping in Hong Kong. Mountain Research and Development, 22(1): 40-47.

Dai, F.C. and Lee, C.F. (2002b). Landslide Characteristics and Slope Instability Modeling Using GIS, Lantau Island, Hong Kong. Geomorphology, 42(3-4): 213-228.

Davis, C.J. and Reisinger, T.W. (1990). Evaluating Terrain for Harvesting Equipment Selection. Journal of Forest Engineering, 2(1): 9-16.

Davis, S.N. and Karzulovic, K.J. (1963). Landslides at Lago Rinihue, Chile. Bulletin of the International Association of Engineering Geology, 53(6): 1403-1414.

Dietrich, W.E., Bellugi, D. and de Asua, R.R. (2001). Validation of the Shallow Landslide Model, SHALSTAB, for Forest Management. In: Wigmosta, M.S. and Burges, S.J. (Eds), Land Use and Watersheds - Human Influence on Hydrology and Geomorphology in Urban and Forest Areas. Water Science and Application. American Geophysical Union, Vol 2: Washington, D.C., 195-227.

Ellen, S.D. and Fleming, R.W. (1987). Mobilization of Debris Flows from Soil Slips, San Francisco Bay Region, California. In: Costa, J.E. and Wieczorek, G.F. (Eds), Debris Flows/Avalanches: Process, Recognition and Mitigation. Geological Society of America, Reviews in Engineering Geology, Vol 7: Boulder, CO, 31-40.

Espizua, L.E. and Bengochea, J.D. (2002). Landslide Hazard and Risk Zonation Mapping in the Rio Grande Basin, Central Andes of Mendoza, Argentina. Mountain Research and Development, 22(2): 177-185.

Gao, J. (1992). Modeling Landslide Susceptibility from a DTM in Nelson County, Virginia: A Remote Sensing-GIS Approach. PhD Dissertation, University of Georgia, Athens, GA.

Gao, J. (1993). Identification of Topographic Settings Conducive to Landsliding from DEM in Nelson County, Virginia, U.S.A. Earth Surface Processes and Landforms, 18: 579-591.

Glade, T. (2001). Landslide Hazard Assessment and Historical Landslide Data - an Inseparable Couple? In: Frances, F. (Ed), The Use of Historical Data in Natural Hazard Assessments. Kluwer Academic, Vol 17: Dordrecht, Netherlands, 153-168.

Glade, T. (2003). Landslide Occurrence as a Response to Land Use Change: A Review of Evidence from New Zealand. CATENA, 51(3-4): 297-314.

Gritzner, M.L., Marcus, A.W., Aspinall, R. and Custer, S.G. (2001). Assessing Landslide Potential Using GIS, Soil Wetness Modeling and Topographic Attributes, Payette River, Idaho. Geomorphology, 37(1-2): 149-165.

Gupta, R.P. and Joshi, B.C. (1990). Landslide Hazard Zoning Using the GIS Approach--a Case Study from the Ramganga Catchment, Himalayas. Engineering Geology, 28(1-2): 119-131.

Guthrie, R.H. (2002). The Effects of Logging on Frequency and Distribution of Landslides in Three Watersheds on Vancouver Island, British Columbia. Geomorphology, 43(3-4): 273-292.

Guzzetti, F., Carrara, A., Cardinali, M. and Reichenbach, P. (1999). Landslide Hazard Evaluation: A Review of Current Techniques and Their Application in a Multi-Scale Study, Central Italy. Geomorphology, 31(1-4): 181-216.

Hack, J.T. and Goodlett, J.C. (1960). Geomorphology and Forest Ecology of a Mountain Region in the Central Appalachians. U.S. Geological Survey, Professional Paper 347, 66 pp.

Hammond, C., Hall, D., Miller, S. and Swetik, P. (1992). Level I Stability Analysis (LISA) Documentation for Version 2.0. U.S.D.A. Forest Service, General Technical Report INT-285, 121 pp.

Hansen, A. (1984). Landslide Hazard Analysis. In: Prior, D.B. (Ed), Slope Instability. John Wiley & Sons, Vol Chichester, U.K., 523-602.

Harrison, P. and Pearce, F. (2000). AAAS Atlas of Population and Environment. American Association for the Advancement of Science and the University of California Press, Berkeley. 204 pp.

Hutchinson, J.N. (1968). Mass Movement. In: Fairbridge, R.W. (Ed), Encyclopedia of Geomorphology. Reinhold Book Corporation, Vol New York, 688-696.

IDNDR (1987). International Decade for Natural Disaster Reduction. 42nd Session of the General Assembly, United Nations. Available at http://www.un.org/documents/ga/res/42/a42r169.htm April 16 2004.

IFRCRCS (1993). World Disasters Report 1993. International Federation of Red Cross and Red Crescent Societies, Martinus Nijhoff Publishers, Dordrecht. 124 pp.

IFRCRCS (1994). World Disasters Report 1994. International Federation of Red Cross and Red Crescent Societies, Martinus Nijhoff Publishers, Dordrecht. 176 pp.

Iverson, R.M. (2000). Landslide Triggering by Rain Infiltration. Water Resources Research, 36(7): 1897-1910.

Ives, J.D. and Messerli, B. (1989). The Himalayan Dilemma: Reconciling Development and Conservation. Routledge, New York. 295 pp.

Jade, S. and Sarkar, S. (1993). Statistical Models for Slope Instability Classification. Engineering Geology, 36(1-2): 91-98.

Jakob, M. (2000). The Impacts of Logging on Landslide Activity at Clayoquot Sound, British Columbia. CATENA, 38(4): 279-300.

Kienholz, H. (1977). Kombinierte Geomorphologische Gefahrenkarte 1 : 10 000 Von Grindelwald. CATENA, 3(3-4): 265-294.

Kienholz, H., Schneider, G., Bichsel, M., Grunder, M. and Mool, P. (1984). Mapping of Mountain Hazards and Slope Stability. Mountain Research and Development, 4(3): 247-266.

Kleim, R.F. and Skaugset, A.E. (2003). Modelling Effects of Forest Canopies on Slope Stability. Hydrological Processes, 17(7): 1457-1467.

Leroi, E., Rouzeau, O., Scanvic, J.Y., Weber, C.C. and Vargas, G. (1992). Remote-Sensing and GIS Technology in Landslide Hazard Mapping in the Colombian Andes. Episodes, 15(1): 32-35.

Lin, M.-L. and Tung, C.-C. (2003). A GIS-Based Potential Analysis of the Landslides Induced by the Chi-Chi Earthquake. Engineering Geology, In Press, Corrected Proof.

Lin, P.-S., Lin, J.-Y., Hung, J.-C. and Yang, M.-D. (2002). Assessing Debris-Flow Hazard in a Watershed in Taiwan. Engineering Geology, 66(3-4): 295-313.

Luzi, L. and Pergalani, F. (1996). Applications of Statistical and GIS Techniques to Slope Instability Zonation (1:50.000 Fabriano Geological Map Sheet). Soil Dynamics and Earthquake Engineering, 15(2): 83-94.

Montgomery, D.R. and Dietrich, W.E. (1994). A Physically Based Model for the Topographic Control on Shallow Landsliding. Water Resources Research, 30(4): 1153-1171.

Montgomery, D.R., Sullivan, K. and Greenberg, H.M. (1998). Regional Test of a Model for Shallow Landsliding. Hydrological Processes, 12(6): 943-955.

Montgomery, D.R., Schmidt, K.M., Greenberg, H.M. and Dietrich, W.E. (2000). Forest Clearing and Regional Landsliding. Geology, 28(4): 311-314.

Morgan, B.A. and Wieczorek, G.F. (1996). Inventory of Debris Flows and Landslides Resulting from the June 27, 1995, Storm in the North Fork Moormans River, Shenandoah National Park. U.S. Geological Survey, Open-File Report 96-503, 10, 1 plate 1:24,000 pp.

Morgan, B.A., Wieczorek, G.F., Campbell, R.H. and Gori, P.L. (1997). Debris-Flow Hazards in Areas Affected by the June 27, 1995, Storm in Madison County, Virginia. U.S. Geological Survey, Open-File Report 97-438, 15 pp.

Morgan, B.A., Iovine, G., Chirico, P. and Wieczorek, G.F. (1999a). Inventory of Debris Flows and Floods in the Lovingston and Horseshoe Mountain, Va, 7.5' Quadrangles, from the August 19/20, 1969, Storm in Nelson County, Virginia. U.S. Geological Survey, Open-File Report 99-518, pp.

Morgan, B.A., Wieczorek, G.F. and Campbell, R.H. (1999b). Historical and Potential Debris-Flow Hazard Map of Area Affected by the June 27, 1995, Storm in Madison County, Virginia. U.S. Geological Survey, Geologic Investigation Series Map I-2623B, 1:24,000.

Morgan, B.A., Wieczorek, G.F. and Campbell, R.H. (1999c). Map of Rainfall, Debris Flows, and Flood Effects of the June 27, 1995 Storm in Madison County, Virginia. U.S. Geological Survey, Geologic Investigation Series Map I-2623A, 1:24,000.

Morgan, B.A., Eaton, L.S. and Wieczorek, G.F. (2003). Pleistocene and Holocene Colluvial Fans and Terraces in the Blue Ridge Region of Shenandoah National Park. U.S. Geological Survey, Open-File Report 03-410, 25 pp., 1 plate 1:100,000.

Morgan, B.W. (1968). An Introduction to Bayesian Statistical Decision Process. Prentice-Hall, New York. 116 pp.

Morrissey, M., Wieczorek, G.F. and Morgan, B.A. (2001a). A Comparative Analysis of Hazard Models for Predicting Debris Flows in Madison County, Virginia. U.S. Geological Survey, Open-File Report 01-0067, 14 pp.

Morrissey, M., Wieczorek, G.F. and Morgan, B.A. (2001b). Regional Application of a Transient Hazard Model for Predicting Initiation of Debris Flows in Madison County, Virginia. U.S. Geological Survey, Open File Report 01-481, 7 pp.

Ohlmacher, G.C. and Davis, J.C. (2003). Using Multiple Logistic Regression and GIS Technology to Predict Landslide Hazard in Northeast Kansas, USA. Engineering Geology, 69(3-4): 331-343.

O'Loughlin, E.M. (1986). Prediction of Surface Saturation Zones in Natural Catchments by Topographic Analysis. Water Resources Research, 22: 794-804.

Pachauri, A.K. and Pant, M. (1992). Landslide Hazard Mapping Based on Geological Attributes. Engineering Geology, 32(1-2): 81-100.

Pachauri, A.K., Gupta, P.V. and Chander, R. (1998). Landslide Zoning in a Part of the Garhwal Himalayas. Environmental Geology, 36(3-4): 325-334.

Pack, R.T., Tarboton, D.G. and Goodwin, C.N. (1998). SINMAP, a Stability Index Approach to Terrain Stability Hazard Mapping. Available at http://www.engineering.usu.edu/dtarb/sinmap.htm April 16 2004.

Prandini, L., Guidicini, G., Bottura, J.A., Poncano, W.L. and Santos, A.R. (1977). Behavior of the Vegetation in Slope Stability: A Critical Review. Bulletin of the International Association of Engineering Geology, 16: 51-55.

Rowbotham, D.N. and Dudycha, D. (1998). GIS Modelling of Slope Stability in Phewa Tal Watershed, Nepal. Geomorphology, 26(1): 151-170.

Saha, A.K., Gupta, R.P. and Arora, M.K. (2002). GIS-Based Landslide Hazard Zonation in the Bhagirathi (Ganga) Valley, Himalayas. International Journal of Remote Sensing, 23(2): 357-369.

Sarkar, S. and Kanungo, D.P. (2004). An Integrated Approach for Landslide Susceptibility Mapping Using Remote Sensing and GIS. Photogrammetric Engineering & Remote Sensing, 70(5): 617-625.

Schuster, R.L. and Krizek, R.J. (Editors) (1978). Landslides: Analysis and Control. Transportation Research Board Special Report, Vol. 176. National Academy of Sciences, Washington D.C., 243 pp.

Schuster, R.L. (1996). Socioeconomic Significance of Landslides. In: Turner, A.K. and Schuster, R.L. (Eds), Landslides: Investigation and Mitigation. Transportation Research Board Special Report. National Academy Press, Vol 247: Washington D.C., 12-35.

Schuster, R.L. and Highland, L.M. (2001). Socioeconomic and Environmental Impacts of Landslides in the Western Hemisphere. U.S. Geological Survey, Open-file Report 01-0276, 23 pp.

Sharpe, C.F.S. (1938). Landslides and Related Phenomena. Columbia University Press, New York. 137 pp.

Shaw, S.C. and Johnson, D.H. (1995). Slope Morphology Model Derived from Digital Elevation Data. In: Proceedings of the Northwest ARC/INFO Users Conference, Coeur d'Alene, ID, pp. 16.

Sidle, R.C., Pearce, A.J. and O'Loughlin, C.L. (1985). Hillslope Stability and Land Use. Water Resources Monograph, 11. American Geophysical Union, Washington D.C., 140 pp.

Sidle, R.C. (1992). A Theoretical-Model of the Effects of Timber Harvesting on Slope Stability. Water Resources Research, 28(7): 1897-1910.

Sidle, R.C. and Wu, W.M. (2001). Evaluation of the Temporal and Spatial Impacts of Timber Harvesting on Landslide Occurrence. In: Wigmosta, M.S. and Burges, S.J. (Eds), Land Use and Watersheds - Human Influence on Hydrology and Geomorphology in Urban and Forest Areas. Water Science and Application. American Geophysical Union, Vol 2: Washington, 179-193.

Smith, K. (1991). Environmental Hazards: Assessing Risk and Reducing Disaster. Routledge Physical Environment. Routledge, London. 391 pp.

Soeters, R. and van Westen, C.J. (1996). Slope Instability Recognition, Analysis, and Zonation. In: Turner, A.K. and Schuster, R.L. (Eds), Landslides: Investigation and Mitigation. Transportation Research Board Special Report. National Academy Press, Vol 247: Washington D.C., 129-177.

Stampfer, K., Lexer, M.J., Vacik, H., Hochbichler, E., Durrstein, H. and Spork, J. (2001). CONES - a Computer Based Multiple Criteria Decision Support Tool for Timber Harvest Planning in Steep Terrain. In: Proceedings of the 24th Annual Meeting of the Council on Forest Engineering, Appalachian Hardwoods - Managing Change, Snowshoe, West Virginia, pp. 15-19.

Stevenson, P.C. (1977). An Empirical Method for the Evaluation of Relative Landslide Risk. Bulletin of the International Association of Engineering Geologists, 16: 69-72.

Tang, S.M., Franklin, J.F. and Montgomery, D.R. (1997). Forest Harvest Patterns and Landscape Disturbance Processes. Landscape Ecology, 12(6): 349-363.

Temesgen, B., Mohammed, M.U. and Korme, T. (2001). Natural Hazard Assessment Using GIS and Remote Sensing Methods, with Particular Reference to the Landslides in the Wondogenet Area, Ethiopia. Physics and Chemistry of the Earth, Part C: Solar, Terrestrial & Planetary Science, 26(9): 665-675.

Terlien, M.T.J., van Westen, C.J. and van Asch, T.W.J. (1995). Deterministic Modelling in GIS-Based Landslide Hazard Assessment. In: Guzzetti, F. (Ed), Geographical

Information Systems in Assessing Natural Hazards. Advances in Natural and Technological Hazards Research. Kluwer Academic Publishers, Vol 5: Dordrecht, 57-77.

Terzaghi, K. (1950). Mechanisms of Landslides. In: Application of Geology to Engineering Practice, Berkey Volume. Geological Society of America, Vol New York, 83-123.

Turner, A.K. and Schuster, R.L. (Editors) (1996). Landslides: Investigation and Mitigation. Transportation Research Board Special Report, Vol. 247. National Academy Press, Washington, D.C., 673 pp.

Turrini, M.C. and Visintainer, P. (1998). Proposal of a Method to Define Areas of Landslide Hazard and Application to an Area of the Dolomites, Italy. Engineering Geology, 50(3-4): 255-265.

U.S. Dept of Agriculture, N.R.C.S. (2003). National Soil Survey Handbook, Title 430-VI. Available at: http://soils.usda.gov/technical/handbook/ August 24 2004.

van Westen, C.J. (1994). GIS in Landslide Hazard Zonation: A Review, with Examples from the Colombian Andes. In: Heywood, D.I. (Ed), Mountain Environments and Geographic Information Systems. Taylor and Francis, Vol 1: London, 135-165.

van Westen, C.J. (1997a). Deterministic Landslide Hazard Zonation. In: Ardanza, G.C. (Ed), ILWIS 2.1 for Windows Application Guide. ITC, Vol 1: Enschede, Netherlands, 85-98.

van Westen, C.J. (1997b). Statistical Landslide Hazard Analysis. In: Ardanza, G.C. (Ed), ILWIS 2.1 for Windows Application Guide. ITC, Vol 1: Enschede, Netherlands, 73-84.

van Westen, C.J., Rengers, N., Terlien, M.T.J. and Soeters, R. (1997). Prediction of the Occurrence of Slope Instability Phenomena through GIS-Based Hazard Zonation. Geologische Rundschau, 86(2): 404-414.

Varnes, D.J. (1958). Landslide Types and Processes. In: Eckel, E.B. (Ed), Landslides and Engineering Practice. Highway Research Board Special Report. National Research Council, Vol 29: Washington D.C., 20-47.

Varnes, D.J. (1978). Slope Movement Types and Processes. In: Schuster, R.L. and Krizek, R.J. (Eds), Landslides: Analysis and Control. Transportation Research Board Special Report. National Academy of Sciences, Vol 176: Washington, D.C., 11-33.

Varnes, D.J. (1984). Landslide Hazard Zonation: A Review of Principles and Practice. UNESCO, Paris. 63 pp.

Vaugeois, L.M. and Shaw, S.C. (2000). Modeling Shallow Landslide Potential for Watershed Management. Available at http://www.gisvisionmag.com/vision.php?article=/GISVision/TechPaper/paper2000.html April 16 2004.

Veblen, T.T. (1982). Natural Hazards and Forest Resources in the Andes of South-Central Chile. GeoJournal, 6(2): 141-150.

Visser, R. and Adams, J. (2002). Risk Management of Steep Terrain Harvesting. In: Proceedings of the Annual Meeting of the Council on Forest Engineering, Forest Engineering Challenges - A Global Perspective, Auburn University. Auburn, AL, pp. 4.

Wieczorek, G.F. (1984). Preparing a Detailed Landslide-Inventory Map for Hazard Evaluation and Reduction. Bulletin of the Association of Engineering Geologists, 21(3): 337-342.

Wieczorek, G.F. (1996). Landslide Triggering Mechanisms. In: Turner, A.K. and Schuster, R.L. (Eds), Landslides: Investigation and Mitigation. Transportation Research Board Special Report. National Academy Press, Vol 247: Washington, D.C., 76-90.

Wieczorek, G.F., Morgan, B.A., Campbell, R.H., Orndorff, R.C., Burton, W.C., Southworth, C.S. and Smith, J.A. (1996). Preliminary Inventory of Debris-Flow and Flooding Effects of the June 27, 1995, Storm in Madison County, Virginia Showing Time Sequence of Positions of Storm-Cell Center. U.S. Geological Survey, Open-File Report 96-13, 8, 1 plate 1:24,000 pp.

Wieczorek, G.F., Morgan, B.A. and Campbell, R.H. (2000). Debris-Flow Hazards in the Blue Ridge of Central Virginia. Environmental and Engineering Geoscience, 6(1): 3-23.

Wieczorek, G.F., Mossa, G.S. and Morgan, B.A. (2004). Regional Debris-Flow Distribution and Preliminary Risk Assessment from Severe Storm Events in the Appalachian Blue Ridge Province, USA. Landslides, 1(1): 53-59.

Williams, G.P. and Guy, H.P. (1973). Erosional and Depositional Aspects of Hurricane Camille in Virginia, 1969. U.S. Geological Survey, Professional Paper 804, 80 pp.

Wright, C. and Mella, A. (1963). Modifications to the Soil Pattern of South-Central Chile Resulting from Seismic and Associated Phenomena During the Period May to August 1960. Bulletin of the International Association of Engineering Geology, 53(6): 1367-1402.

Wu, S., Shi, L., Wang, R., Tan, C., Hu, D., Mei, Y. and Xu, R. (2001). Zonation of the Landslide Hazards in the Forereservoir Region of the Three Gorges Project on the Yangtze River. Engineering Geology, 59(1-2): 51-58.

Yin, K.L. and Yan, T.Z. (1988). Statistical Prediction Models for Slope Instability of Metamorphosed Rocks. In: Proceedings., 5th International Symposium on Landslides Vol 2: Lausanne, Switzerland, 1269-1272.

Zaruba, Q. and Mencl, V. (1982). Landslides and Their Control. 2nd ed. Elsevier, Amsterdam, Netherlands. 324 pp.

APPENDICES

APPENDIX A. MADISON UNIFIED WEIGHTS

Soil Description	MUSYM	Unified Group	Weight
Alluvial land, cobbly	Ad	SC-SM	1
Alluvial land, mixed	Ac	SM	1
Altavista loam, clayey subsoil variant	Al	SC	5
Appling fine sandy loam, very deep	Ar	ML	5
Augusta silt loam, clayey subsoil variant	Au	CL	1
Baile stony silt loam	Ba	CL	1
Braddock-Thurmont loams	Bc	SC	5
Brandywine fine gravelly loam	Bd	GM	10
Brandywine loam, very deep	Be	GM	10
Brandywine stony loam, very deep	Bn	GM	10
Chester-Brandywine loams, very deep	Ck	GM	10
Chewacla silt loam	Cm	SC	5
Codorus loam, cobbly subsoil variant	Cn	GM	1
Colluvial land, extremely stony	Cu		10
Colluvial land, very stony	Cr		10
Congaree fine sandy loam	Cv	CL	1
Congaree loam	Cw	CL	1
Dyke loam	Dk	CL	1
Elioak fine sandy loam	El	SC	5
Elioak loam	Em	SC	5
Elioak silty clay loam	En	SC	5
Eubanks loam, very deep	Et	SC	5
Eubanks-Lloyd clay loams	Eu	SC	5
Eubanks-Lloyd loams	Ey	SC	5
Glenelg loam	Gl	CL	1
Hazel loam	Ha	SM	10
Hiwassee loam	Hs	CL	1
Iredell silt loam	Ir	CL	1

APPENDIX A CONTINUED

Soil Description	MUSYM	Unified Group	Weight
Lloyd loam	Ll	CL	1
Lloyd loam, thin solum variant	Lm	CL	1
Made land	Ma		5
Manor silt loam	Mo	SC-SM	7
Meadowville loam	Mv	SC	5
Myersville-Catoctin very stony silt loam	My	GC	5
Porters very stony loam	Po	SM	10
Riverwash	Rh		1
Rock land, acidic	Rn		10
Rock land, basic	Ro		7
Rock land, myersville and catoctin materials	Rr		7
Rock land, porters and hazel materials	Rt		10
Rock outcrop	Ru		5
Starr silt loam	Sr	SC	5
Trego loam	Tr	GC	5
Tusquitee stony loam	Tu	SC-SM	7
Unison loam	Un	CL	1
Unison very stony silt loam	Us	CL	1
Water	W		0
Wehadkee silt loam	We	SC	5
Wickham loam, clayey subsoil variant	Wh	CL	1
Worsham loam	Wm	CL	1

APPENDIX B. NELSON UNIFIED WEIGHTS

Soil Description	Unified Group	Weight
Belvoir sandy loam	CL	1
Chatuge loam	SM	10
Codorus silt loam	SM	10
Colleen gravelly loam	GC	5
Colvard fine sandy loam	SM	10
Craigsville very cobbly loam	SC-SM	7
Delanco loam	CL	1
Edneytown loam	SM	10
Edneytown-Peaks complex	SM	10
Elioak clay loam	CL	1
Elioak loam	CL	1
Fauquier loam	CH	1
Glenelg silt loam	CL	1
Hatboro loam	SC	5
Hayesville clay loam	CL	1
Hayesville loam	CL	1
Hazel channery loam	GC	5
Hazel loam	GC	5
Minnieville loam	CL	1
Myersville-Catoctin complex	GC	5
Occoquan loam	SC	5
Peaks-Rock outcrop complex	GC-GM	7
Pineywoods silt loam	CL	1
Pits		1
Saunook loam	SM	10
Sketerville silt loam	CL	1
Spriggs loam	SC	5
Suches loam	SC	5
Sylco-Sylvatus complex	GC	5
Thurmont loam	SC	5

APPENDIX B CONTINUED

Soil Description	Unified Group	Weight
Unison loam	CL	1
Water		0
Wintergreen clay loam	CH	1
Wintergreen loam	CH	1

APPENDIX C. SMALL-SCALE INSTABILITY MAPS

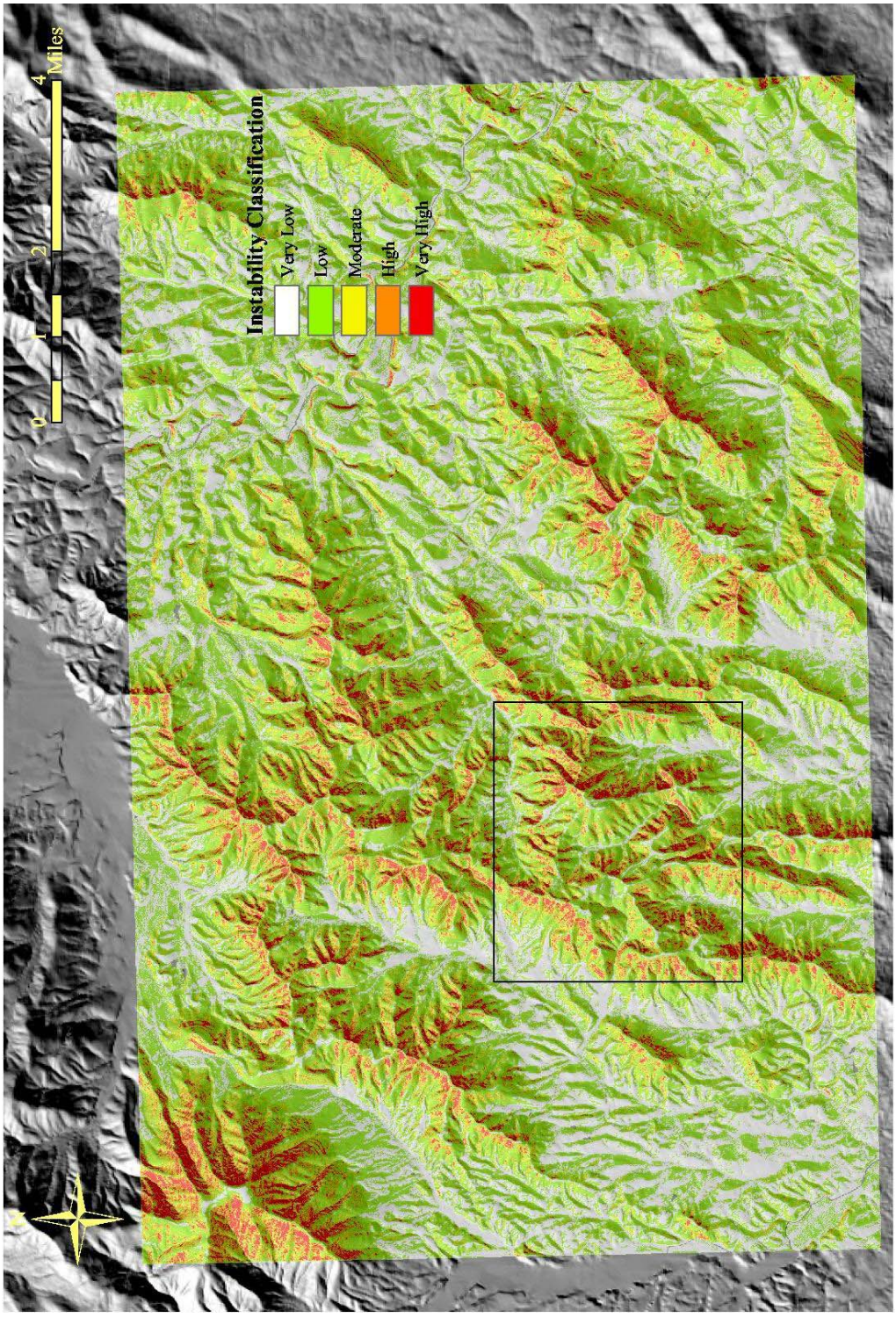

10-meter Instability Map created using the Bivariate Statistical Analysis in Nelson County (box shows area shown in Figures 9-13)

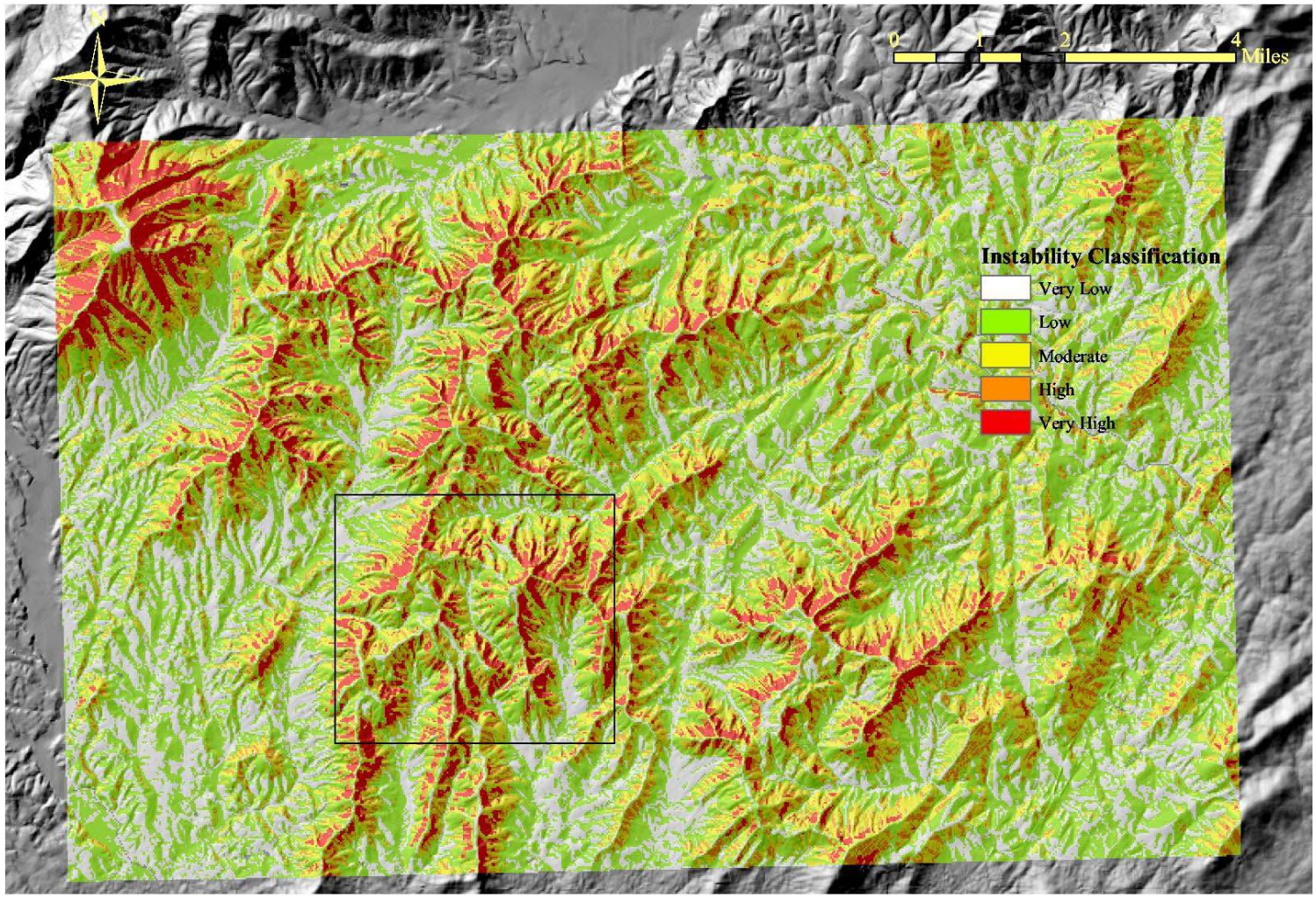

30-meter Instability Map created using the Bivariate Statistical Analysis Run 1 in Nelson County (box shows area shown in Figures 9-13)

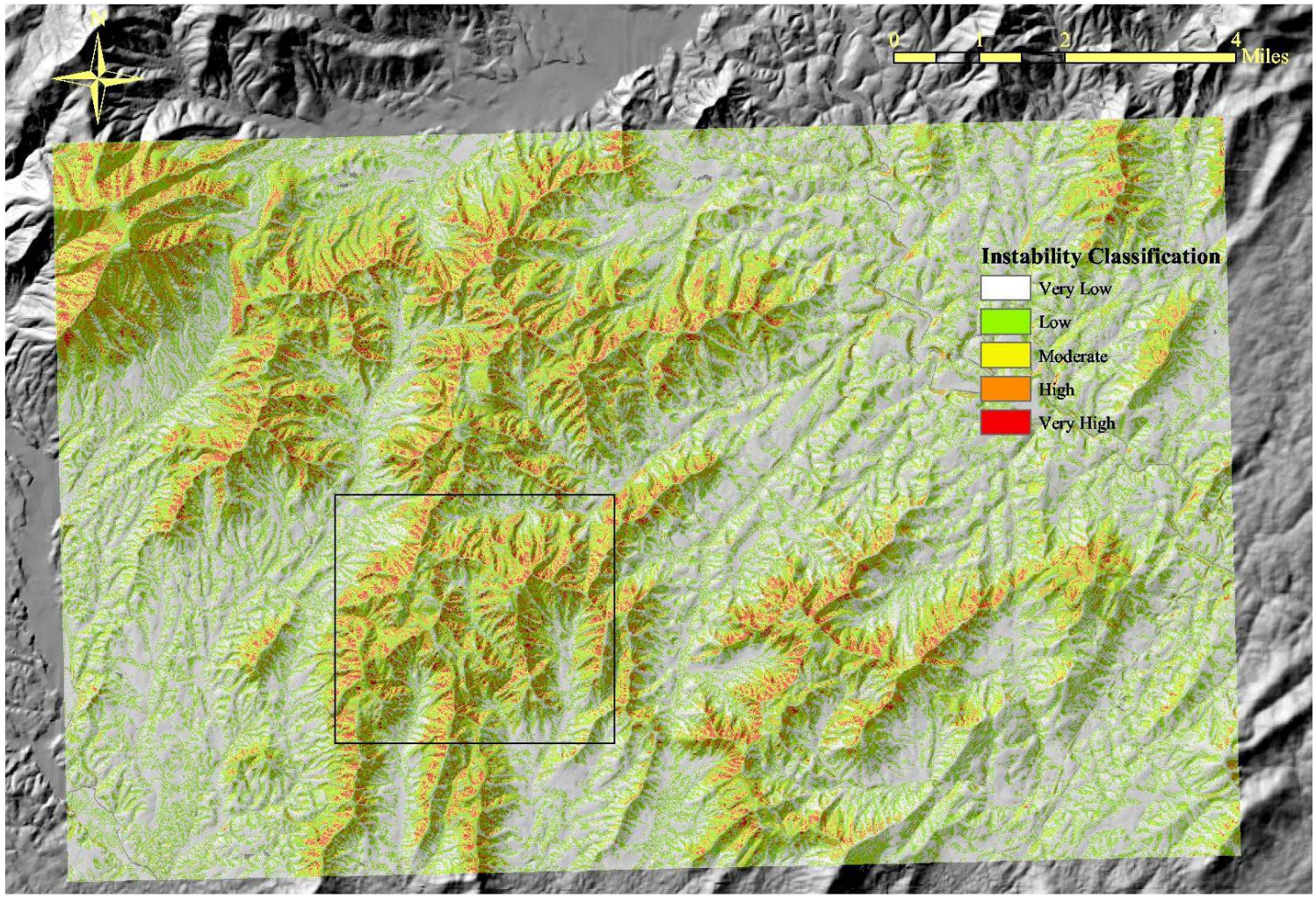

10-meter Instability Map created using the Qualitative Map Combination Run 1 in Nelson County (box shows area shown in Figures 9-13)

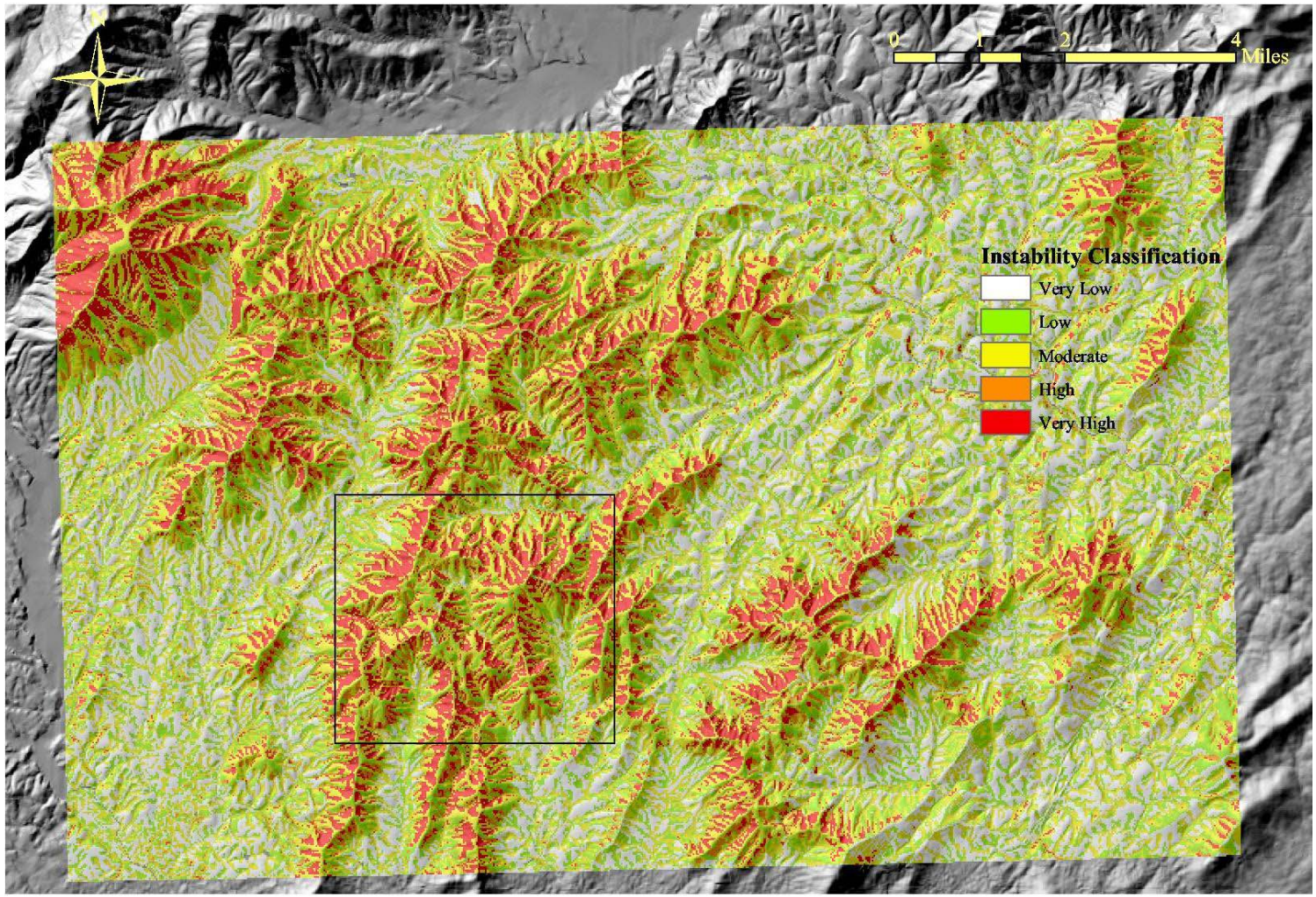

30-meter Instability Map created using the Qualitative Map Combination Run 1 in Nelson County (box shows area shown in Figures 9-13)

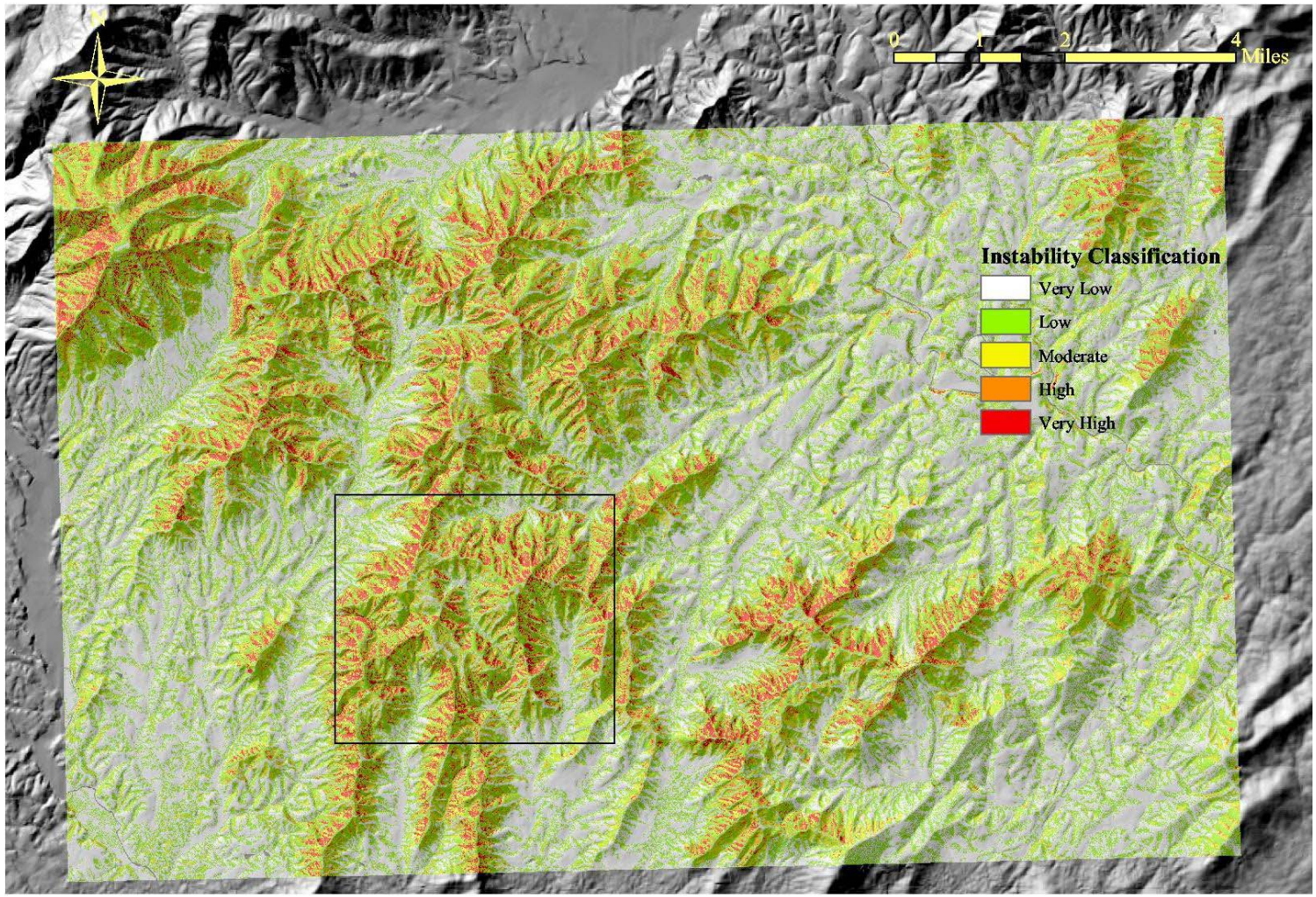

10-meter Instability Map created using the Qualitative Map Combination Run 2 in Nelson County (box shows area shown in Figures 9-13)

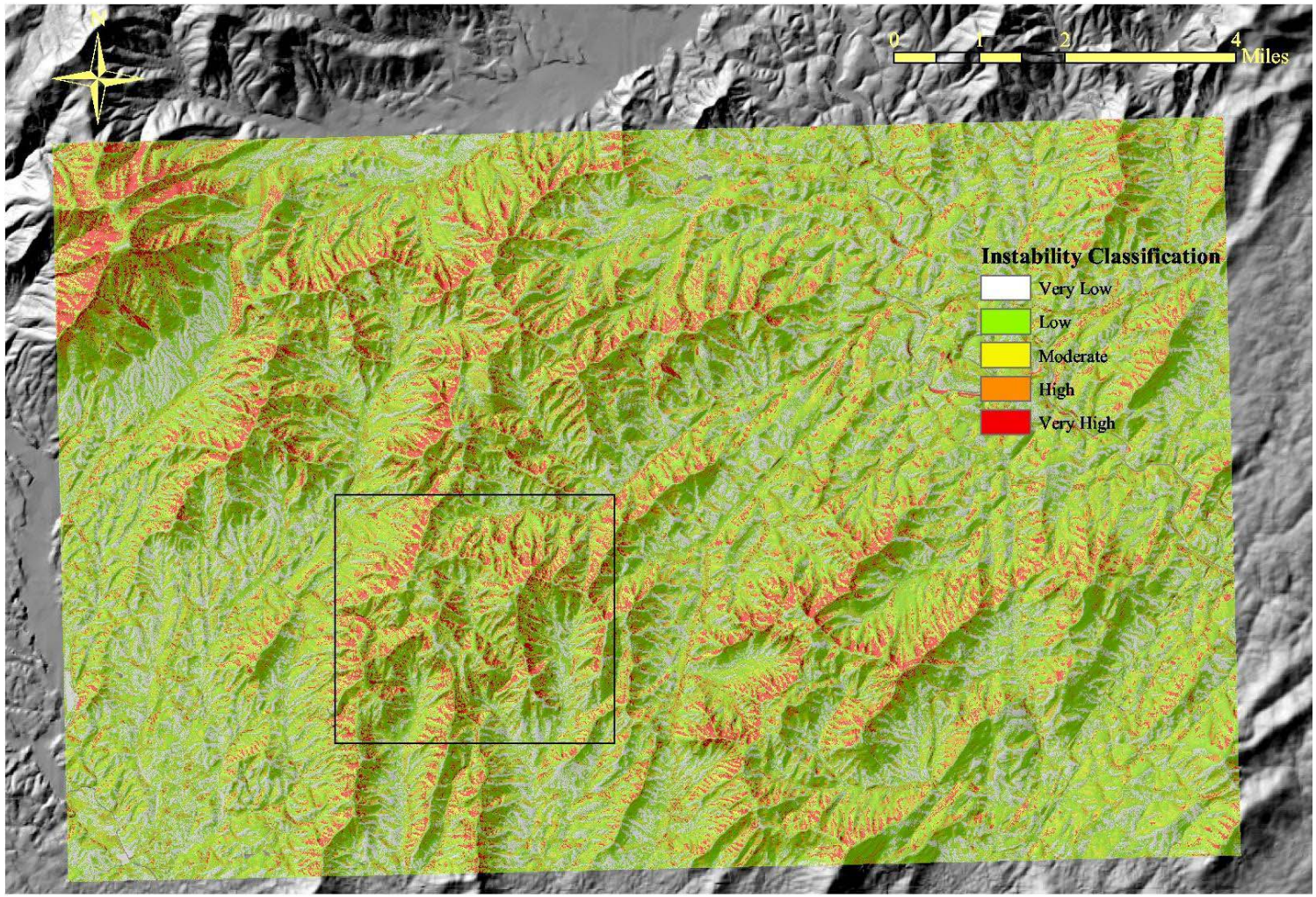

10-meter Instability Map created using the Qualitative Map Combination Run 3 in Nelson County (box shows area shown in Figures 9-13)

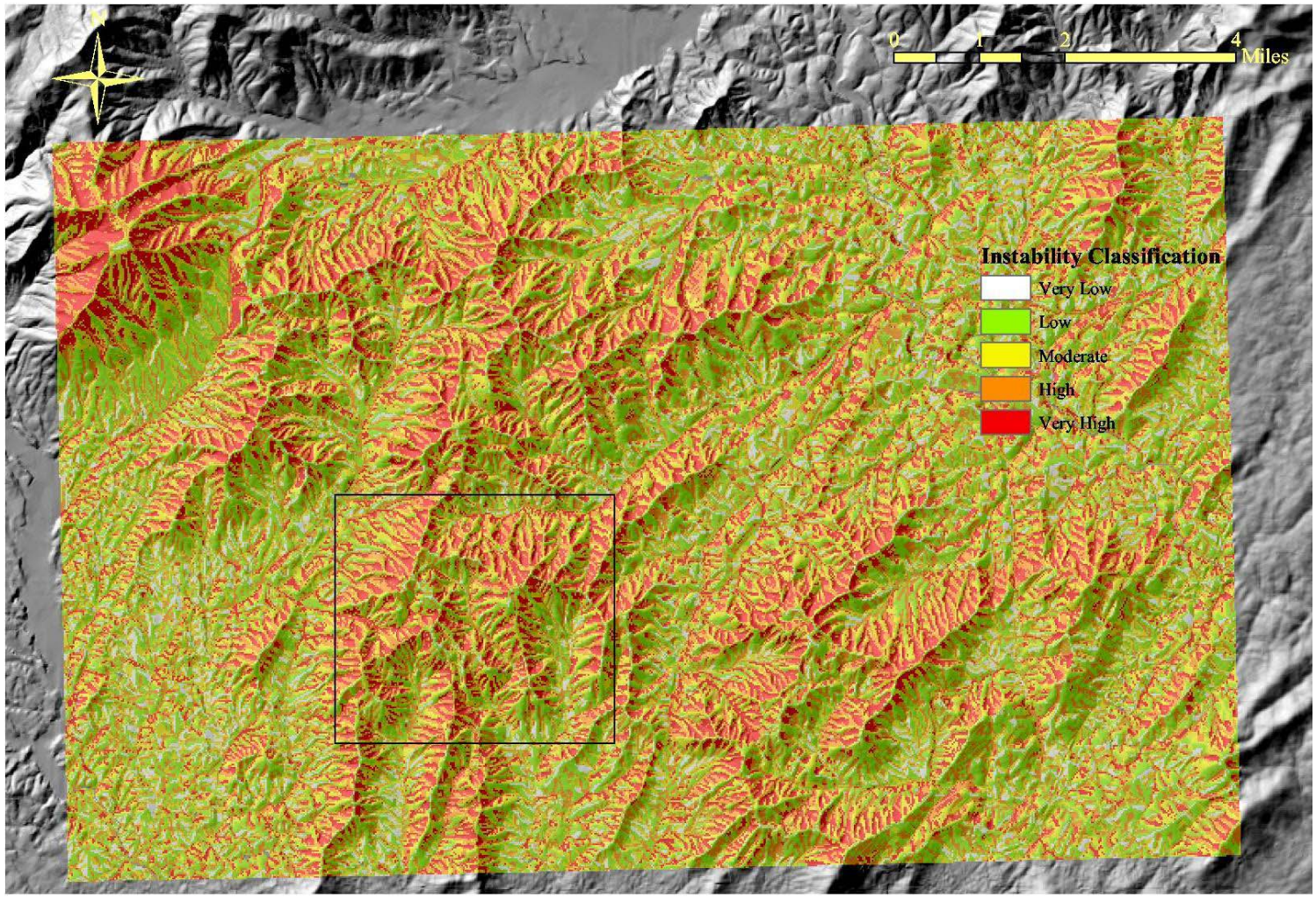

30-meter Instability Map created using the Qualitative Map Combination Run 3 in Nelson County (box shows area shown in Figures 9-13)

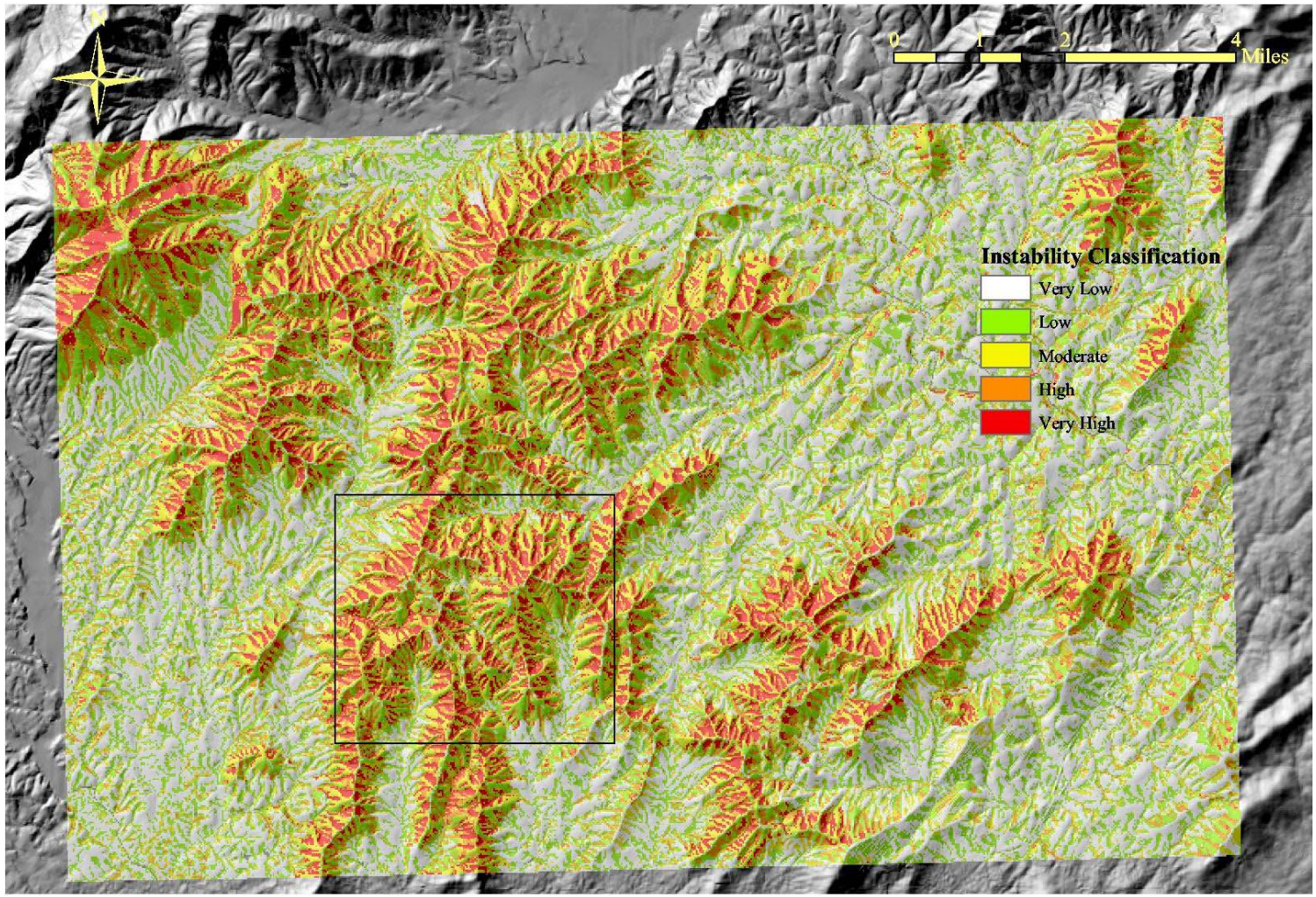

30-meter Instability Map created using the Qualitative Map Combination Run 2 in Nelson County (box shows area shown in Figures 9-13)

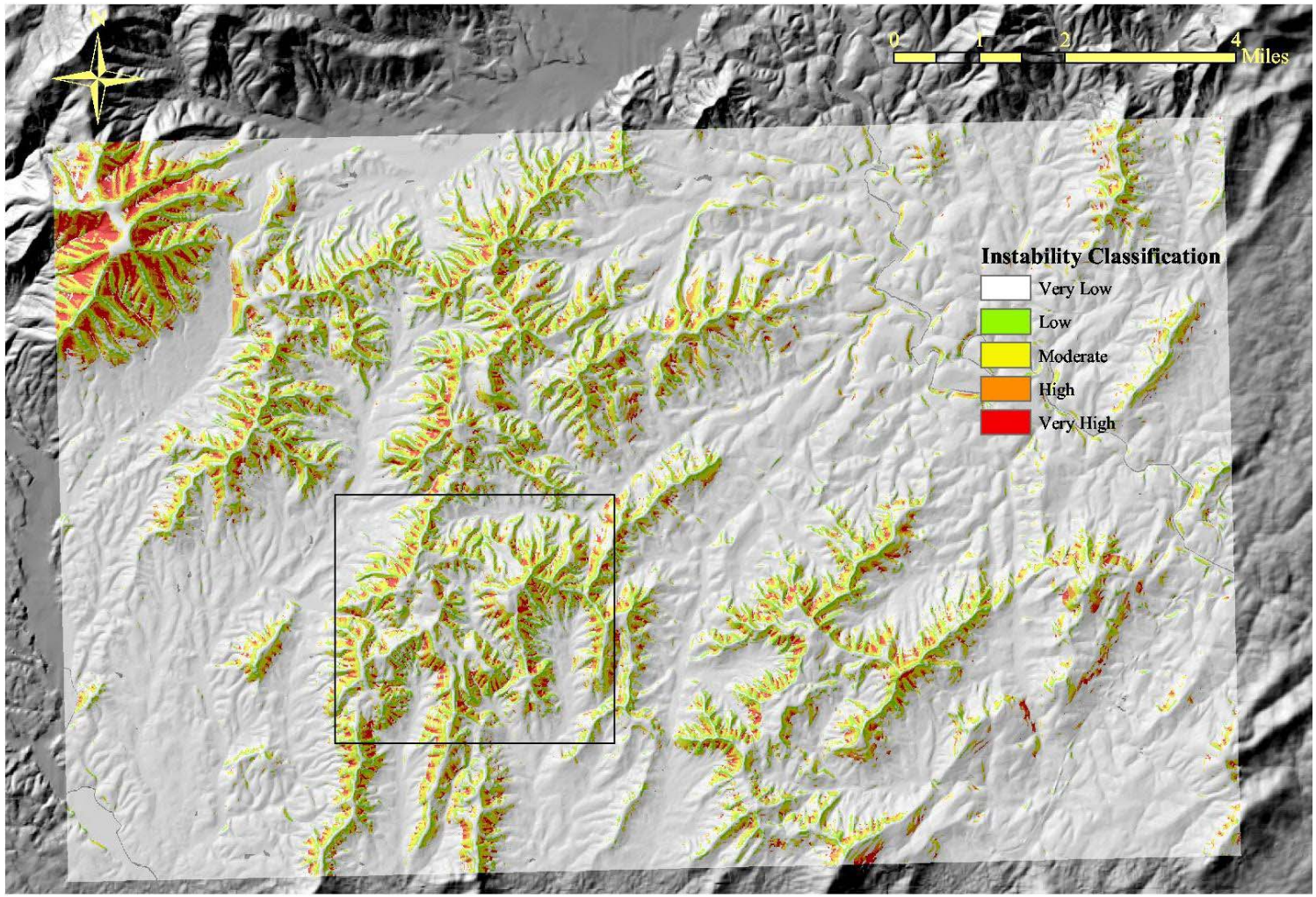

10-meter Instability Map created using SHALSTAB Run 1 in Nelson County (box shows area shown in Figures 9-13)

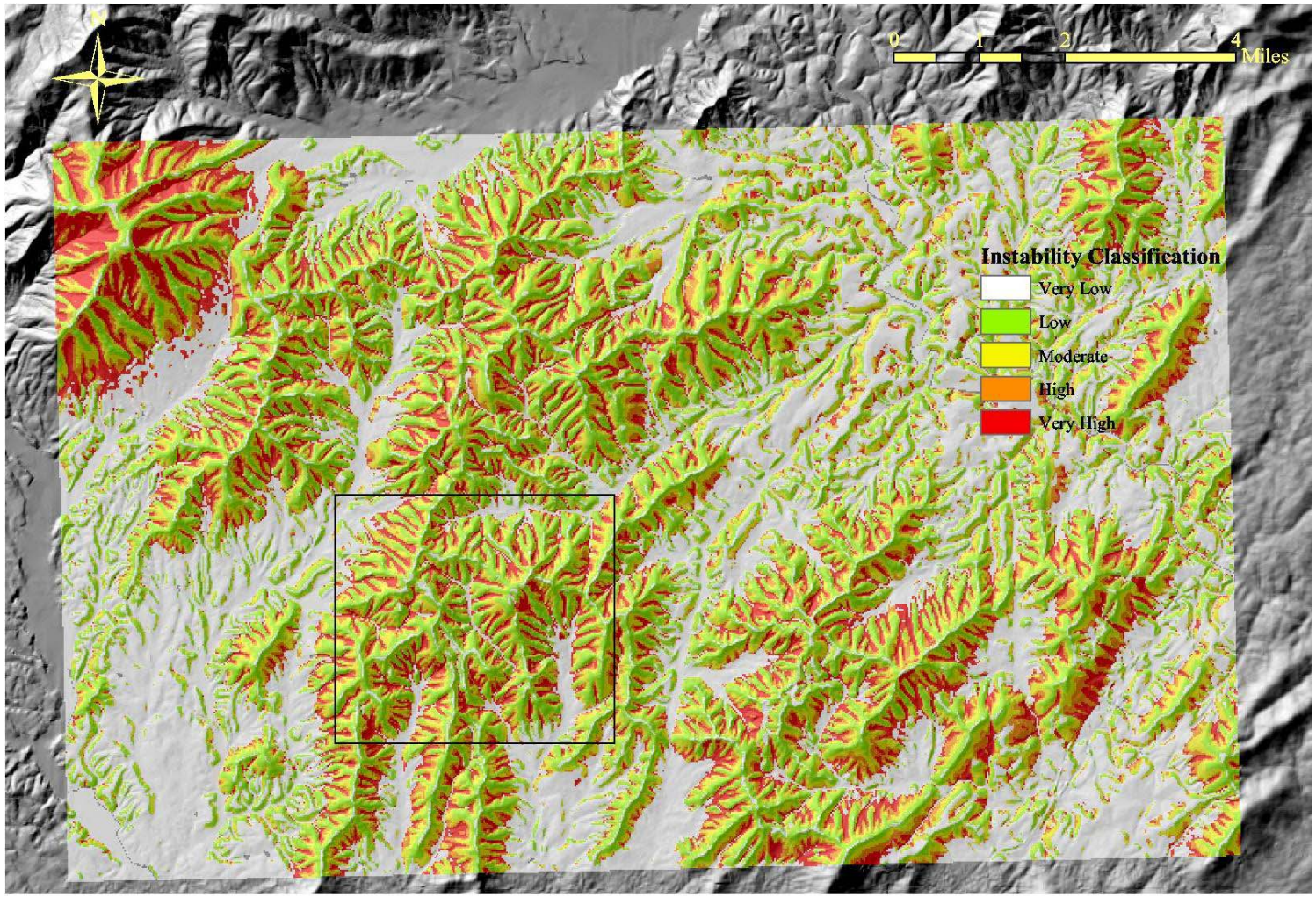

30-meter Instability Map created using SHALSTAB Run 1 in Nelson County (box shows area shown in Figures 9-13)

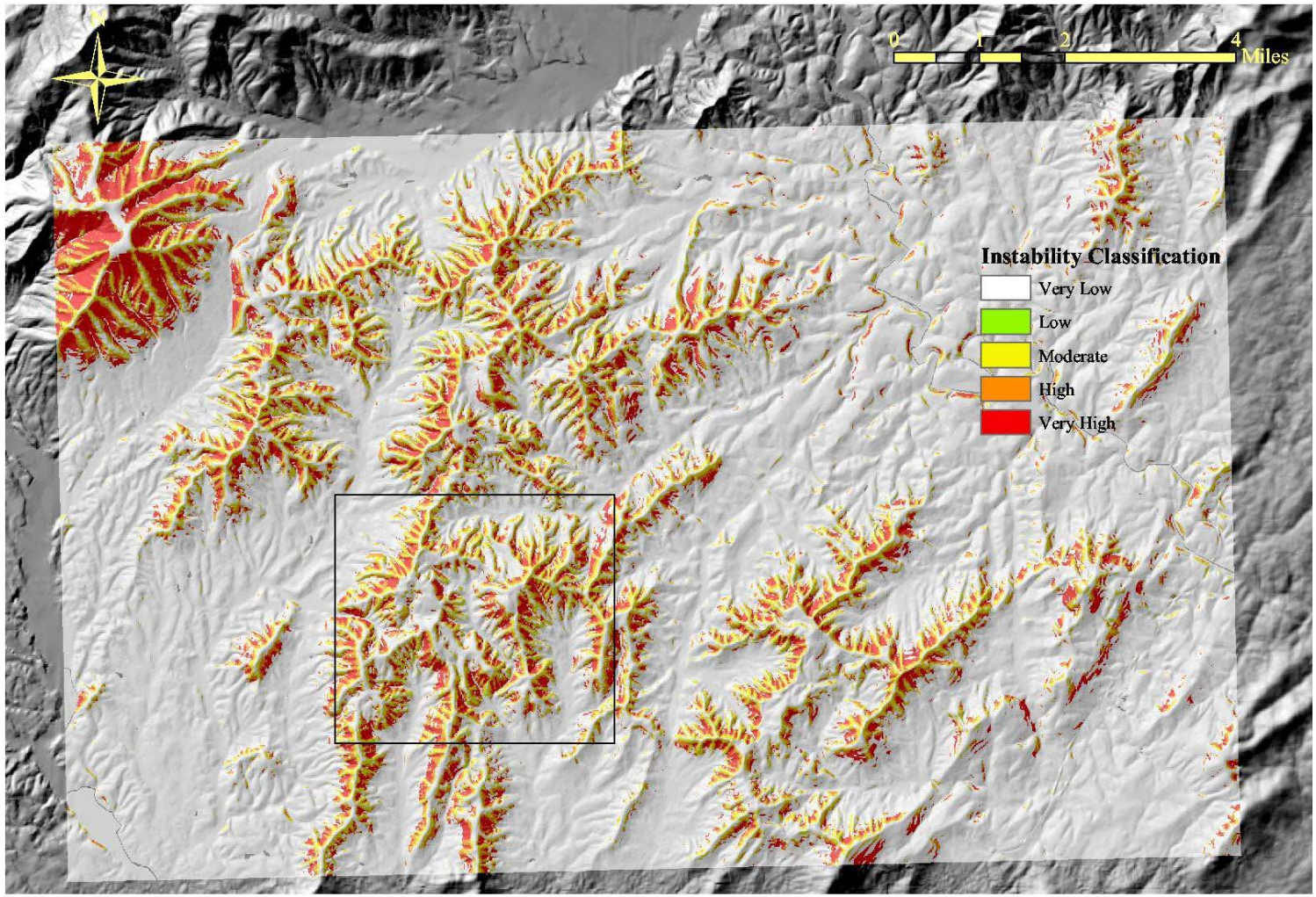

10-meter Instability Map created using SHALSTAB Run 2 in Nelson County (box shows area shown in Figures 9-13)

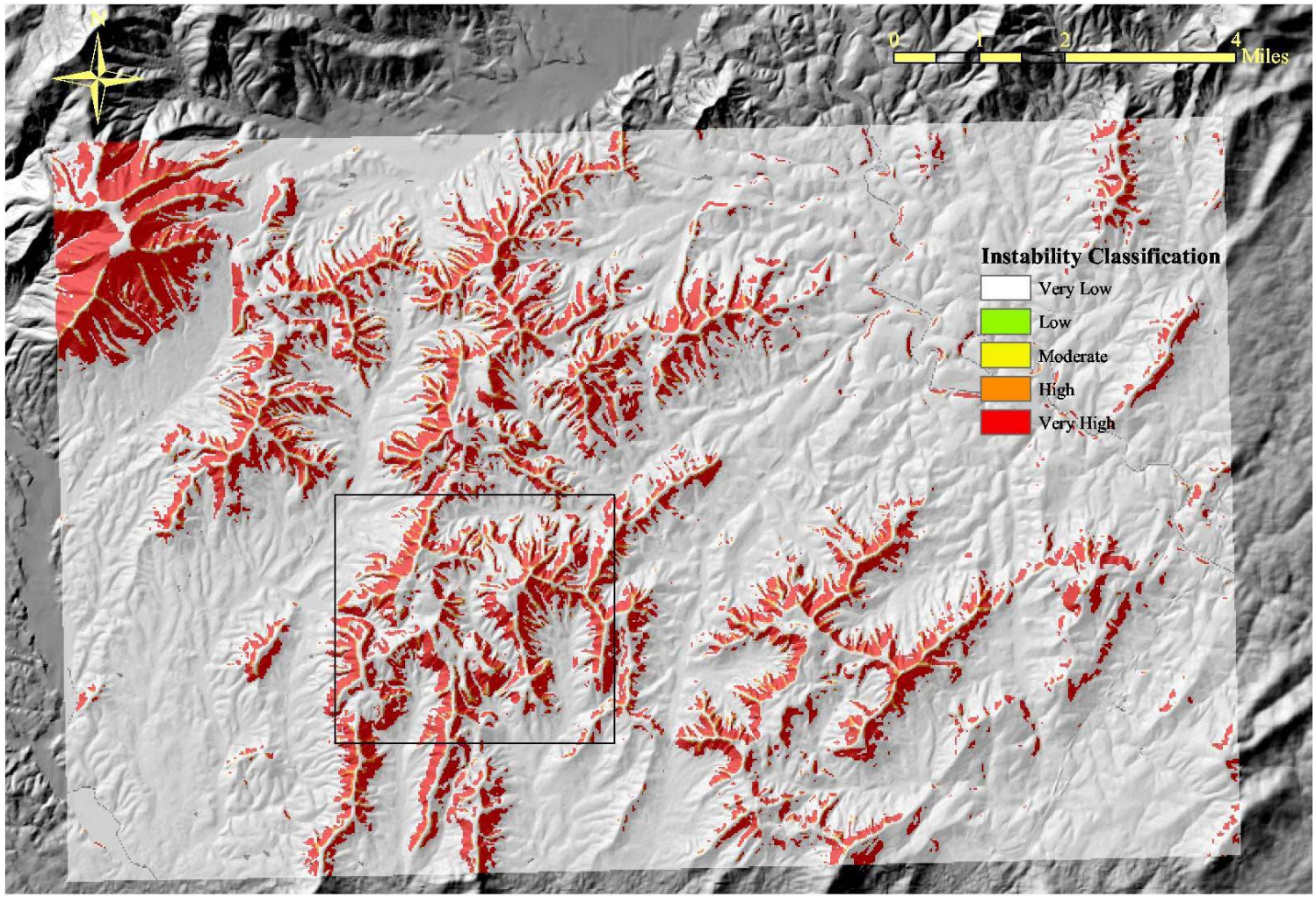

30-meter Instability Map created using SHALSTAB Run 2 in Nelson County (box shows area shown in Figures 9-13)

APPENDIX D. CONTINGENCY TABLES FOR SENSITIVITY ANALYSES

SHALSTAB Run 1

10 meter \ 30 meter	Very Low	Low	Moderate	High	Very High	Total
Very Low	**1102483**	637308	326565	147951	235699	2450006
Low	4504	**159272**	24337	4154	4654	196921
Moderate	95	44394	**148136**	37207	17927	247759
High	21	209	15564	**45582**	22388	83764
Very High	6	111	1014	12823	**51111**	65065
Total	1107109	841294	515616	247717	331779	**3043515**

SHALSTAB Run 2

10 meter \ 30 meter	Very Low	Low	Moderate	High	Very High	Total
Very Low	**2411621**	20	54	8979	29332	2450006
Low	184	**0**	2	30	0	216
Moderate	79846	51	**152**	65701	79439	225189
High	33321	1	2	**2702**	147331	183357
Very High	28812	0	6	237	**155692**	184747
Total	2553784	72	216	77649	411794	**3043515**

QMC Run 3

10 meter \ 30 meter	Very Low	Low	Moderate	High	Very High	Total
Very Low	**124908**	299802	93072	77723	11752	607257
Low	64230	**486572**	455255	435440	166627	1608124
Moderate	6613	59329	**52815**	129948	73814	322519
High	1482	21166	52448	**54118**	113791	243005
Very High	212	4902	27172	64622	**165702**	262610
Total	197445	871771	680762	761851	531686	**3043515**

QMC Run 2

10 meter \ 30 meter	Very Low	Low	Moderate	High	Very High	Total
Very Low	**833103**	351964	94831	40117	3956	1323971
Low	207465	**379132**	302439	117376	57305	1063717
Moderate	12616	69026	**64116**	147391	58875	352024
High	1261	13064	30258	**30191**	66781	141555
Very High	364	4206	25956	29262	**102460**	162248
Total	1054809	817392	517600	364337	289377	**3043515**

APPENDIX D CONTINUED

QMC Run 1

10 meter	30 meter: Very Low	Low	Moderate	High	Very High	Total
Very Low	**617977**	487706	278624	23365	8741	1416413
Low	129521	**192499**	603752	75925	94952	1096649
Moderate	1728	15582	**88266**	34171	118188	257935
High	854	12707	51183	**15945**	84200	164889
Very High	31	2049	19267	7021	**79261**	107629
Total	750111	710543	1041092	156427	385342	**3043515**

BVS Run 1

10 meter	30 meter: Very Low	Low	Moderate	High	Very High	Total
Very Low	**514174**	322720	25431	2515	63	864903
Low	168611	**804417**	385928	78289	22081	1459326
Moderate	6097	93351	**127354**	130734	41609	399145
High	851	13414	54246	**36205**	82956	187672
Very High	239	2643	17595	28933	**83059**	132469
Total	689972	1236545	610554	276676	229768	**3043515**

VITA

Jeffrey Sterling Galang was born to Mario and Judith Galang on September 18, 1974 in Harrisonburg, Virginia. He attended Turner Ashby High School in Bridgewater, VA and graduated in 1993. After a few years away from academics, Jeff attended Blue Ridge Community College in Weyers Cave, VA and transferred to Virginia Tech in the fall of 1999 to pursue a Bachelor's degree in Forestry. During this time, Jeff had the fortunate opportunity to spend time in the Khumbu region of Nepal underneath the shadows of Mt. Everest. After finishing his undergraduate degree in May of 2002, he began his Master's degree in Forestry during the fall of 2002 and finished in December of 2004.